Copyright Warning & Restrictions

The copyright law of the United States (Title 17, United States Code) governs the making of photocopies or other reproductions of copyrighted material.

Under certain conditions specified in the law, libraries and archives are authorized to furnish a photocopy or other reproduction. One of these specified conditions is that the photocopy or reproduction is not to be "used for any purpose other than private study, scholarship, or research." If a, user makes a request for, or later uses, a photocopy or reproduction for purposes in excess of "fair use" that user may be liable for copyright infringement,

This institution reserves the right to refuse to accept a copying order if, in its judgment, fulfillment of the order would involve violation of copyright law.

Please Note: The author retains the copyright while the New Jersey Institute of Technology reserves the right to distribute this thesis or dissertation

Printing note: If you do not wish to print this page, then select "Pages from: first page # to: last page #" on the print dialog screen

ABSTRACT

MODELLING OF IN-SITU BIOREMEDIATION WITH EMPHASIS ON INHIBITORY KINETICS AND BIOMASS GROWTH

by
Dilip Kumar Mandal

This thesis was motivated by the need for better engineering tools to predict the extent of contaminant plume migration in the saturated zone. The principal result was a mathematical model analogous to a catalytic packed-bed reactor, in which the subsurface was considered to be composed (conceptually) of soil aggregates (the "catalyst" particles, in which biodegradation, diffusion, and sorption take place), and a mobile phase (groundwater) passing around the aggregates, in which convection, axial diffusion, and mass transfer from the aggregates take place.

The modelling emphasis was on a more detailed exposition of the biokinetics of the system (including an inhibitory expression for biomass growth, and oxygen limitation) than is the case in most prior models (which place greater emphasis on physical effects such as sorption, diffusion, and hydrodynamics).

Several coupled partial differential equations were used to describe the processes taking place, and these were solved numerically in dimensionless form by the Method of Lines. Model parameters were determined by a combination of laboratory experiments, existing empirical correlations, and estimates based on the literature. Sensitivity analyses of these parameters showed that the biokinetic constants indeed dominated the system

response, which justified the emphasis placed on those factors in the model development.

A laboratory soil column was used to test the model, and the results showed good agreement with model simulations. However, the simulations were particularly sensitive to three interrelated parameters (one of the inhibitory biokinetic constants, another related to the rate of loss of active microorganisms from the system, and the initial biomass concentration), two of which (bacterial loss rate, and initial biomass concentration) were not known. The loss rate was presumably a function of both the rate of cell death as well as transport out of the system. Thus, some estimation and adjustment of these parameters was necessary in order to obtain a fit of the data.

The effect of oxygen limitation was simulated only. Confirmatory experiments proved difficult to conduct. The simulations indicated the dominant effect that oxygen has on the performance of the system. Even with a saturated feed, oxygen can be rapidly depleted in the direction of groundwater flow, leading to a substantial decrease in the rate of biodegradation.

Field tests of the model are currently being planned.

MODELLING OF IN-SITU BIOREMEDIATION WITH EMPHASIS ON INHIBITORY KINETICS AND BIOMASS GROWTH

by
Dilip Kumar Mandal

A Dissertation
Submitted to the Faculty of
New Jersey Institute of Technology
in Partial Fulfillment of the Requirements for the Degree of
Doctor of Philosophy

Department of Chemical Engineering
Chemistry, and Environmental Science

May 1998

APPROVAL PAGE

MODELLING OF IN-SITU BIOREMEDIATION WITH EMPHASIS ON INHIBITORY KINETICS AND BIOMASS GROWTH

Dilip Kumar Mandal

Dr. Gordon A. Lewandowski, Dissertation Advisor — Date
Distinguished Professor of Chemical Engineering,
and Department Chairperson, NJIT

Dr. Piero M. Armenante, Committee Member — Date
Professor of Chemical Engineering, NJIT

Dr. Basil C. Baltzis, Committee Member — Date
Professor of Chemical Engineering, NJIT

Dr. Norman W. Loney, Committee Member — Date
Associate Professor of Chemical Engineering, NJIT

Dr. Edward J. Bouwer, Committee Member — Date
Professor of Environmental Engineering, Johns Hopkins University, MD

Dr. David Kafkewitz, Committee Member — Date
Professor of Biology, Rutgers University, Newark, NJ

BIOGRAPHICAL SKETCH

Author: Dilip Kumar Mandal

Degree: Doctor of Philosophy in Chemical Engineering

Date: May 1998

Undergraduate and Graduate Education:

- Doctor of Philosophy in Chemical Engineering
  New Jersey Institute of Technology, New Jersey, 1998
- Master of Science in Chemical Engineering
  Ohio University, Athens, Ohio, 1993
- Bachelor of Science in Chemical Engineering
  University of Calcutta, Calcutta, India, 1990
- Bachelor of Science in Chemistry (Honours)
  University of Calcutta, Calcutta, India, 1987

Major: Chemical Engineering

Publications:

D. K. Mandal, A.K. Guha, and K.K. Sirkar, "Membrane-based Isomer Separation by Hollow Fiber Contained Liquid Membrane Permeator," *J. of Membrane Science* (in press).

G. A. Lewandowski, D.K. Mandal, R. Gourdon, and R. Bayard, "French/American Collaboration on Transport/Sorption/Biokinetic Interactions During In-Situ Bioremediation", *In: Proceedings of the Fourth International In-Situ and On-Site Bioremediation Symposium*, New Orleans, Louisiana, April 28 - May 1, 1997.

Section on isomer separation in "*Hollow Fiber Contained Liquid Membranes for Separations: An Overview* - by Dr. K.K. Sirkar" of ACS Symposium Series on "*Chemical Separations with Liquid Membranes*" edited by R.A. Bartsch and J.D. Way, 1996.

Presentations:

G. A. Lewandowski, D. K. Mandal, M.E. Rosar, and D.T. Papageorgiou, "Modelling of In-Situ Bioremediation: Coupling of Non-Equilibrium Sorption and Growth Inhibition," American Institute of Chemical Engineers 1995 Annual Meeting, Miami Beach, Florida, November 12-17, 1995.

D. K. Mandal, G. A. Lewandowski, M.E. Rosar, and D.T. Papageorgiou, "Modelling of In-Situ Bioremediation: Coupling of Non-Equilibrium Sorption and Growth Inhibition," 1995 Five Centers' Research Conference, Oregon Water Resources Research Institute, Oregon State University, Salishan Lodge, Gleden Beach, Oregon, July 23-26, 1995.

D. K. Mandal, "Modelling of In-Situ Bioremediation: Coupling of Non-Equilibrium Sorption and Growth Inhibition," Fifth Annual Mini-Tech Conference, New Jersey Institute of Technology, Newark, April 21, 1995.

K.K. Sirkar, D.K. Mandal, A.K. Guha, and Z.-F. Yang, "Liquid Membranes for Product Separations," Annual Pfizer in-house Technical Conference, Wakefield, Massachusetts, October 24-28, 1994.

D. K. Mandal, A.K. Guha, Z.-F. Yang, and K.K. Sirkar, "Equipment for Pollution Prevention - Isomer and Bioproduct Separation by Hollow Fiber Contained Liquid Membrane Permeator, 20th anniversary of the NSF Industry/University Cooperative Research Centers, Washington, D.C., January 11, 1994.

This dissertation is dedicated to
my parents

ACKNOWLEDGMENT

Primary recognition goes to my advisor, Dr. Gordon A. Lewandowski for believing in me, guidance, encouragement, criticism, and patience throughout this research, and I do consider myself fortunate to have been under his tutelage.

I would like to thank Dr. Piero M. Armenante, Dr. Basil C. Baltzis, Dr. Edward Bouwer, Dr. David Kafkewitz, and Dr. Norman Loney for serving as members of my dissertation committee. Further appreciation goes to Dr. Bouwer for a thorough revision and helpful comments on my dissertation.

Financial support for this work comes from the Hazardous Substance Management Research Center (HSMRC) and the National Science Foundation (NSF), which is highly appreciated.

I would like to express special thanks to Dr. Sudipto Majumdar for his valuable comments and suggestions during this research.

I would like to thank my fellow colleagues and friends: Mr. Jay Best, Mr. Syamalendu Bhaumik, Dr. Sitaram Dikshitulu, Dr. Socrates Ioannides, Mr. Anjaneya Kovvali, Mr. Christos Mpanias, Mr. Sachin Purekar, and Dr. Uttam Shanbhag.

I also thank my family in India for their endless patience, support, and constant moral encouragement.

Finally, I do express my sincere appreciation to my wife Aparna for her love and support. Late nights, bad moods, and times when my mind was miles away have not changed her love for me.

TABLE OF CONTENTS

TABLE OF CONTENTS
(Continued)

TABLE OF CONTENTS
(Continued)

Chapter **Page**

TABLE OF CONTENTS
(Continued)

Chapter **Page**

TABLE OF CONTENTS
(Continued)

LIST OF TABLES

LIST OF TABLES
(Continued)

Table **Page**

LIST OF TABLES
(Continued)

LIST OF FIGURES

LIST OF FIGURES
(Continued)

Figure **Page**

LIST OF FIGURES
(Continued)

Figure **Page**

LIST OF FIGURES
(Continued)

LIST OF FIGURES
(Continued)

Figure **Page**

LIST OF FIGURES
(Continued)

Figure **Page**

LIST OF SYMBOLS

a_v	external surface area per unit volume of the aggregate (cm^{-1})
A_d	rate of adsorption (mg/L ·sec)
b	biomass concentration (mg/L)
B_d	biodegradation rate of pollutant (mg/L ·sec)
B_{do}	rate of oxygen consumption due to biodegradation (mg/L ·sec)
b_o	initial biomass concentration (mg/L)
C	concentration of the pollutant in the aqueous phase (mg/L)
c	tracer concentration (mg/L)
C_a	concentration of the pollutant in the aggregate phase (mg/L)
$C_a\|_{r=R}$	concentration of the pollutant at the surface of the aggregates (mg/L)
C_{a0}	initial concentration of the pollutant in the aggregate phase (mg/L)
C_a^*	concentration of pollutant in pore liquid in equilibrium with soil phase concentration (q) (mg/L)
C_b	concentration of the pollutant in the mobile phase (mg/L)
C_{bL}	concentration of pollutant (up to acceptable limit) at the column exit (mg/L)
C_{b0}	initial concentration of pollutant in the mobile phase (mg/L)
C_o	concentration of dissolved oxygen in the mobile phase (mg/L)
C_{o0}	initial concentration of dissolved oxygen in the aggregate (mg/L)
$C_o\|_{r=R}$	concentration of the oxygen at the surface of the aggregates (mg/L)
C_{mo}	concentration of dissolved oxygen in the mobile phase (mg/L)
C_{mo}^0	initial concentration of the oxygen in the mobile phase (mg/L)

$C_{moz_{o}}$ concentration of the oxygen just before entering into the reactor (mg/L)

$C_{z_{o}}$ concentration of the pollutant just before entering into the reactor (mg/L)

$C_{moz_{o}}$ concentration of the oxygen just before entering into the reactor (mg/L)

D_{le} dispersion coefficient of 2-CP (cm^2/sec)

D_{lo} dispersion coefficient of oxygen (cm^2/sec)

D_{se} diffusion coefficient of 2-CP (cm^2/sec)

D_{so} diffusion coefficient of oxygen (cm^2/sec)

k_d adsorption rate constant (sec^{-1})

k_m mass transfer coefficient (cm/sec)

k_{m0} mass transfer coefficient of oxygen (cm/sec)

k_p Freundlich parameter $(L/kg)^{1/n}$

K_i Andrews parameter (mg/L)

K_S Andrews parameter (mg/L)

k_{so} mass transfer coefficient of oxygen (cm/sec)

K_{SO} Monod kinetic constant of oxygen (mg/L)

L length of the column (cm)

n Freundlich parameter

Pe Peclet number of the pollutant ($=\bar{v}_z \cdot L/D_{le}$)

Pe_o Peclet number of oxygen ($=\bar{v}_z \cdot L/D_{lo}$)

q concentration of pollutant in the soil (mg pollutant/kg of soil)

q_0 initial concentration of pollutant in the soil (mg pollutant/kg of soil)

$-r_s$ rate of substrate consumption (mg/L·sec)

r	radial distance (cm)
R	aggregate radius (cm)
R_m	rate of mass transfer of the pollutant to the surface of the soil aggregates (mg/L ·sec)
s	substrate concentration (mg/L)
Sh_a	sherwood number of pollutant ($Sh_a = k_m \cdot R/D_{se}$)
Sh_{ao}	sherwood number of oxygen ($Sh_{ao} = k_{mo} \cdot R/D_{so}$)
Sh_b	modified sherwood number of pollutant [$Sh_b = (3(1-\varepsilon_b)/\varepsilon_b) \cdot Sh_a$]
Sh_{bo}	modified sherwood number of oxygen [$Sh_{bo} = (3(1-\varepsilon_b)/\varepsilon_b) \cdot Sh_{ao}$]
t	time (sec)
$\bar{t}$	mean residence time (sec)
t_{lag}	lag period (sec)
u	average pore velocity (cm/sec)
$\bar{v}_z$	average pore velocity (cm/sec)
Y	yield coefficient (mg biomass per mg substrate degraded)
Y_{Expt}	experimentally obtained yield coefficient (mg biomass per mg substrate degraded)
Y_o	yield coefficient due to oxygen (mg biomass per mg oxygen consumed)
z	axial distance (cm)

Greek Symbols

β	dimensioless biomass concentration

β_o dimensionless initial biomass concentration

γ_a normalized liquid phase pollutant concentration in the aggregate

$\gamma_a|_{\eta=1}$ dimensionless concentration of oxygen at the surface of the aggregates

γ_{a0} normalized initial liquid phase pollutant concentration in the aggregate

γ_a^* concentration of pollutant in pore liquid in equilibrium with soil phase concentration (γ_s)

γ_b dimensionless concentration of pollutant in the mobile phase

γ_{b0} dimensionless initial concentration of pollutant in the mobile phase

γ_{mo} dimensionless concentration of dissolved oxygen in the mobile phase

γ_{mo}^0 dimensionless initial concentration of the oxygen in the mobile phase

γ_{moz_0} dimensionless concentration of the oxygen just before entering into the reactor

γ_o normalized liquid phase oxygen concentration in the aggregate

γ_{o0} normalized initial liquid phase oxygen concentration in the aggregate

γ_s normalized solid phase pollutant concentration in the aggregate

γ_{s0} normalized initial solid phase pollutant concentration in the aggregate

γ_{z_0} dimensionless concentration of the pollutant just before entering into the reactor

ε_a void fraction of the aggregates (cm^3 void/cm^3 total)

ε_b void fraction of the mobile phase (cm^3 void/cm^3 total)

Φ_a dimensionless group ($\Phi_a = R^2 \cdot k_d / D_{se}$)

Φ_b dimensionless group ($\Phi_b = R^2 \cdot \hat{\mu} / D_{se}$)

Φ_c dimensionless group ($\Phi_c = R^2 \cdot \hat{\mu}_c / D_{se}$)

Φ_k dimensionless group ($\Phi_k = K_{so}/K_s$)

ξ dimensionless axial distance

η dimensionless radial distance

μ specific growth rate (sec^{-1})

$\hat{\mu}$ Andrews parameter (sec^{-1})

μ_c specific death rate (sec^{-1})

$\hat{\mu}_C$ specific death rate constant (sec^{-1})

ρ_S soil density (g/cm^3)

Ψ dimensionless group ($\Psi = \bar{v}_z \cdot R^2 / L \cdot D_{se}$)

σ^2 variance (sec^2)

σ_θ^2 dimensionless variance ($\sigma_\theta^2 = \sigma^2 / \bar{t}^2$)

τ dimensionless time ($\tau = t \cdot u / L$)

θ dimensionless time ($\theta = D_{se} \cdot t / R^2$)

CHAPTER 1

INTRODUCTION

As a result of more than two hundred years of industrial activity, there are a large number of sites worldwide (Table 1.1) that are contaminated with industrial chemicals, both organic and inorganic. Rainfall causes these chemicals to migrate down through the soil, often reaching groundwater (i.e. below the water table).

Table 1.1 Estimate of the number of contaminated sites on a global basis [EPA (1997) and Smith (1991)].

Country	Number of contaminated sites	Estimated high risk sites
Canada	10,000	1000
Finland	20,000	100-1000
United States	217,083	547
Germany	100,000	not known
United Kingdom	est. 100,000	not known
Netherlands	110,000	6000

The focus in this dissertation will be on organic contaminants capable of being biodegraded. A schematic of generic contaminant distribution is shown in Figure 1.1. Organic contaminants may be:

- present as a separate non-aqueous phase liquid (NAPL), which may be lighter or denser

than water

- sorbed on the soil matrix
- present as vapor within soil pore space
- dissolved in water
- undergoing biodegradation

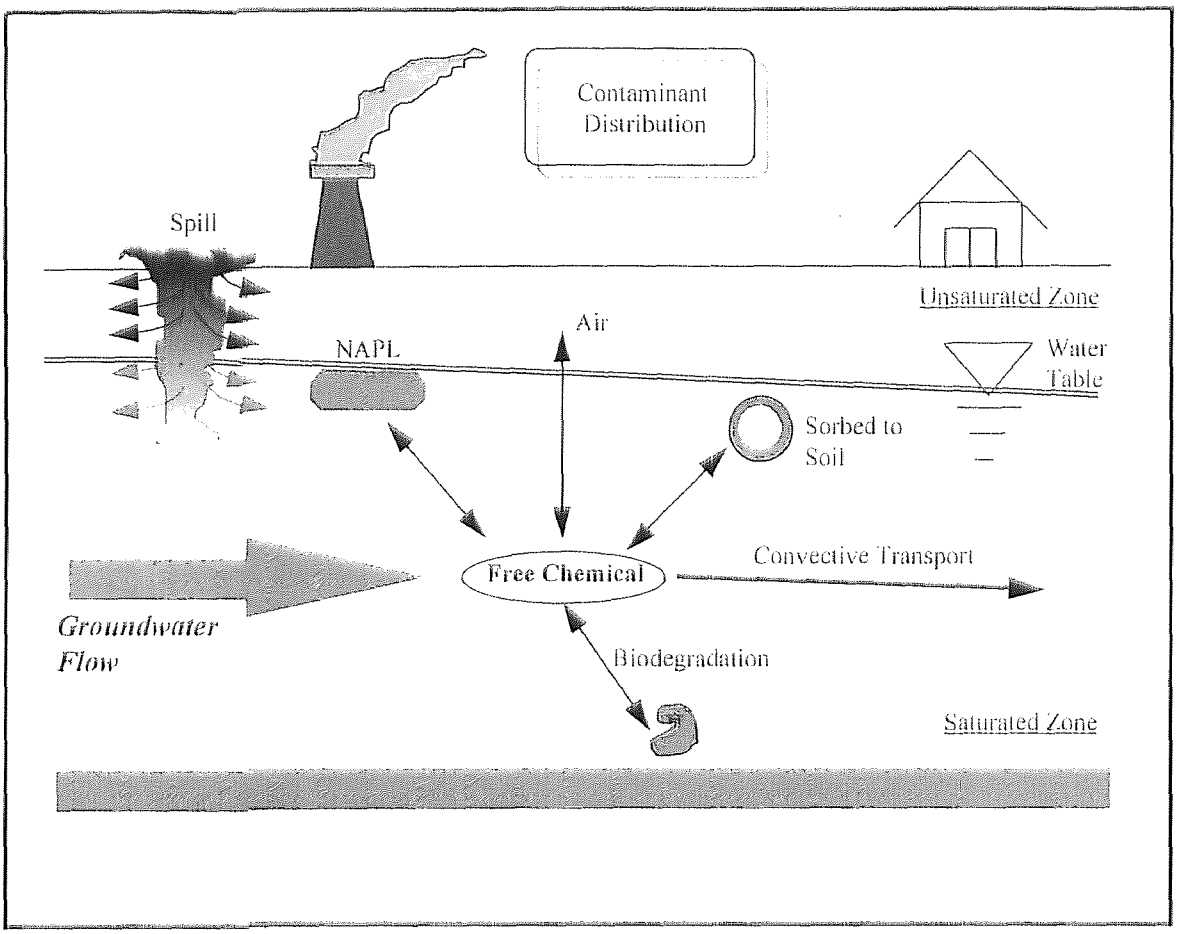

Figure 1.1 Schematic of generic contaminant distribution at a site.

In-situ bioremediation technology has the potential of offering cost-effective remediation of contaminated sites, by using the metabolic activity of indigenous or introduced microorganisms to transform hazardous organic compounds to harmless products [Bouwer (1992)]. Although bioremediation can occur without human intervention (called "natural" attenuation, or "intrinsic" bioremediation), most often engineers must intervene to protect water supplies, and achieve desired clean up levels in a timely manner. An example of engineered in-situ bioremediation is shown in Figure 1.2 which seeks to alter nutrient concentrations (e.g. nitrogen, phosphorous, etc.) and the concentration of electron acceptors (e.g. oxygen, nitrate, sulfate, etc.) to increase the rate of in-situ bioremediation [Bouwer (1992)]. In addition, other environmental conditions like redox potential, pH, and moisture must be favorable for microorganisms to biotransform organic contaminants [Hrudey and Pollard (1993)].

This is a very complex process, which is exacerbated by the heterogeneity of the "reactor" being employed, and the difficulty of influencing "reactor" parameters such as soil type, percent natural organic matter (i.e. humic substances), moisture content, temperature, nature of the microbial population, etc. As a result, traditional trial-and-error methods of implementing in-situ bioremediation technology at a contaminated site can be inefficient and costly.

It is therefore essential to develop reliable structured engineering models that can analyze in-situ treatment options, predict the extent of contaminant migration, estimate treatment time and cost, and diagnose problems arising in the field prior to the

irreversible commitment of resources. Such a structured model must at a minimum include the effect of transport processes, sorption, and biokinetic phenomena.

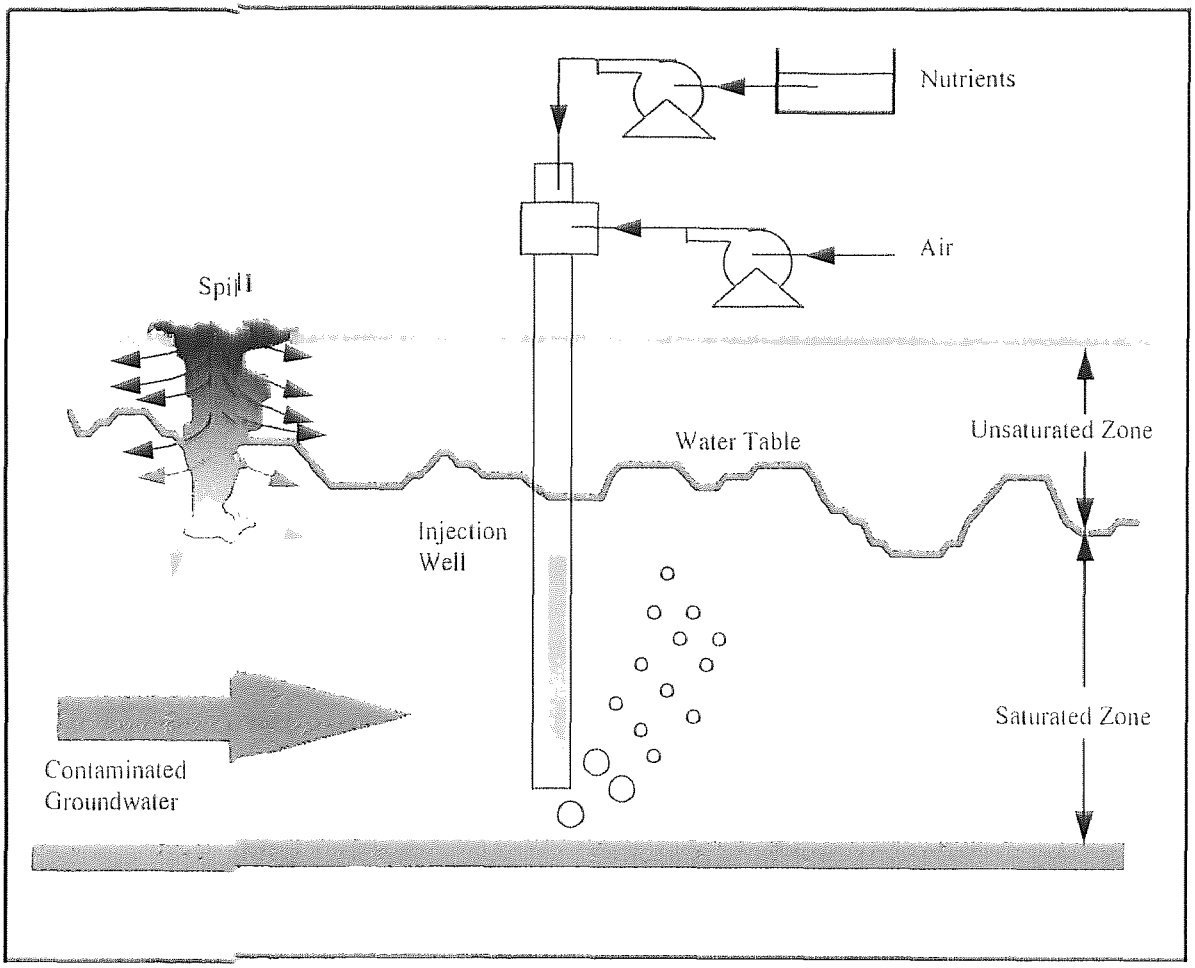

Figure 1.2 Pictorial representation of an in-situ bioremediation system.

CHAPTER 2

LITERATURE REVIEW

2.1 Overview of Model Development

Cerniglia (1993), Sims et al (1990), and Bouwer (1992a) among others, have pointed out that there are several critical factors (e.g. soil type, moisture content, temperature, pH, electron acceptor and pollutant concentrations, hydraulic conductivity, permeability, and environmental conditions as a whole) which profoundly influence field applications of in-situ bioremediation technology. It is easier to qualitatively address these factors, than elucidate a quantitative model incorporating them.

Over the years, several models have been proposed to simulate the transport of organic contaminants in abiotic systems (i.e. in the absence of biodegradation) [Abriola (1989), Abriola and Pinder (1985a,b), Brusseau (1992), Crittenden et al. (1986), Freeman and Schroy (1986), Goltz and Roberts (1988), Parker and van Genuchten (1984), Pinder and Abriola (1986), Rao et al. (1980a, 1980b, 1982), Roberts et al. (1987), and van Genuchen et al. (1977)].

Crittenden et al. (1986) utilized a "two-compartment" model incorporating mass balance equations based on the movement of a non-degradable organic compound in a saturated soil column. Their model included advection/convection, axial dispersion, liquid-phase mass transfer, diffusion, and local adsorption equilibrium, in mobile and immobile water (the two compartments). They obtained analytical solutions for the one-dimensional concentration profile.

Goltz and Roberts (1986, 1988) described another physical (abiotic) model for mobile phase advection/dispersion, combined with diffusion of solute into immobile water regions, in two and three dimensions. Although this model agreed, in part, with some aspects of the observed behavior, other factors such as a decrease in organic solute concentration in the mobile phase, retardation of the sorbing solute, and the long-tailing of the breakthrough responses at the near field well, were not consistent with the model results.

In addition to these abiotic models there are a number of engineering models that also incorporate biokinetic factors, albeit in first-order or Monod expression [Borden and Bedient (1986), Bouwer and Cobb (1987), MacQuarrie et al. (1990), Molz et al. (1986), Rifai and Bedient (1990), Semprini and McCarty (1991), Srinivasan and Mercer (1988), Sykes et al. (1982), Widdowson et al. (1988)].

Sykes et al. (1982) developed a very basic engineering model to predict the concentration of leachate organics, measured as chemical oxygen demand (COD), in the ground water below sanitary landfill sites. To model the subsurface biodegradation, they included convective transport, dispersion, and biokinetic substrate utilization with biomass production. However, their solutions reduced the Michaelis-Menten-type model to a first-order expression (which may be the case when the substrate concentration is very low), and eliminated any adsorption term. Simulation results from the model appeared to over-estimate the COD (or leachate) concentrations.

Borden and Bedient (1986), and Borden et al. (1986), attempted to incorporate an aerobic biotransformation term in their mathematical model to simulate the transport and

fate of contaminants in the natural environment. They considered growth, decay, and transport of microorganisms, as well as transport of contaminants (hydrocarbons) and oxygen. This approach differed from Sykes in that they accounted for the mechanisms of adsorption and rate-limiting oxygen transport from the neighboring unsaturated zone. However, as is often the case with these attempts, when solutions for the model were finally developed, they assumed that for oxygen-limited biodegradation, consumption of oxygen and hydrocarbon can be approximated as an instantaneous reaction, and this enormously simplified their model simulations in one and two dimensions (although they appeared to obtain reasonable agreement with experimental data at a creosote-contaminated site).

Srinivasan and Mercer (1988) also aimed at simulating one dimensional contaminant transport in the presence of sorption and biodegradation. Advection and dispersion effects were considered for substrate (hydrocarbon) and oxygen transport. Biological transformation for both substances included three different kinetic expressions: (1) aerobic kinetics using a Monod model, (2) anaerobic kinetics using a Michaelis-Menten equation, and (3) a first-order model. Adsorption was assumed to be in local equilibrium. As with many other published models, the initial mathematical description was simplified prior to solution, in this case by assuming constant biomass. However, they conceded that this assumption was a major limitation of their model, even though their simulations fit reasonably well with the data obtained by Borden et al. (1984).

Several other researchers formulated their models based on "biofilm concepts". In subsurface environments, microorganisms tend to attach to solid surfaces, forming clusters enveloped by excreted extracellular polymeric materials [Costerton et al. (1981)]. That assembly of microbial clusters is termed a "biofilm". Models have then been developed that consider transport and biodegradation in these biofilms [Bakke (1986), Bouwer (1989), Bouwer and McCarty (1984 and 1985), Bouwer et al. (1992), Kissel et al. (1984), Rittmann and McCarty (1980a, b), Semprini and McCarty (1991), Wanner and Reichert (1996), Zhang and Bishop (1994)].

Semprini and McCarty (1991) presented an unsteady state transport model for in-situ bioremediation in saturated porous media, which was very similar to that of Borden and Bedient (1986). This model included physical transport, microbial growth, substrate utilization, and rate-limited sorption. Monod kinetics were assumed for microbial growth and substrate utilization based on the concept of a biofilm. It was further assumed that biofilms were completely penetrable, and there were no mass transfer limitations as such. Similar concepts had already been developed by Rittmann and McCarty (1980a). Solution of the governing equations showed a reasonably good fit with observed data. However, the compounds used for their experimental studies did not sorb to the soil. Thus, the model may need further modifications for situations in which there are significant sorption effects.

Typically soil may have wide pore size distributions, which are altered by microbial growth, resulting in time-dependent changes to porosity, tortuosity, and

dispersivity [Cunningham (1991), Taylor et al. (1990), Rittmann (1993), Taylor and Jaffé (1990a,b), Vandevivere and Baveye (1992)].

Sorption, whether linear or non-linear, can have a pronounced effect on the persistence of organic chemicals in an in-situ bioremediation process [McCarty et al. (1981, 1984)]. Excellent review articles have been published that have discussed many fundamental aspects of sorption and desorption processes commonly occurring in soil [Brusseau and Rao (1989), Calvet (1989), Harmon et al. (1989), Sabatini et al. (1989), Weber and Smith (1987)]. Calvet (1989) has mentioned that it is difficult to generalize the relationship between the shape of the isotherm and the nature of the adsorbate-adsorbent systems, which can include ion exchange, hydrogen bonding, charge transfer, and London-van der Waals dispersion forces. Additional factors affecting sorption processes include the molecular structure of the sorbing material, organic carbon content of the soil matrix, and temperature.

Miller and Weber (1986) presented a one dimensional model to predict the transport behavior of a solute (lindane or nitrobenzene) in a soil column. This model included advection, desorption, and rate-limited sorption. Their model predictions were in close agreement with observed column results. This agreement between simulation and data were even closer when dual-resistance, rate-controlled mechanisms were included. They concluded that for a wide variety of soils and organic solute systems, sorption equilibria are generally non-linear. They also mentioned that the equilibration rate is not instantaneous, but rather a combination of two steps: an initial fast step,

followed by a slower rate step. This is similar to observations made in this dissertation, as well as those of Bayard (1997).

A similar observation was made by Bouchard et al. (1988). They performed several batch sorption experiments to quantitatively describe the effects of pore-water velocity, solute hydrophobicity, and soil organic-carbon content, and proposed a slow intra-organic-carbon diffusional mechanism to describe non-equilibrium sorption during solute transport.

Batch soil-microcosm experiments were performed by Robinson et al. (1990) to determine the sorption and bioavailability of toluene in soil with high organic content. It was determined that there are two different steps through which sorption of toluene occurred. The first step involved a rapid sorption followed by slow rate-based sorption until equilibrium was reached. This study suggested that sorption is a non-linear process. It was also concluded that toluene desorbs very slowly from the soil particles, and therefore biodegradation may be limited by the desorption rate.

Pickens et al. (1981) performed radial injection dual tracer studies in a sandy aquifer to determine dispersive and adsorptive properties. They observed the extreme tailing of tracer breakthrough curves. This showed the non-equilibrium nature of the adsorption/desorption phenomenon. Another field study for soil flushing at Gloucester Landfill by Bahr (1989) also supported the concept of non-equilibrium desorption-rate-limited biodegradation.

Laboratory experiments were performed by Ogram et al. (1985) to determine the effects of sorption on the biodegradation rate of 2,4-dichlorophenoxy acetic acid (2,4-D)

in soils. They showed that biodegradation occurred for that portion of 2,4-D which was free in solution. Even bacteria that were attached to the soil particles were not able to degrade the sorbed 2,4-D. Investigators postulated that this may be the result of: (1) the inability of the microcolonies to metabolize sorbed 2,4-D; and (2) sorption of 2,4-D deep into the soil matrix that limited its bioavailability.

Brusseau et al. (1991) performed several experiments in preparative chromatographic columns in order to identify/elucidate the mechanisms/processes responsible for the nonlinear sorption of hydrophobic organic chemicals, e.g. pentafluorobenzoic acid, anthracene, quinoline, etc. A first order model was used to analyze the data. They concluded that the sorption observed in their experiments was nonequilibrium in nature and may have been caused by diffusion into intra-organic matter. They also mentioned that for this approach to adequately describe nonequilibrium sorption, the polymeric nature of organic matter, and diffusant-polymer interactions, must be taken into account.

Ball and Roberts (1990), Dhawan et al. (1991), Chung et al. (1993), and Ahn et al. (1996) have outlined the importance of intra-aggregate diffusion and sorption/desorption in the remediation process. Particularly, Dhawan et al. (1991) have stressed the fact that diffusion, sorption, and biotransformation inside the aggregate must be considered in order to obtain a quantitative understanding of soil remediation.

Ahn et at. (1996) proposed a very comprehensive mathematical model to describe sorption, transport, and biodegradation in the saturated zone. They used naphthalene as the test compound for simulation. This was entirely a theoretical work, in which

macroscale-predictions were based on the knowledge of microscale kinetics and macroscopic fluid dynamics. Although this model was very fundamental in its formulation, it required a very large number of parameters (about 50). All of these model parameters were either taken from the literature or assumed. In fact, obtaining these parameters experimentally (especially those at the microscale) would be a difficult task.

In general, these models do not consider oxygen limitation, and [except for Dhawan (1993), and Ahn et at. (1996)] depend on first order or Monod (non-inhibitory) kinetics. Furthermore, they treat biodegradation and sorption as independent (decoupled) processes.

The Monod kinetic model assumes that the pollutant does not inhibit growth of the microorganisms at any concentration. Furthermore, it is only strictly applicable to a pure culture, or a stable functional population under growth conditions, with only one substrate limiting the rate of reaction [Monod (1942)]. For chemicals with higher toxicity, kinetic patterns may be highly inhibitory in nature, leading to a model proposed by Andrews (1968). In this model, increasing concentration of pollutant eventually inhibits the specific growth rate of the microorganisms, which is often the case with chemicals found in subsurface contaminated sites.

The research described in this dissertation places greater emphasis than previously on the dynamic interplay between sorption and biodegradation, and takes into account simultaneous growth and decay of biomass, inhibitory biokinetics, and oxygen limitation.

2.2 Biodegradation Kinetics of Chlorinated Phenolics

In this study, emphasis is on the development of a more reliable in-situ bioremediation model, and testing it using laboratory soil column experiments. To meet this objective, one needs to obtain parameter values that are an integral part of the model equations. Of these, the biokinetic parameters are of paramount importance. 2-chlorophenol (*ortho*-chlorophenol) was selected as the model compound.

In general, chlorophenols (e.g. mono-, di-, and tri- etc.) are of environmental concern due to their toxicity and presence at many sites. They have been used as biocides [Kobayashi (1978)], pesticides [Häggblom (1992)], are formed as by-products during chlorine-bleaching of pulp [Kringsted and Lindstorm (1984)] and degradation of pesticides [Pritchard et al. (1987)], and result from chlorination of surface and wastewaters [Jolly et al. (1976)]. Chlorophenolics, particularly di- and tri-, being relatively soluble in water [Boyd (1982)], become easily mobile and leachable, and thereby contaminate ground water [Valo et al. (1984)].

Considerable progress has been made in aerobic [Baker et al. (1980), Dorn et al. (1974), Fava et al. (1995), Janke et al. (1989), Kafkewitz et al. (1996), Knackmuss and Hellwig (1978), Smith and Novak (1987), Spain and Gibson (1988), Wang (1995)] and anaerobic [Armenante et al. (1993), Boyd et al. (1983), Boyd and Shelton (1984), Dietrich and Winter (1990), Hrudey et al. (1987)] biodegradation of chlorinated phenols in the past several years using bacteria, fungi, and activated sludge. In addition, there are a few excellent review articles [Reineke and Knackmuss (1988), Chaudhry and

Chapalamadagu (1991), Häggblom (1992)] that have outlined various aspects of aerobic and anaerobic biodegradation of chlorophenolics.

Anaerobic biodegradation proceeds via removal of the chlorine substituent, followed by reactions leading eventually to methane and carbon dioxide [Boyd et al. (1983), Boyd and Shelton (1984), Mikesell and Boyd (1986), Suflita et al. (1982)].

Aerobic biodegradation generally proceeds by initial oxidation, followed by reactions leading to inorganic chloride and carbon dioxide [Chaudhry and Chapalamadagu (1991), Häggblom (1992), Häggblom et al. (1988)]. For example, 2-chlorophenol (2-CP) first undergoes *ortho*-cleavage to form 2-chloro-cis,cis-muconates (or chloromuconates), followed by release of the chlorine substituent to form 4-carboxy-methylene-but-2-en-4-olide [Schmidt and Knackmuss (1980)]. Similar degradation pathways have been postulated by Spain and Gibson (1988) and Kaschabek and Reineke (1993). Studies by Bartels et al. (1984) showed that *meta*-cleavage of chlorocatechols gave rise to some metabolites (e.g. acylchlorides) which deactivated the precursor enzyme. Thus, *meta*-cleavage did not lead to complete mineralization.

A typical aerobic biodegradation pathway (via *ortho*-cleavage) of 2-CP by a *Pseudomonas* strain is shown in Figure 2.1 [Knackmuss and Hellwig (1978), Reineke and Knackmuss (1988), and Schmidt and Knackmuss (1980)].

Nevertheless, there is a lack of detailed biokinetic rate constants for 2-CP, particularly using an inhibitory (Andrews) rate model (which is necessary since 2-CP is an inhibitory substrate). Obtaining such constants was therefore an essential part of the present work.

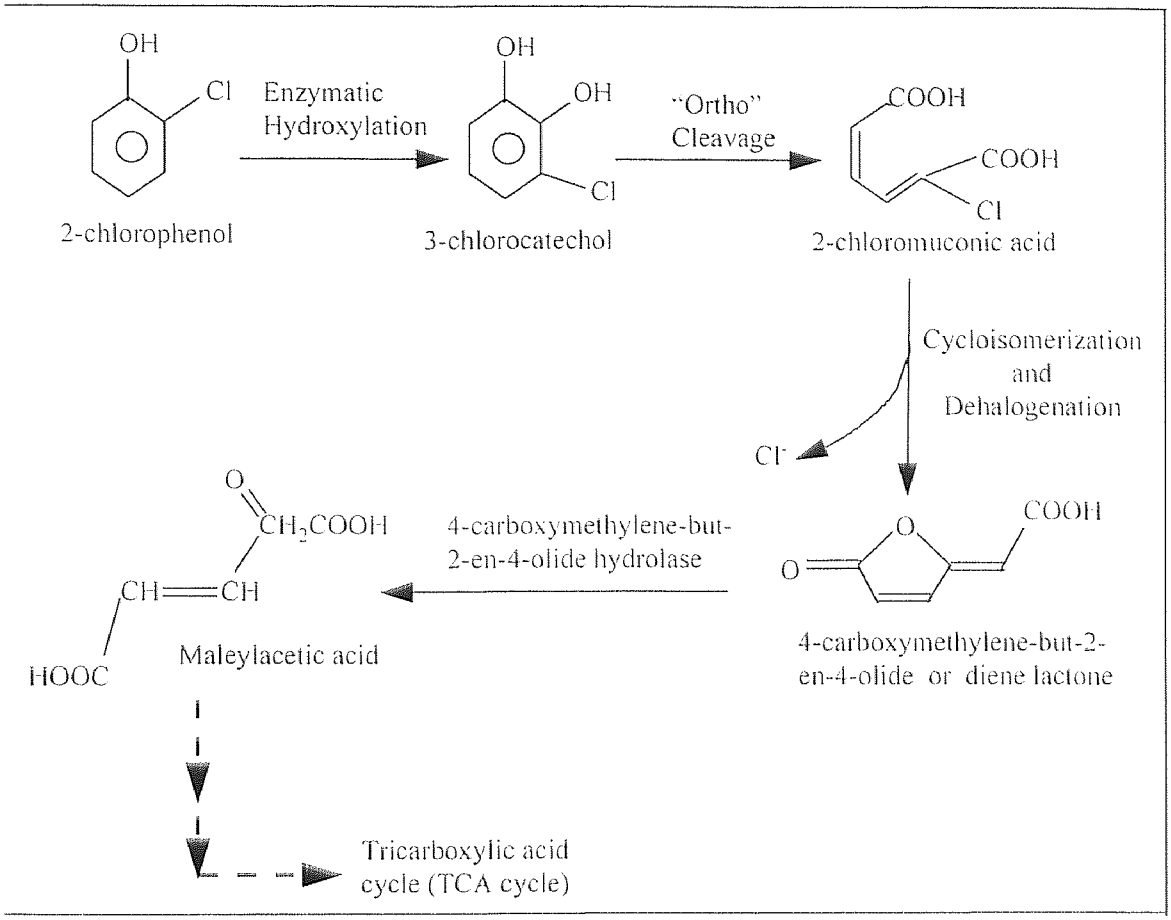

Figure 2.1 Aerobic biodegradation pathway of 2-chlorophenol by *Pseudomonas sp.*

CHAPTER 3

OBJECTIVES

The primary objective in this dissertation was to develop a more reliable, structured mathematical model of in-situ bioremediation and pollutant migration, that would emphasize biokinetic effects (inhibitory biomass growth, oxygen dependence), coupled sorption, and mass transfer. To reach this objective the following steps were followed:

(1) a porous biocatalyst model was developed and solved numerically (by method of lines), with and without consideration of oxygen limitation.
(2) model parameters were determined from the literature, estimates, or experiments.
(3) biodegradation kinetic parameters for 2-chlorophenol (2-CP) were determined in shake flasks and batch reactors using a pure culture (*Pseudomonas pickettii*) derived from activated sludge [Fava et al. (1995)].
(4) a model soil (from Pequest, NJ) was chosen, and sorption parameters determined for 2-CP.
(5) a laboratory soil column was constructed and axial dispersion determined.
(6) the column was seeded with *P. pickettii*, and the concentration profiles determined for different feed rates of 2-CP.
(7) the experimental results were compared to the model predictions.

CHAPTER 4

MATERIALS AND EXPERIMENTAL METHODS

4.1 Materials

4.1.1 Chemicals

2-Chlorophenol (2-CP) was purchased from Sigma Chemical Company, St. Louis, MO. A 2000 mg/L stock solution of 2-CP was prepared in DI water, and stored at 4 °C. Methanol and acetic acids used for HPLC analysis were ACS certified and obtained from Fisher Scientific, Fair Lawn, NJ. Nutrient broth (BBL-11479) was purchased from Becton Dickinson and Co., Cockeysville, MD, and nutrient agar (Model# 001-01-8) from Difco Laboratory, Detroit, MI.

A list of the chemicals used for the preparation of the synthetic inorganic medium is given in Table 4.1. Mercuric chloride (#M159-100) and sodium chloride (# S671-500) were purchased from Fisher Scientific Company, Fair Lawn, NJ.

Table 4.1 Chemicals used for preparing growth medium in DI water.

Components	Concentration (g/L)	Source and Grade
Potassium Phosphate, Dibasic K_2HPO_4	5.802	Fisher Scientific, ACS Certified, Fair Lawn, NJ
Potassium Phosphate, Monobasic KH_2PO_4	2.268	Fisher Scientific, ACS Certified, Fair Lawn, NJ
Ammonium Sulfate $(NH_4)_2(SO_4)$	0.50	Fisher Scientific, ACS Certified, Fair Lawn, NJ
Magnesium Sulfate, Heptahydrate $MgSO_4$	0.10	Aldrich, ACS Reagent
Manganous Sulfate, Monohydrate $MnSO_4$	0.001	Baker, Baker analyzed Reagent
Ferrous Sulfate, $FeSO_4$*	0.50 mg/L	Fisher Scientific, ACS Certified Fair Lawn, NJ

*$FeSO_4$ was not added if tap water was used instead of DI water for medium preparation

The test soil was obtained from a site in Pequest, NJ. The composition is given in Table 4.2. This soil was used for all the soil-related experiments.

Table 4.2 Soil characteristics.

Constituents	This Study Pequest, NJ (PNJ)	USEPA ("Standard" Soil)	Eurosoil, #3
Sand	44%	60%	47%
Silt	44%	28%	36%
Clay	12%	12%	17%
Total Organic Carbon	2.1%	3.2%	3.7%
pH	5.2	8.5	5.3

4.1.2 Preparation of Synthetic Growth Medium and Nutrient Broth

The synthetic inorganic growth medium was prepared by adding the appropriate amounts of different chemicals as listed in Table 4.1 in deionized (DI) water. The medium was sterilized by autoclaving at 121°C for about 2 hours. The pH of the medium was 7.15-7.2. In order to maintain pH, a buffer of 5% potassium dihydrogen phosphate was added when necessary.

Nutrient broth was prepared (as instructed on the container label) by adding 4g of "BBL nutrient powder" to 0.5L of DI water, which was then autoclaved at 121 °C for about 2 hours. This solution was then stored in a refrigerator and used whenever necessary for the purpose of reviving frozen cultures. Also, nutrient agar was prepared occasionally for the purpose of checking the purity of the cultures.

4.2 Preparation of Pure Microbial Culture and Acclimation to 2-CP

While consortia of mixed microbial species are the norm in nature, it is difficult to obtain consistent results in the laboratory using mixed cultures, since the relative microbial composition can change with time. As a result, a pure culture capable of degrading 2-CP was isolated from the mixed liquor of the Passaic Valley Sewerage Commissioners (PVSC) Treatment Plant in Newark, NJ. This isolation had been accomplished previously by Dr. Fava (visiting NJIT from the University of Bologna). The culture was identified as *Pseudomonas pickettii*. Stocks of this culture (as a suspension in a sealed tube) were frozen and used subsequently as needed.

The pure culture of *Pseudomonas pickettii* was reconstituted by growing in a nutrient broth according to the following procedure. About 10 mL of the nutrient broth was inoculated and placed in an incubator at 29 °C. After about 2 days, the culture indicated signs of growth by becoming turbid. About 2-3 mL of that suspension was transferred into 100 mL of the synthetic growth medium in a 250 mL flask. A specific amount of 2000 ppm 2-CP stock solution (roughly enough to attain a final concentration of 5 ppm) was added to the flask in order to acclimate the cultures to 2-CP as sole carbon source. The flask was stoppered with a cotton plug and placed in an incubator shaker (New Brunswick Scientific Co.), which was set at 200 rpm and 26~29 °C. Air entered through the cotton plug by shaking, and the headspace in the flask thus served as an oxygen supply zone. When the 2-CP was depleted, again a small portion (~2-3 mL) was transferred to 100 mL fresh inorganic medium, and the entire process repeated to obtain secondary, and then tertiary, cultures. The tertiary culture was used for all subsequent

biodegradation experiments. This culture was also stored in a refrigerator and kept active by periodic additions of 2-CP stock solution and fresh growth medium. Stocks of the primary, secondary, and tertiary cultures were also streaked on agar plates, and stored frozen for potential future use.

4.3 Experimental Set Up

4.3.1 Shake Flasks

Most of the initial kinetic experiments were performed in shake flasks. This simple setup (given in Figure 4.1) typically consisted of one to three 250 mL glass Erlenmeyer flasks, stoppered with cotton plugs, and placed in an incubator/shaker apparatus (Series 25, New Brunswick Scientific Co.) at 200 rpm and 26-29 °C. Seed cultures needed for initiating other experiments were also grown in this type of apparatus. During kinetic experiments, samples were taken (e.g. at an interval of 10 to 15 min) by opening the cotton plug momentarily and inserting a pipette (P-5000, Rainin Instrument Co.) fitted with a disposable microliter pipette tip (C-5000, Rainin Instrument Co.).

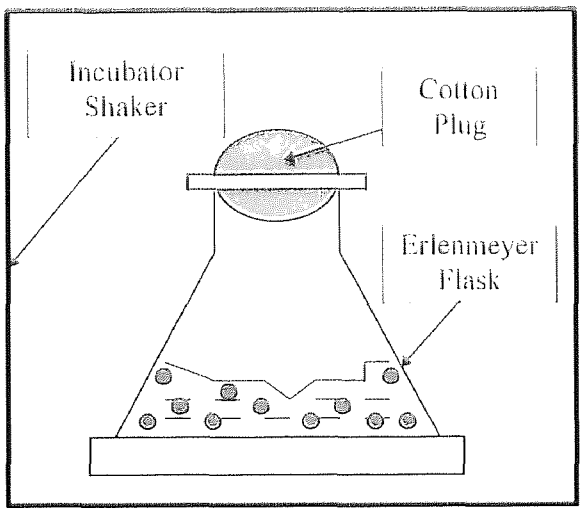

Figure 4.1 Schematic of the shake flask reactor.

4.3.2 Batch Reactor

Having performed some preliminary kinetic experiments it was observed that there were difficulties in obtaining consistent results in the shake flasks. These are discussed in the Results and Discussion section. In order to avoid those observed discrepancies, it then was decided to use a larger reactor with improved control. This 4.5-liter jacketed reactor was custom-designed at NJIT using 13.7 cm ID (6" OD) Lucite tubing obtained from Grewe Plastic Inc., Newark, N.J.

The temperature of the reactor contents was controlled by a water jacket surrounding the exterior of the reactor. The water-bath and temperature controller was a Neslabs Endocal RTE-8 system. The water-bath temperature was typically set at 28 °C to 29 °C.

A schematic diagram is shown in Figure 4.2. Two air dispersion tubes (Pyrex brand-coarse) were fitted through two of the lid ports. Aeration was provided by a small Dynatomic air bladder pump, and also by laboratory-based compressed air lines through glass tubes with fritted ends. Flowmeters (Cole-Parmer Instrument Co.) were placed in-line to maintain control of the air flow rates. Also included was an in-line air filter (Nalgene Co.).

Other lid ports were used to insert a probe (New Brunswick Scientific Co., 900 Series) for measuring dissolved oxygen, a thermometer, and a vent line. Sampling was accomplished at a regular interval of 10 to 15 min, by opening the seal of one port (which was kept covered at all other times) and inserting a 5000 microliter pipette fitted with a disposable microliter pipette tip. For the kinetic experiments, the reaction volume was

maintained at 1.5-2L in most cases. Contents inside the reactor were continuously stirred using a teflon coated magnetic bar (Fisher Scientific Co.). Finally, special attention was given to cleaning and sterilizing the reactor and all probes.

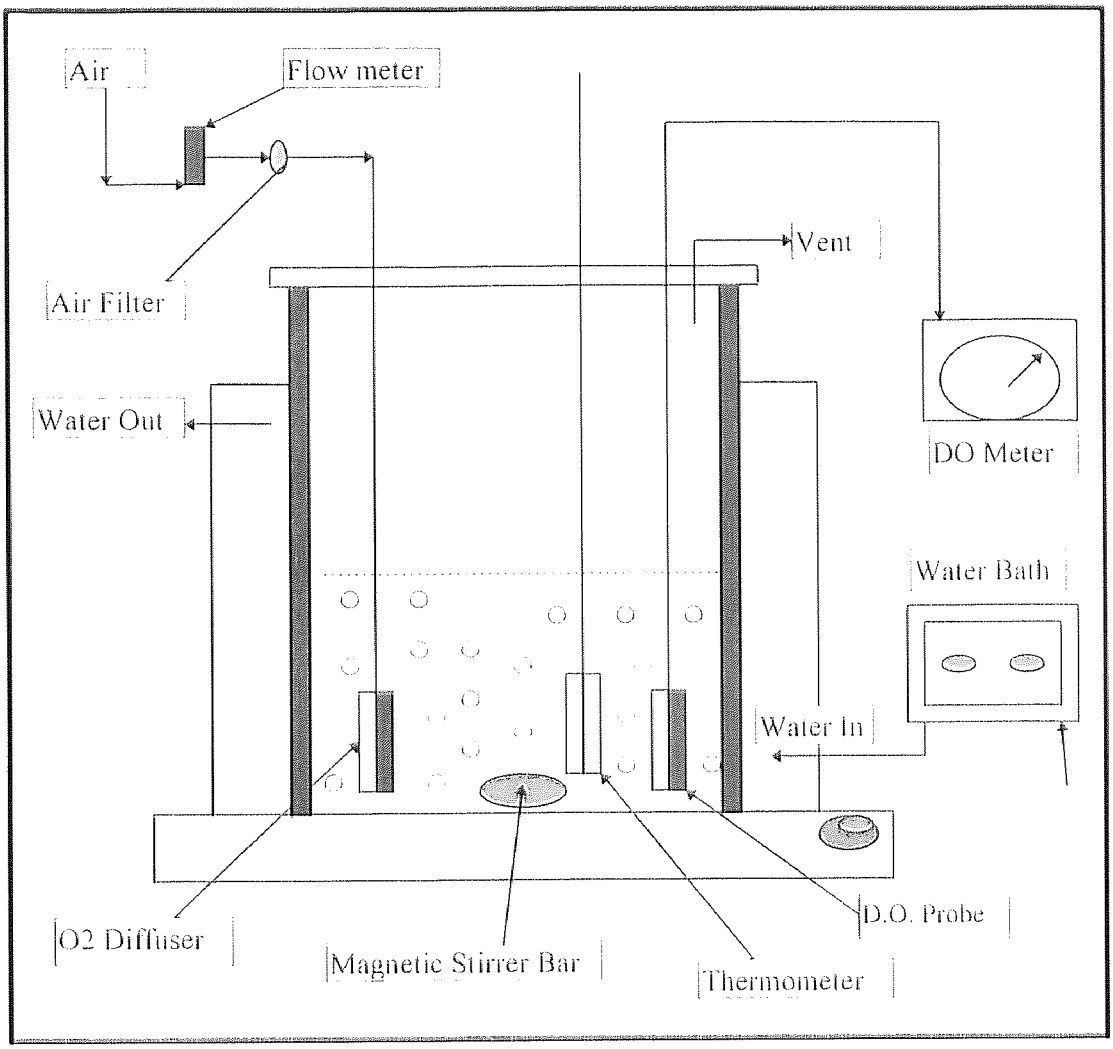

Figure 4.2 Schematic of the batch reactor used for kinetic experiments.

4.3.3 Soil Column Reactor

A schematic of the apparatus used in the soil column studies is presented in Figure 4.3. The two identical columns used in this study were custom-made and purchased from Ace

Glass, Vineland, NJ. They were 24 cm long, heavy-walled, glass process pipe, with a 5 cm inside diameter. There were 5 sampling ports along the height of each column, located at 2, 7, 12, 17, and 22 cm from the base of the column. Two thick polymeric end plates, machined to the same inside diameter of the column, were tightly connected to each end of the column using a rubber o-ring and teflon tape. Both of these end-plates were equipped with a flow channel of about 5 mm in diameter.

A stainless steel screen (fine mesh) was placed at the bottom of the column. A thin layer of glass beads of 3 mm diameter (Fisher Scientific Co.) was placed on top of that screen to prevent fine particles from clogging the inlet port. This bottom layer of glass beads also served to provide a mixing zone to distribute the inlet flow uniformly across the column cross-section. Successive layers of soil (previously sieved through 2 mm mesh and air dried) were added to the column and tapped evenly with the edge of a rectangular bar. This tapping process was accomplished with water in the column to prevent air from being trapped in the soil interstices. This packing continued until the height of the first sampling port (which is located at 2 cm), where a thin layer of glass beads was placed to facilitate sampling via syringes inserted through the sampling port septa. This layer of glass beads also acted as an internal redistributor to help maintain uniform flow and eliminate channeling.

This whole process of soil addition and tapping was repeated several times until the top of the column was reached. The final layer on top was glass beads covered by a fine 1 mm plastic mesh. Another end-plate was tightly connected to the top end of the column. It is to be noted that soil used for packing was always autoclaved twice (for

about 2 hours each time at 121 °C) to make sure it was thoroughly sterilized prior to packing. In a similar way, all other autoclavable portions of the setup were sterilized, and throughout the experiments careful attention was paid to system sterility.

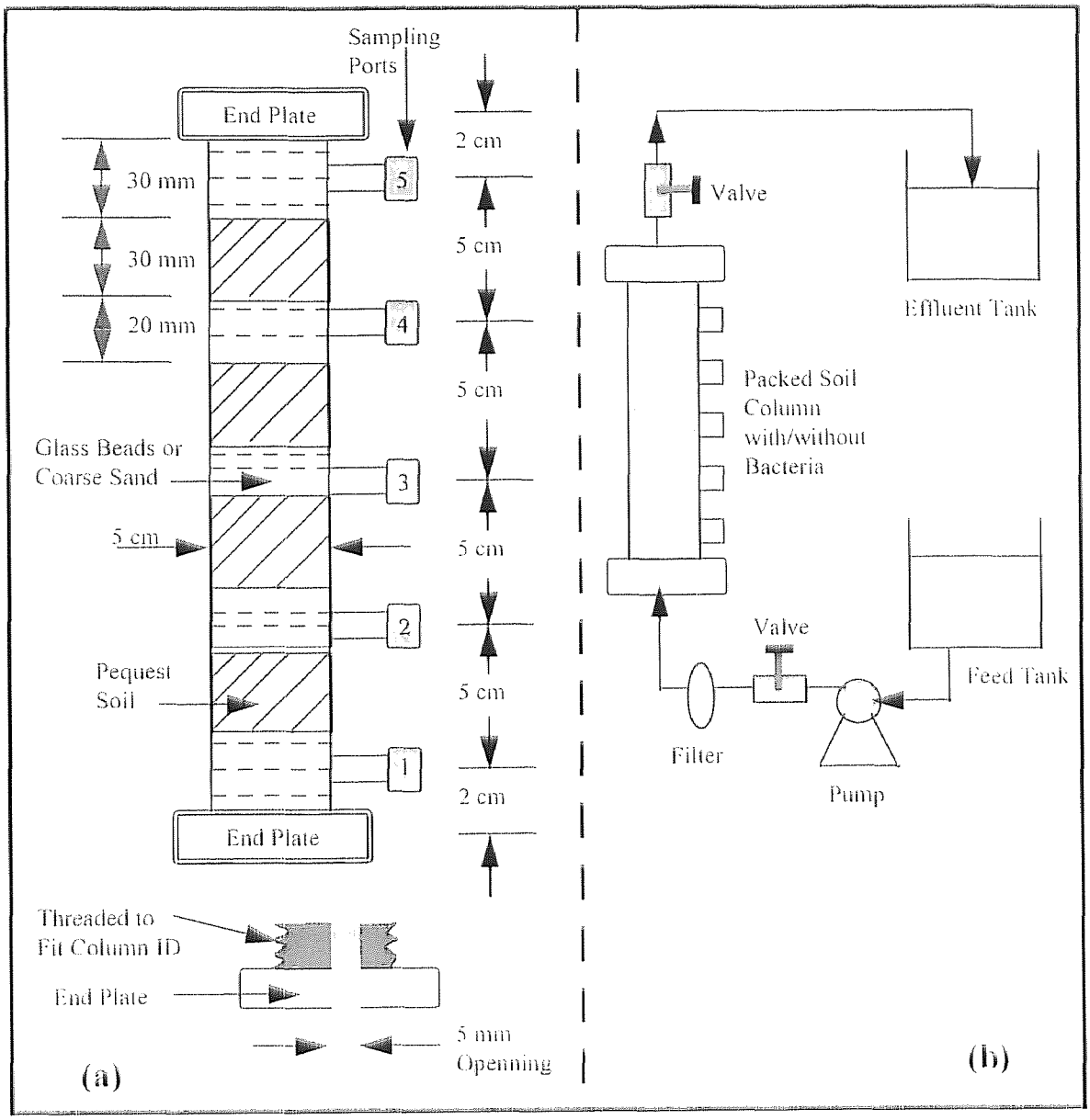

Figure 4.3 Schematic of the apparatus used in soil column studies: (a) column details and (b) experimental set-up.

4.4 Analytical Procedures

4.4.1 2-Chlorophenol (2-CP)

Concentrations of 2-CP were measured using a Waters HPLC (Millipore, Milford, MA), equipped with: (1) Tunable Absorbance Detector (Model# 484); (2) System Controller (Model# 600E); (3) Multisolvent Delivery System (Model# 600); and (4) Ultra WISP Sample Processor (Model# 715). In some cases, a rough estimate of 2-CP concentration was obtained by UV-scanning in a spectrophotometer (Varian DMS-200).

Sample preparation proceeded as follows. About 4 mL liquid sample was collected using either an adjustable micropipette (Pipetman® # P-5000, Rainin Instrument Co.) or disposable syringes (B-D®). To that collected sample one drop of 6M HCl was added, not only to kill the active microorganisms, but also to maintain 2-CP in its non-ionized form. The solution was then filtered through 0.2 μm Nylaflo membrane filter (Gelman Sciences Inc.). Most samples were analyzed immediately, but a few samples (collected from soil column runs) were analyzed after about 12 hours. During this period, samples were stored frozen.

In order to have a quantitative estimate of the variability in concentration measurement at different times, three sample vials were prepared from one original solution. Vial #1 was stored in the freezer, vial #2 was stored in the refrigerator, and vial #3 was analyzed immediately using the protocol described later (at room temperature of 20 °C). Vials #1 and #2 were analyzed after 48 hours and 24 hours, respectively. The measured concentrations were almost the same in all three cases, with very little variation (e.g., vial #1: 10.23 ppm; vial #2: 10.17 ppm; and vial #3: 10.28 ppm).

Isocratic elution of 2-CP was obtained by a mobile phase consisting of 55% methanol and 45% water (Milli-Q Ultrapure). Both methanol and water were vacuum filtered through a 0.45 μm membrane filter and preserved by adding 1% acetic acid. The solutions were then degassed by a continuous helium purge (Ultra High Purity, Matheson gas Products). The flow rate of the mobile phase was maintained at 1 mL/min. The UV-detector was set at a wavelength of 280 nm. The chromatographic column was a 25x4 cm Licrosphere 60® RP-Select B (EM Separations, Gibstown, NJ). The retention time of 2-CP was approximately 3.5 min, but it was observed to fluctuate with varying room temperature. The data were processed and integrated by Nelson Chromatography Software (PE Nelson Model 2600, rev. 5.10) using a Nelson 900 Series interface. A calibration curve (given in Figure C-1 in Appendix C) was generated by 5 known standard 2-CP solutions, and checked periodically.

4.4.2 Biomass

The concentration of microorganisms (or biomass) in suspended growth was determined by optical density (OD). The optical density of the suspension was measured by a UV-Visible spectrophotometer (Varian DMS 200) at a wavelength of 540 nm using DI-water as reference. About 2.5~3 mL sample was placed in a 1x1 cm quartz cuvette. A detailed study of OD calibration was conducted by Dikshitulu (1993) using *Pseudomas sp.* He showed that there is a linear relationship between optical density and biomass concentration up to an OD value of 0.6. In our study, the OD was always below 0.6. At high biomass concentrations (above 300 mg/L), individual organisms combine to form

visible flocs, which have a much lower optical density than the mass concentration would indicate. With an assumption of similar size, shape, and light absorbing behavior of the *Pseudomas sp.* of this study and that of Dikshitulu (1993), the same linear relationship of 273 g/m^3 biomass per unit optical density was used for our calculations (see Figure C-3 in Appendix C).

4.4.3 Chloride

The concentration of chloride ions was measured using an IonPlus Chloride Electrode (Model 96-17B, Orion Research Inc., Boston, MA) with an Ion Specific Chloride Meter (Model SA 720, Orion Research Inc., Boston, MA). The meter readings were given in millivolts (mV) and these were then converted to the desired concentrations in ppm with the help of calibration curves. The calibration curves were generated according to the procedure specified by the manufacturer for low-level measurements (below 30 ppm chloride ion concentration). A standard chloride ion solution was prepared by adding 1 gm of sodium chloride to 1 liter of Milli-Q deionized water to obtain a final chloride concentration of 607 ppm (or 1000 ppm NaCl). A low-level ionic strength adjuster (ISA), 1.0 % $NaNO_3$, was prepared by adding 80 mL of DI water to 20 mL of ISA (Orion Cat. No. 940011, 5.0 % $NaNO_3$). Calibration was accomplished as follows. To 100 mL of distilled water in a 150 mL beaker, 1 mL of low-level ISA solution was added. The solution was stirred thoroughly and the electrode was then placed into the beaker. To the resulting solution, increments of the standard solution were added in the sequence of 0.1, 0.1, 0.2, 0.2, 0.4, 2.0, and 2.0 mL. After each addition, the solution was stirred and a

stable millivolt reading was recorded (about 3-4 mins was needed for stable reading). The chloride ion concentration after each addition was 0.6, 1.2, 2.4, 3.6, 6.0, 17.5, and 28.6 ppm, respectively. A typical calibration curve of concentration (log scale) versus mV (linear axis) was plotted, as shown in Figure C-2 in Appendix C.

4.4.4 pH

pH was measured using a combination pH electrode (Model 91-56, Orion Research Inc., Boston, MA) with an Expandable Ion Analyzer (Model EA 920, Orion Research Inc., Boston, MA). Typically, the electrode was dipped into a vial of about 4~5 mL solution, and after stabilization the pH was read. It is to be noted that the presence of foreign particles in the solution appeared to cause fluctuations in the pH measurement. The meter was calibrated periodically using standard buffer solutions at two different pHs (4.0 and 7.0).

4.5 Experimental Procedures

4.5.1 Biodegradation Kinetics of 2-Chlorophenol

The kinetics of 2-CP biodegradation by *Pseudomonas pickettii* were studied in detail in both shake flask and jacketed batch reactors. Experimental procedures for each type of reactor are given separately as follows.

4.5.1.1 In Shake Flask: Shake flask experiments served many purposes, from growing cultures (i.e. acclimation) to kinetic parameter evaluation. For a kinetic experiment, the

culture-growing steps were the same as described in Section 4.2. Similar preparative steps for the kinetic experiments (as described in detail in Section 4.5.1.2) were employed in shake flasks as well. To obtain an estimate of specific growth rate parameters, many shake flask experiments were conducted using different initial 2-CP concentrations. Samples were periodically obtained and quantified analytically for biomass (via OD) and 2-CP.

It was observed that the shake flask experiments suffered from some important flaws: (1) even though the temperature of the incubator shaker was set at 26 °C, it was still found to vary by ±4 °C; (2) oxygen might have been a limiting factor in biomass growth; (3) the smaller working volume created sampling problems toward the end of the reaction. These factors were minimized by using a larger batch reactor with better control of the system.

4.5.1.2 In Batch Reactor: A jacketed batch reactor helped eliminate the problems in shake flask experiments mentioned earlier. In spite of a wide room temperature variation (15-28 °C), the jacketed batch reactor was maintained at 28±1 °C. In addition, it was possible to provide positive oxygen control, as described in section 4.3.2.

To begin any kinetic experiment, the reactor and other accessories were cleaned using either a dilute solution of hydrogen peroxide, or a 60% methanol solution, which was followed by a thorough washing using sterilized DI water. Any autoclavable materials or solutions were always sterilized prior to use. Experiments were started from a pure culture grown earlier on nutrient broth, followed by acclimation of the pure culture

to 2-CP (as described in section 4.2). This acclimation procedure generally started with a low concentration (~5 ppm) of 2-CP, and ultimately reached about 120 ppm.

For the kinetic experiments, about 1.5L growth medium was placed in the reactor, with constant stirring and a flow of constant temperature water through the outer jacket. 2-CP stock solution was added to attain a desired initial working concentration (5 to 100 ppm). Aeration was started, and once a constant temperature of 28 °C was attained, the acclimated inoculum was added. It was decided to start with a low biomass concentration (about 12-14 ppm), which in turn, produced an extended exponential growth phase, and thereby facilitated kinetics determination.

During these experiments, the pH of the reaction mixture decreased slightly from 7.2 to 7.1, and in few cases to 7.0. Samples of about 5 mL were collected periodically and analyzed for 2-CP and biomass concentrations. During some experiments, the consumption pattern of dissolved oxygen uptake was measured using a DO probe. Typically for a kinetic run, the reactor solution was initially about 96-100% saturated with oxygen, and it stayed at that value for about 30-60 mins (lag phase). After that, the % saturation started to fall (exponential phase) to about 75-80, and then went back up to the initial level (stationary phase). In a few cases, the reactor culture was sampled and streaked on an agar plate to check for purity. Biomass growth along the wall of the reactor was never observed. However, during experiments with 100 ppm 2-CP (which took almost 6-8 hours), some growth on the edges of the oxygen diffuser was noticed toward the end.

4.5.2 Soil Column Bioreactor with Continuous Feed

The preparative technique of a soil-column bioreactor has been discussed in detail earlier in Section 4.3.3. A simple schematic is shown in Figure 4.3. To consistently pack and seed such a reactor turned out to be a very complicated task. Many trials were made before obtaining consistent results

Trial#1: A fresh growth medium was simultaneously prepared, sterilized, and 2-CP stock solution was added to obtain a concentration of about 6 mg/L. Then, initial acclimation and growth of the pure culture were accomplished in a batch reactor as described before. The contents of the batch reactor were continuously fed upflow to the soil column at 1.1 mL/min using a Digital Cartridge Pump (Masterfelx® 7519-10, Pump with Digital Console Drive, Cole Parmer) through Masterflex® tubing (Model 6426-13, Cole Parmer). Optical density measurement of samples from the outlet of the column did not indicate any significant loss of biomass. After about 4 hours, the column was inverted and the feeding process was repeated for about 4 more hours.

Once the seeding process was completed, a feed solution containing 34 mg/L 2-CP was fed continuously through the bottom of the column in an upflow manner. The feed solution also contained $CaCl_2$ (about 2~3 mM) to keep the soil intact (otherwise the soil starts to disintegrate and fines exit the top of the column). Samples were collected from the middle and exit of the column. However, it was found that biodegradation was primarily occurring at the inlet zone of the column. This was perhaps due to the way the column was seeded, so a different approach was undertaken next.

Trial#2: Preparative methods for feed solution, growth medium, and 2-CP degrading culture were the same as that of Trial#1. However, instead of preparing the soil column first and then feeding organisms and growth medium, the soil was first contacted with seed organisms in growth medium, and then the column was packed. This ensured a uniform distribution of organisms throughout the column. Furthermore, after packing, growth medium containing 2-CP was injected through each port (0.5 mL over the first 2.5-3 hours) in order to further encourage more uniform growth.

Then the feed was introduced as before in an upflow fashion (first passing through a Nylaflo membrane filter). Samples were collected from the middle-port and exit of the column initially, and then only from the exit. Samples were also collected periodically from the feed container. These experiments lasted for about five to six days.

A number of problems were encountered in column packing and obtaining consistent results. Ultimately two successful biodegradation runs were made on one packed column. A separate set of experiments was also performed without any biomass present on another column, as a control. In this control experiment, the sterilized feed contained about 200 ppm mercuric chloride and 4 mM $CaCl_2$ to maintain sterility and soil integrity, respectively. NaCl tracer runs, and the calculated dispersivities, were nearly the same for both columns. Results are discussed in Chapter 6.

4.5.3 Axial Dispersion Measurements in Soil Column

Axial dispersion within the soil column was experimentally obtained using chloride ion (NaCl) tracer. The column was initially flushed for about 12 hrs with Milli-Q deionized

water at a flow rate of 1.1 mL/min, in order to minimize background chloride ion concentration and establish a uniform flow distribution throughout the entire cross section of the column. A pulse of 0.2 mL of 2000 ppm NaCl was injected into the column through port 1. A sample volume of 3 mL was collected at 10 minute intervals in a clean 10 cc vial from the column exit. To that sample, 1 drop of low-level ISA (ionic strength adjuster, i.e. 1% $NaNO_3$ solution) was added, stirred, and then the chloride electrode was placed inside to obtain a mV reading. Each experiment required up to 7.5 hrs. Results are given and discussed in Chapter 6.

4.5.4 Porosity in the Soil Column

The column and soil used for measuring the total porosity of the bed was the same as described in section 4.3.3, except that the amount of water added during packing was accurately measured. The system was then allowed to equilibrate, and water was added or subtracted so that the liquid and soil levels were identical. Porosity was obtained by dividing the volume of water added to the soil column by the volume of the empty column. This procedure was repeated. The average porosity was 0.42 (±0.009), and this assumed to be the value of ε_b. It is very difficult to distinguish between ε_a and ε_b. As a result, ε_a was estimated [Hausenbuiller (1978), and Hutzler et al. (1986)], while ε_b was considered to be the measured value.

4.5.5 Soil Density

A 50 mL graduated cylinder was cleaned, dried, and weighed. Soil (as received and sieved through 2 mm mesh screen) was placed inside and packed incrementally almost the same way as column packing without any water. Packing was done up to a volume of 40 mL and weighed. Soil density was obtained by dividing the weight of the soil by 40 mL. This procedure was repeated two more times. The average soil density was found to be 1.70 mg/L (±0.019).

4.6 Adsorption Experiments

4.6.1 Adsorption Kinetics

The soil preparation, equipment preparation, solution preparation, and sterilization procedure were the same as mentioned in Section 4.6.2. Out of 13 serum bottles prepared, 10 were for the adsorption measurements and 3 were for controls. To about 25±0.04 g of soil, 75 mL (14.7 ppm 2-CP) of aqueous solution were quickly added. The bottles were then sealed and placed in a shaker at 200 rpm. After 10 mins, the first bottle was removed from the shaker and a 5 mL sample was taken with a syringe. It was immediately filtered and analyzed in duplicate by HPLC. The remaining bottles were each sampled periodically (e.g. second one was removed after 30 min, third one after 45 min, fourth one after 60 min, etc.). With each adsorption sample, one control sample was always analyzed. This whole set of adsorption rate experiments was repeated at a 2-CP concentration of 21.8 ppm. Results are discussed in Chapter 6.

4.6.2 Batch Equilibrium Isotherm

Adsorption of 2-CP was measured at room temperature, which varied from 16.3 to 20 °C. Pequest soil (PNJ) was air dried and then sieved through a 2 mm mesh screen. The soil was further dried in an oven at 105 °C for about 24 hours. Of ten 125 mL serum bottles, one was a control and the remaining nine contained 2-CP concentrations of 9.8, 12.5, 15.3, 20.0, 30.6, 40.3, 47.4, 59.0, 60.2 mg/L. About 75 mL of 2-CP solution and 25±0.04 gm of soil were used in each case. The bulk phase also contained 3 mM $CaCl_2$, which helped prevent desegregation of clays and maintained the integrity of the soil, as before. All the serum bottles, septa, aqueous solutions, and soils were sterilized prior to their use. After preparation, the serum bottles were sealed with septa and crimptops and placed in a shaker for about 48 hours to reach equilibrium, then removed, and allowed to settle. Two samples of supernatant were taken from each bottle and filtered. Filtrates were immediately analyzed in duplicate by HPLC. Results are given in Chapter 6.

CHAPTER 5

MATHEMATICAL MODEL FORMULATION

5.1 Model Development without Oxygen Limitation

This model was developed for biodegradation in the saturated zone (i.e. below the water table). Conceptually, it's analogous to that used in chemical engineering practice to model the dynamic behavior of a packed bed of porous catalyst particles. In the present case, the column is horizontal rather than vertical, and the "catalyst" particles are considered to be soil agglomerates, in which the diameter of individual soil particles is much less than that of the aggregates. Thus while most of the biomass is probably attached to individual soil particles, it is assumed to be relatively evenly distributed throughout the aggregate. The fluid within the aggregates is assumed to be stagnant, and the concentration profiles are a function of radial diffusion, biodegradation, and sorption processes.

Groundwater is moving around and between the aggregates. The groundwater, or "mobile phase", concentration profiles in the direction of flow are a function of axial diffusion, convective transport, and mass transfer from the aggregates. A schematic diagram of the aggregate and mobile phases is given in Figure 5.1.

5.1.1 Model Description

The present model differs from existing ones in two important ways:

- coupling of non-equilibrium sorption with mass transfer, and
- biomass growth, with inhibitory kinetics

both of which are very important to real in-situ situations.

In developing the resulting equations, the following assumptions were made:

1. Biomass is assumed to be uniformly distributed inside each aggregate.

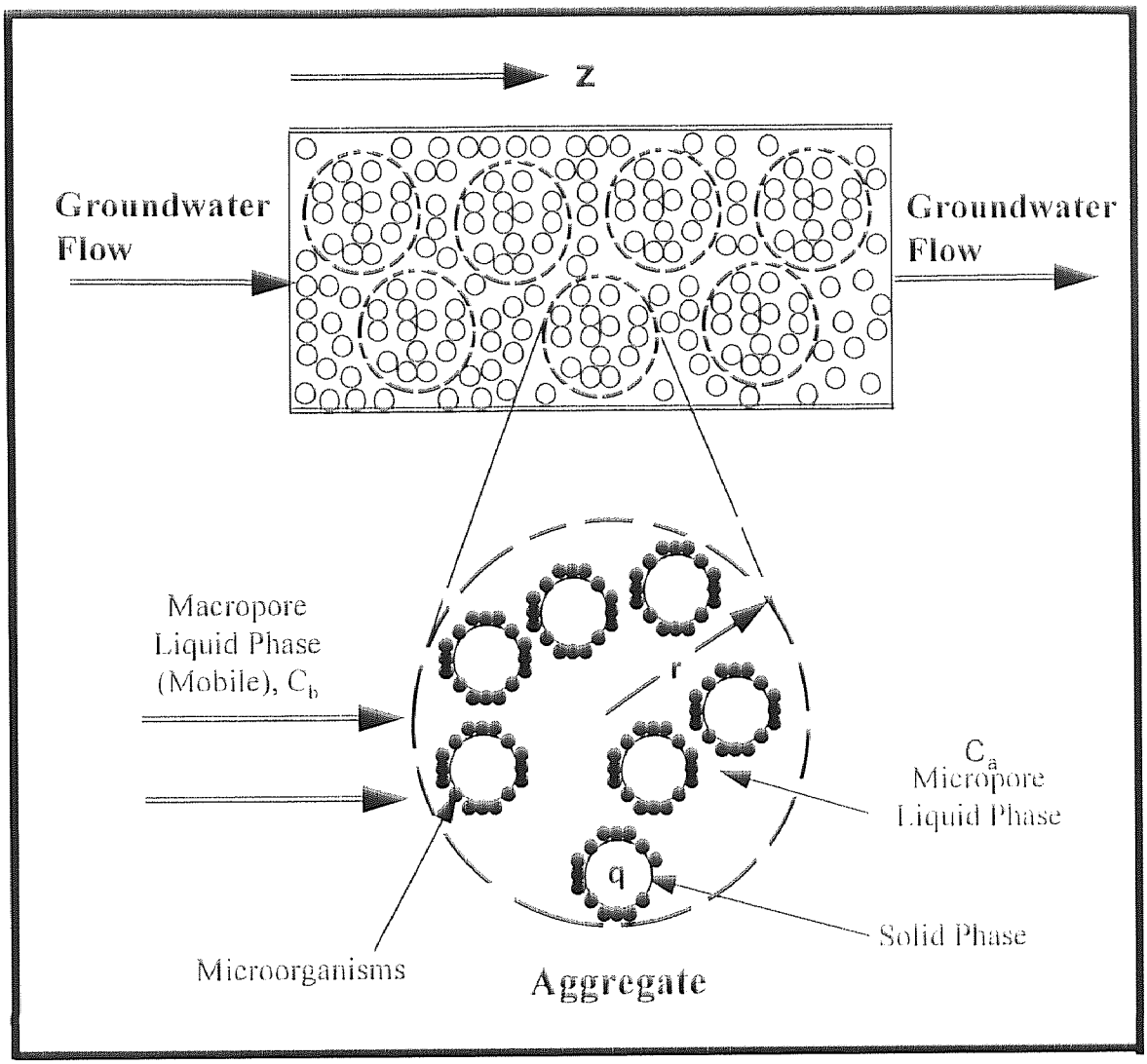

Figure 5.1 Schematic of the soil column bioreactor.

2. Biodegradation occurs in the aggregates only (i.e. there is a negligible amount of suspended biomass in the mobile phase).
3. Oxygen limitation is not accounted for.
4. The organic pollutant is the only significant carbon source.
5. The specific growth rate could be described by an inhibitory biokinetic model (e.g. Andrews model).
6. Plug-flow with axial dispersion in the mobile phase is assumed.
7. Chemotaxis is assumed to be negligible.
8. Temperature variation is not considered.
9. End effects are neglected.
10. Mass transfer within the particles is assumed to be governed only by Fick's law-type diffusion, with effective diffusion coefficients that are constant over the entire particle radius.
11. The groundwater flow rate is assumed constant.
12. Mass transfer between the bulk phase and surface of the particle is described by an external film coefficient.

5.1.1.1 Aggregate Phase: The material balance of the biodegradable component in a differential segment of the spherical aggregates is represented by the following equation:

$$\frac{\partial C_a}{\partial t} = \frac{D_{se}}{r^2}\left[\frac{\partial}{\partial r}\left(r^2 \frac{\partial C_a}{\partial r}\right)\right] - B_d - A_d \qquad (5.1)$$

The first term on the right describes the intra-aggregate diffusion, the second term represents the rate of biodegradation, and the third term is the sorption rate. The

biodegradation rate (B_d), and the associated biomass growth rate, are given by equations (5.2) and (5.3) respectively:

$$B_d = \frac{b}{Y}\left(\frac{\hat{\mu}C_a}{K_S + C_a + \frac{C_a^2}{K_i}}\right) \tag{5.2}$$

$$\frac{\partial b}{\partial t} = \left(\frac{\hat{\mu}C_a}{K_S + C_a + \frac{C_a^2}{K_i}}\right)\cdot b - \left(\hat{\mu}_c\right)\cdot b \tag{5.3}$$

The rate of sorption (A_d) is given by equation (5.4).

$$A_d = k_d\left(C_a - C_a^*\right) \tag{5.4}$$

The solid phase concentration (q) in equilibrium with C_a^* is given by:

$$q = k_p \cdot \left(C_a^*\right)^{\frac{1}{n}} \tag{5.5}$$

and the rate of change in solid phase concentration is:

$$\frac{\partial q}{\partial t} = \frac{\varepsilon_a}{(1-\varepsilon_a)\cdot\rho_S}\cdot k_d \cdot \left(C_a - C_a^*\right) = \frac{\varepsilon_a}{\left(1-\varepsilon_a\right)\cdot\rho_S}\cdot A_d \tag{5.6}$$

Initial conditions:

(i) t=0 $C_a = C_{a0}$ (r,z,0) (5.7)

$q = q_0$ (r,z,0) (5.8)

$b = b_0$ (r,z,0) (5.9)

Boundary conditions:

@ r=0 C_a = finite (5.10)

or $\frac{\partial C_a}{\partial r} = 0$ (symmetry) (5.10a)

@ r= R $-D_{se}\frac{\partial C_a}{\partial r} = k_m\left(C_a - C_b\right)$ (mass transfer to mobile phase) (5.10b)

5.1.1.2 Mobile Phase

$$\varepsilon_b \cdot \frac{\partial C_b}{\partial t} = \varepsilon_b \cdot D_{le}\frac{\partial^2 C_b}{\partial z^2} - \varepsilon_b \cdot \bar{v}_z \cdot \frac{\partial C_b}{\partial z} - R_m \quad (5.10c)$$

The first term on the right corresponds to axial diffusion, the second term describes convection, and the third term describes mass transfer from the mobile phase. R_m (i.e. the rate of mass transfer of the pollutant from the groundwater to the surface of the soil aggregates) is given by:

$$R_m = k_m \cdot a_m \cdot (1-\varepsilon_b) \cdot \left[C_b - C_a\Big|_{r=R} \right] \quad (5.10d)$$

Substituting R_m in equation (5.10c) and rearranging:

$$\frac{\partial C_b}{\partial t} = D_{le}\frac{\partial^2 C_b}{\partial z^2} - \bar{v}_z\frac{\partial C_b}{\partial z} + k_m \cdot \frac{3}{R} \cdot \frac{1-\varepsilon_b}{\varepsilon_b} \cdot \left[C_a\Big|_{r=R} - C_b \right] \quad (5.11)$$

Initial condition:

@ t=0 $C_b = C_{b0}$ (r,z,0) (5.12)

Boundary conditions:

$$@\ z=0 \qquad -D_{le}\frac{\partial C_b}{\partial z} + \bar{v}_z C_b = \bar{v}_z C_{z_0} \tag{5.13}$$

In the case of an "old" spill, in which clean water flows toward the contaminant zone, $C_{Z_0}=0$. In the case of a "new" spill, in which a reservoir of contamination is brought into a previously clean zone, C_{Z_0} = constant (non-zero).

$$@\ z=L \qquad C_b = C_{bL} \text{ (acceptable environmental limit)} \tag{5.14}$$

$$\text{or } \frac{\partial C_b}{\partial z} = 0 \text{ (flux is zero)} \tag{5.15}$$

A detailed discussion of these boundary conditions is given in Appendix A.

5.1.2 Dimensionless Forms

To facilitate the solution methodology these equations were converted to dimensionless form as follows:

5.1.2.1. Aggregate Phase

Dimensionless groups:

$$\gamma_a = \frac{C_a}{K_s} \qquad \text{pollutant concentration} \tag{5.16}$$

$$\gamma_s = \frac{\rho_s}{K_s}\cdot q \qquad \text{solid phase concentration} \tag{5.17}$$

$$\theta = \frac{D_{se}}{R^2}\cdot t \qquad \text{time} \tag{5.18}$$

$$\eta = \frac{r}{R} \qquad \text{radial distance} \tag{5.19}$$

$$\beta = \frac{b}{K_s} \qquad \text{biomass concentration} \tag{5.19a}$$

Dimensionless equations:

$$\frac{\partial \gamma_a}{\partial \theta} = \frac{1}{\eta^2}\left[\frac{\partial}{\partial \eta}\left(\eta^2 \frac{\partial \gamma_a}{\partial \eta}\right)\right] - B_d \cdot \frac{R^2}{D_{se} K_s} - A_d \cdot \frac{R^2}{D_{se} K_s} \tag{5.20}$$

$$A_d \cdot \frac{R^2}{D_{se}\, K_s} = \Phi_a \left(\gamma_a - \gamma_a^*\right) \tag{5.21}$$

$$\gamma_a^* = \frac{K_s^{n-1}}{k_p^n \rho_s^n} (\gamma_s)^n \tag{5.22}$$

alternatively, γ_a^* can also be written as, $\gamma_a^* = \left(\frac{K_s^{1-\frac{1}{n}}}{k_p \rho_s} \cdot\right)^n \cdot \gamma_s^n$ (5.22a)

$$\frac{\partial \gamma_s}{\partial \theta} = \frac{\varepsilon_a}{(1-\varepsilon_a)} \cdot \Phi_a \cdot \left(\gamma_a - \gamma_a^*\right) = \frac{\varepsilon_a}{(1-\varepsilon_a)} \cdot \left(A_d \cdot \frac{R^2}{D_{se}\, K_s}\right) \tag{5.23}$$

$$B_d \cdot \frac{R^2}{D_{se} K_s} = \Phi_b \cdot \frac{1}{Y} \cdot \left(\frac{\gamma_a}{1 + \gamma_a + \gamma_a^2 \left(\frac{K_S}{K_i}\right)}\right) \beta \tag{5.24}$$

$$\frac{\partial \beta}{\partial \theta} = \Phi_b \left(\frac{\gamma_a}{1 + \gamma_a + \gamma_a^2 \left(\frac{K_S}{K_i}\right)}\right) \beta - \Phi_c\, \beta \tag{5.25}$$

where, $\Phi_a = \frac{R^2 k_d}{D_{se}}$, $\Phi_b = \frac{R^2 \hat{\mu}}{D_{se}}$, and $\Phi_c = \frac{R^2 \hat{\mu}_c}{D_{se}}$.

Initial conditions:

@ θ=0 $\qquad \gamma_a = \gamma_{a0}$ (r,z,0) (5.26)

$\beta = \beta_0$ (r,z,0) (5.26a)

$$\gamma_s = \gamma_{s0} \quad (r,z,0) \tag{5.26b}$$

Boundary conditions:

$$@\ \eta=0 \qquad \frac{\partial \gamma_a}{\partial \eta} = 0 \tag{5.27}$$

$$\text{or } \gamma_a = \text{finite} \tag{5.27a}$$

$$@\ \eta=1 \qquad -\frac{\partial \gamma_a}{\partial \eta} = Sh_a\left(\gamma_a - \gamma_b\right) \tag{5.28}$$

where, $Sh_a = \dfrac{k_m R}{D_{se}}$.

5.1.2.2. Mobile Phase

Dimensionless groups:

$$\gamma_b = \frac{C_b}{K_s} \qquad \text{pollutant concentration} \tag{5.29}$$

$$\gamma_{z_a} = \frac{C_{z_a}}{K_s} \qquad \text{pollutant concentration before entering into the bed.} \tag{5.29a}$$

$$\theta = \frac{D_{se}}{R^2} \cdot t \qquad \text{time} \tag{5.30}$$

$$\xi = \frac{z}{L} \qquad \text{axial distance} \tag{5.31}$$

Dimensionless equation:

$$\frac{\partial \gamma_b}{\partial \theta} = \frac{\Psi}{Pe}\left(\frac{\partial^2 \gamma_b}{\partial \xi^2}\right) - \Psi \frac{\partial \gamma_b}{\partial \xi} + Sh_b\left[\gamma_a\Big|_{\eta=1} - \gamma_b\right] \tag{5.32}$$

where, $\Psi = \frac{\bar{v}_z \cdot R^2}{L \cdot D_{se}}$, $Sh_b = \frac{3(1-\varepsilon_b)}{\varepsilon_b} \cdot \frac{k_m \cdot R}{D_{se}}$, and $Pe = \frac{\bar{v}_z L}{D_{le}}$.

Initial condition:

@ $\theta=0$ $\qquad \gamma_b = \gamma_{b0}$ (r,z,0) (5.33)

Boundary conditions:

@ $\xi=0$ $\qquad \gamma_{z_0} - \gamma_b = -\frac{1}{Pe}\left(\frac{\partial \gamma_b}{\partial \xi}\right)$ (5.34)

@ $\xi=1$ $\qquad \gamma_b = \gamma_b$ (acceptable limit) (5.35)

or $\qquad \frac{\partial \gamma_b}{\partial \xi} = 0$ @ $\xi=1$ (5.35a)

5.1.3 Numerical Solution

The dimensionless equations shown in the previous section are highly non-linear and numerically very stiff. In order to obtain a stable numerical solution, a powerful method is needed. Of the different types of numerical methods available in the literature [Lapidus and Seinfeld (1971), Mitchell and Griffiths (1980), Raghavan and Ruthven (1983), Davis (1984), Press et al. (1990), and Walas (1991)], a technique called Method of Lines (MOL) was adopted to solve the non-linear partial differential equations (PDEs) with appropriate initial and boundary conditions. The method of lines technique applies to initial value (time-dependent) problems (IVPs). Essentially, the concept is to make a partial discretization, i.e. to discretize only the spatial gradients. This leads to the formation of a system of ordinary differential equations (ODEs) in time. Boundary

conditions are incorporated into the process of spatial discretization, while initial conditions are used to start the IVP.

The axial (z) and radial (r) distances are discretized into NB and NR points respectively (Figure 5.2). Even though there are several finite difference formulas that could be used, this dissertation employs methodologies previously described by Craver (1976), Brian III et al. (1987), and Bhaumik et al. (1996).

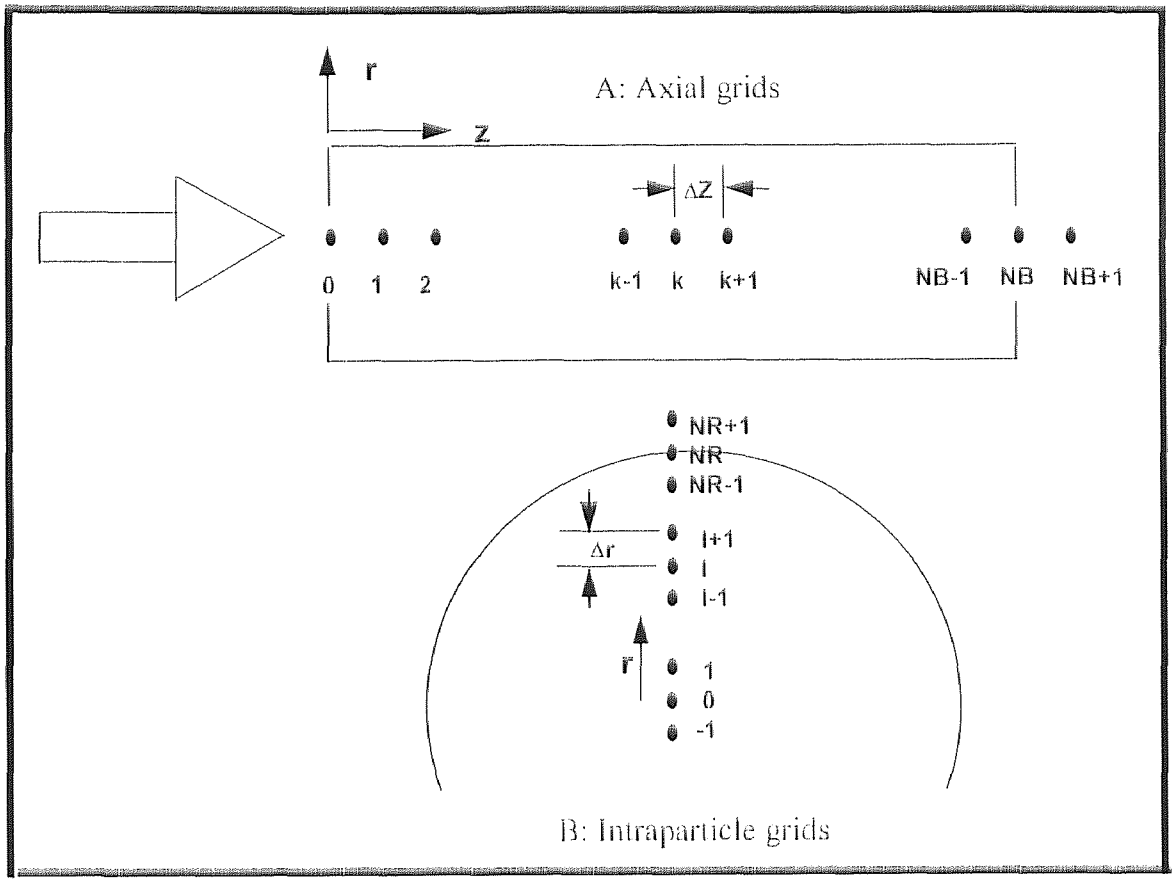

Figure 5.2 Indexed grids for axial and radial directions.

The distance between any two consecutive axial points is Δz and the same between any two consecutive radial points is Δr. Thus the set of PDEs was converted to a total of NT (equal to 1*NB+3*NB*NR) ODEs. Each concentration has a specific location in the concentration vector of NT dimensions. The integration of ODEs starts with the initialization of different concentration vectors, along with the input of initial stepsize, $\Delta\theta$. Integration then proceeded until normalized time, θ, was equal to $\Delta\theta$. Similarly, subsequent integration continued until the new time step ($\theta+\Delta\theta$) was reached. It is to be noted that for each time step, the entire set of equations (i.e. total of NT) are solved. Assume for example that NB=30 and NR=20, then NT would be 1830, which means for each time step, 1830 simultaneous equations have to be solved before it can go to the next updated time. The entire integration proceeded until a stopping criteria was met.

The resulting ODEs in the time domain were numerically integrated with the help of an IMSL subroutine named "DIVPAG" (Double Precision Version of Initial Value Problem, using an Adams-Moulton/Gear method), which has the ability to handle very stiff differential equations. The computer code was written in FORTRAN 77 for a VAX/VMS environment. This code was robust and stable, and convergence criteria were satisfied even with a tolerance value of 10^{-12}.

5.2 Model Development with Oxygen Limitation

In the previous section (5.1), a detailed discussion of the model is given, which takes into account most of the effects considered except the concentration of electron acceptor. This section will focus on inclusion in the model of oxygen-limiting conditions. The need for such consideration stems from the fact that the availability of oxygen in most in-situ situations is a limiting factor in the rate of biodegradation.

5.2.1 Model Description

In addition to the assumptions given in the previous section:

- adsorption of oxygen into soil is neglected
- oxygen enters the saturated zone as a dissolved gas
- the oxygen biokinetic response follows a Monod model (non-inhibitory)

5.2.1.1 Mass Balance Equations for the Aggregates

For pollutant:

$$\frac{\partial C_a}{\partial t} = \frac{D_{se}}{r^2}\left[\frac{\partial}{\partial r}\left(r^2 \frac{\partial C_a}{\partial r}\right)\right] - B_d - A_d \qquad (5.36)$$

$$B_d = \frac{b}{Y}\cdot\mu = \frac{b}{Y}\left(\frac{\hat{\mu} C_a}{K_S + C_a + \left(C_a^2 / K_i\right)}\right)\cdot\left(\frac{C_o}{K_{so} + C_o}\right) \qquad (5.37)$$

$$\text{where, } \mu = \mu\left(C_a, C_o\right) = \left(\frac{\hat{\mu} C_a}{K_S + C_a + \left(C_a^2 / K_i\right)}\right)\cdot\left(\frac{C_o}{K_{so} + C_o}\right) \qquad (5.38)$$

$$\frac{\partial b}{\partial t} = \left(\frac{\hat{\mu}\, C_a}{K_S + C_a + \left(C_a^2 / K_i\right)} \right) \cdot \left(\frac{C_o}{K_{so} + C_o} \right) b \; - \; \hat{\mu}_c\, b \tag{5.39}$$

$$A_d \;\; = k_d \left(C_a - C_a^* \right) \tag{5.40}$$

$$q \;\; = \;\; k_p \cdot \left(C_a^* \right)^{\frac{1}{n}} \tag{5.41}$$

Again, C_a^* can written as $C_a^* = \left(\frac{q}{k_p} \right)^n$ (5.42)

$$\frac{\partial q}{\partial t} = \frac{\varepsilon_a}{\left(1 - \varepsilon_a\right) \cdot \rho_s} \cdot k_d \cdot \left(C_a - C_a^* \right) = \frac{\varepsilon_a}{\left(1 - \varepsilon_a\right) \cdot \rho_s} \cdot A_d \tag{5.43}$$

For oxygen:

$$\frac{\partial C_o}{\partial t} \;\; = \;\; \frac{D_{so}}{r^2} \left[\frac{\partial}{\partial r} \left(r^2 \frac{\partial C_o}{\partial r} \right) \right] \; - B_{do} \tag{5.44}$$

$$B_{do} = \frac{b}{Y_o} \cdot \mu = \frac{b}{Y_o} \left(\frac{\hat{\mu}\, C_a}{K_S + C_a + \left(C_a^2 / K_i\right)} \right) \cdot \left(\frac{C_o}{K_{so} + C_o} \right) \tag{5.45}$$

Initial conditions:

(i) t=0 $\qquad C_a = C_{a0}$ (5.46)

$q \;\; = q_0$ (5.46a)

$b \;\; = b_0$ (5.46b)

$C_o = C_{o0}$ (5.46c)

Boundary conditions:

@ r=0 $C_a = \text{finite} \quad \text{or} \quad \left(\frac{\partial C_a}{\partial r} = 0\right)$ (5.47)

$C_o = \text{finite} \quad \text{or} \quad \left(\frac{\partial C_o}{\partial r} = 0\right)$ (5.48)

@ r= R $-D_{se}\frac{\partial C_a}{\partial r} = k_m\left(C_a - C_b\right)$ (5.49)

$-D_{so}\frac{\partial C_o}{\partial r} = k_{mo}\left(C_o - C_{mo}\right)$ (5.50)

5.2.1.2 Mass Balance Equations for the Mobile Phase

For pollutant:

$$\frac{\partial C_b}{\partial t} = D_{le}\frac{\partial^2 C_b}{\partial z^2} - \bar{v}_z\frac{\partial C_b}{\partial z} + k_m \cdot \frac{3}{R} \cdot \frac{1-\varepsilon_b}{\varepsilon_b} \cdot \left[C_a\Big|_{r=R} - C_b\right] \quad (5.51)$$

For oxygen:

$$\frac{\partial C_{mo}}{\partial t} = D_{lo}\frac{\partial^2 C_{mo}}{\partial z^2} - \bar{v}_z\frac{\partial C_{mo}}{\partial z} + k_{mo} \cdot \frac{3}{R} \cdot \frac{1-\varepsilon_b}{\varepsilon_b} \cdot \left[C_o\Big|_{r=R} - C_{mo}\right] \quad (5.52)$$

Initial conditions:

@ t=0 $C_b = C_{b0}$ (5.53)

$C_{mo} = C_{mo}^{0}$ (5.53a)

Boundary conditions:

@ z=0

$$\text{(pollutant)} \qquad -D_{le}\frac{\partial C_b}{\partial z} + \bar{v}_z C_b = \bar{v}_z C_{z_o} \tag{5.54}$$

$$\text{(oxygen)} \qquad -D_{lo}\frac{\partial C_{mo}}{\partial z} + \bar{v}_z C_{mo} = \bar{v}_z C_{moz_{0-}} \tag{5.55}$$

@ z=L (pollutant) $C_b = C_{bL}$ (acceptable limit) (5.56)

$$\text{or} \quad \frac{\partial C_b}{\partial z} = 0 \tag{5.56a}$$

$$\text{(oxygen)} \quad \frac{\partial C_{mo}}{\partial z} = 0 \quad \text{(oxygen flux is zero at the edge of the plume)} \tag{5.57b}$$

Also note that:

old spill: @ z=0, $C_{Z_o} = 0$ and $C_{moz_o} = \text{constant}$

new spill: @ z=0, $C_{Z_o} = \text{constant}$ and $C_{moz_o} = \text{constant}$

5.2.2 Dimensionless Form

5.2.2.1 Aggregate Phase

Dimensionless groups:

$$\gamma_a = \frac{C_a}{K_s} \qquad \text{pollutant concentration} \tag{5.58}$$

$$\gamma_o = \frac{C_o}{K_s} \qquad \text{oxygen concentration} \tag{5.59}$$

$$\gamma_s = \frac{\rho_s}{K_s}\cdot q \qquad \text{solid phase concentration} \tag{5.60}$$

$$\theta = \frac{D_{se}}{R^2}\cdot t \qquad \text{time} \tag{5.61}$$

$$\eta = \frac{r}{R} \qquad \text{radial distance} \tag{5.62}$$

$$\beta = \frac{b}{K_s} \qquad \text{biomass concentration} \tag{5.63}$$

Dimensionless equations:

For pollutant:

$$\frac{\partial \gamma_a}{\partial \theta} = \frac{1}{\eta^2}\left[\frac{\partial}{\partial \eta}\left(\eta^2 \frac{\partial \gamma_a}{\partial \eta}\right)\right] - B_d \cdot \frac{R^2}{D_{se} K_s} - A_d \cdot \frac{R^2}{D_{se} K_s} \tag{5.64}$$

where,

$$A_d \cdot \frac{R^2}{D_{se} K_s} = \Phi_a \left(\gamma_a - \gamma_a^*\right) \tag{5.65}$$

$$\gamma_a^* = \frac{K_s^{n-1}}{k_p^n \rho_s^n} (\gamma_s)^n \tag{5.66}$$

alternatively γ_a^* can also be written as, $\gamma_a^* = \left(\frac{K_s^{1-\frac{1}{n}}}{k_p \rho_s} \cdot\right)^n \cdot \gamma_s^n$ (5.67)

$$\frac{\partial \gamma_s}{\partial \theta} = \frac{\varepsilon_a}{(1-\varepsilon_a)} \cdot \Phi_a \cdot \left(\gamma_a - \gamma_a^*\right) = \frac{\varepsilon_a}{(1-\varepsilon_a)} \cdot \left(A_d \cdot \frac{R^2}{D_{se} K_s}\right) \tag{5.68}$$

and $B_d \cdot \frac{R^2}{D_{se} K_s} = \Phi_b \cdot \frac{1}{Y} \cdot \left(\frac{\gamma_a}{1 + \gamma_a + \gamma_a^2 \cdot (K_s / K_i)}\right) \cdot \left(\frac{\gamma_o}{\Phi_k + \gamma_o}\right) \cdot \beta$ (5.69)

$$\frac{\partial \beta}{\partial \theta} = \Phi_b \cdot \left(\frac{\gamma_a}{1 + \gamma_a + \gamma_a^2 \cdot (K_s / K_i)}\right) \cdot \left(\frac{\gamma_o}{\Phi_k + \gamma_o}\right) \cdot \beta - \Phi_c \beta \tag{5.70}$$

where, $\Phi_a = \frac{R^2 k_d}{D_{se}}$, $\Phi_b = \frac{R^2 \hat{\mu}}{D_{se}}$, $\Phi_c = \frac{R^2 \hat{\mu}_c}{D_{se}}$, and $\Phi_k = \frac{K_{so}}{K_S}$

For oxygen:

$$\frac{\partial \gamma_o}{\partial \theta} = \frac{D_{so}}{D_{se}} \cdot \frac{1}{\eta^2} \left[\frac{\partial}{\partial \eta} \left(\eta^2 \frac{\partial \gamma_o}{\partial \eta} \right) \right] - B_{do} \cdot \frac{R^2}{D_{se} K_S} \tag{5.71}$$

where,

$$B_{do} \cdot \frac{R^2}{D_{se} K_S} = \Phi_b \cdot \frac{1}{Y_o} \cdot \left(\frac{\gamma_a}{1 + \gamma_a + \gamma_a^2 \cdot (K_s / K_i)} \right) \cdot \left(\frac{\gamma_o}{\Phi_k + \gamma_o} \right) \cdot \beta \tag{5.72}$$

Initial conditions:

@ $\theta=0$ $\gamma_a = \gamma_{a0}$ (5.73)

$\beta = \beta_0$ (5.73a)

$\gamma_s = \gamma_{s0}$ (5.73b)

$\gamma_o = \gamma_{o0}$ (5.73c)

Boundary conditions:

@ $\eta=0$ γ_a = finite or $\left(\frac{\partial \gamma_a}{\partial \eta} = 0 \right)$ (5.74)

γ_o = finite or $\left(\frac{\partial \gamma_o}{\partial \eta} = 0 \right)$ (5.75)

@ $\eta=1$ $-\frac{\partial \gamma_a}{\partial \eta} = Sh_a (\gamma_a - \gamma_b)$ (5.76)

$-\frac{\partial \gamma_o}{\partial \eta} = Sh_{ao} (\gamma_o - \gamma_{mo})$ (5.76a)

where, $Sh_a = \frac{k_m R}{D_{se}}$ and $Sh_{ao} = \frac{k_{mo} R}{D_{so}}$

5.2.2.2 Mobile Phase

Dimensionless groups:

$$\gamma_b = \frac{C_b}{K_s} \qquad \text{pollutant concentration} \tag{5.77}$$

$$\gamma_{z_o} = \frac{C_{z_o}}{K_s} \qquad \text{pollutant concentration before entering into the reactor} \tag{5.77a}$$

$$\gamma_{mo} = \frac{C_{mo}}{K_s} \qquad \text{oxygen concentration} \tag{5.77b}$$

$$\gamma_{moz_o} = \frac{C_{moz_o}}{K_s} \qquad \text{oxygen concentration before entering into the reactor} \tag{5.77c}$$

$$\theta = \frac{D_{se}}{R^2} \cdot t \qquad \text{time} \tag{5.77d}$$

$$\xi = \frac{z}{L} \qquad \text{axial distance} \tag{5.77e}$$

Dimensionless equations:

For pollutant:

$$\frac{\partial \gamma_b}{\partial \theta} = \frac{\Psi}{Pe}\left(\frac{\partial^2 \gamma_b}{\partial \xi^2}\right) - \Psi \cdot \frac{\partial \gamma_b}{\partial \xi} + Sh_b\left[\gamma_a\Big|_{\eta=1} - \gamma_b\right] \tag{5.78}$$

where, $\Psi = \dfrac{\bar{v}_z \cdot R^2}{L \cdot D_{se}}$, $Pe = \dfrac{\bar{v}_z L}{D_{le}}$, and $Sh_b = \dfrac{3(1-\varepsilon_b)}{\varepsilon_b} \cdot \dfrac{k_m \cdot R}{D_{se}}$

For oxygen:

$$\frac{\partial \gamma_{mo}}{\partial \theta} = \frac{\Psi}{Pe_o}\left(\frac{\partial^2 \gamma_{mo}}{\partial \xi^2}\right) - \Psi \cdot \frac{\partial \gamma_{mo}}{\partial \xi} + Sh_{bo}\left[\gamma_o\Big|_{\eta=1} - \gamma_{mo}\right] \tag{5.79}$$

where, $Pe_o = \frac{\bar{v}_z L}{D_{lo}}$ and $Sh_{bo} = \frac{3(1-\varepsilon_b)}{\varepsilon_b} \cdot \frac{k_{mo} \cdot R}{D_{se}}$

Initial conditions:

@ $\theta=0$ $\gamma_b = \gamma_{b0}$ (5.80)

$\gamma_{mo} = \gamma^0_{mo}$ (5.80a)

Boundary conditions:

@ $\xi=0$ (pollutant) $\gamma_{z_{0^-}} - \gamma_b = -\frac{1}{Pe}\left(\frac{\partial \gamma_b}{\partial \xi}\right)$ (5.81)

(oxygen) $\gamma_{moz_{0^-}} - \gamma_{mo} = -\frac{1}{Pe_o}\left(\frac{\partial \gamma_{mo}}{\partial \xi}\right)$ (5.81a)

@ $\xi=1$ (pollutant) $\gamma_b = \gamma_b$ (acceptable limit) (5.82)

or $\frac{\partial \gamma_b}{\partial \xi} = 0$ @ $\xi=1$ (5.82a)

(oxygen) $\frac{\partial \gamma_b}{\partial \xi} = 0$ @ $\xi=1$ (5.83a)

5.2.3 Numerical Solution

The same general methodology described earlier (section 5.1.3) has been used to obtain numerical solutions for the system of equations with oxygen limitation.

CHAPTER 6

RESULTS AND DISCUSSION

6.1 Determination of Biokinetic Parameters

This section deals with obtaining detailed kinetics of 2-chlorophenol biodegradation by a pure culture (*Pseudomonas pickettii*) from both the shake flask and jacketed batch reactors.

6.1.1 In Shake Flasks

In these experiments, the initial substrate concentration varied from 11 to 110 ppm, and the initial biomass concentration varied from 8 to 35 ppm. The results of these kinetic runs are given in Tables D-1 through D-8 in Appendix D. A detailed data analysis is given in section 6.1.2 showing how the kinetic parameters were obtained. Plots of logarithmic biomass concentrations versus time (Figures D-1 through D-8) yielded the specific growth rates for each substrate concentration. Table 6.1 shows the values of the specific growth rate for each run. Figure 6.1 plots the data of specific growth rate versus phenol concentration, and shows the curve obtained from a fit of the data to the Andrews model. Unfortunately the data are scattered, and the resulting fit to the model was unsatisfactory. This may have occurred due to one or more of the following reasons:

(1) The oxygen requirement during exponential growth is high, and since all of the oxygen must diffuse from the surrounding air, through the cotton plug, into the shake flask, and across the liquid/gas interface, these experiments may have suffered from inconsistent oxygen limitation.

(2) Temperature was not controlled, but rather fluctuated with the variation in room temperature.

Table 6.1 Experimental data on specific growth rates in shake flasks.

Expt. Run	2-CP conc. at growth, mg/L	Average 2-CP conc. during growth, mg/L	Expt. Specific growth rate, μ, h^{-1}	Pred. Specific growth rate, μ, h^{-1}	% error
9	10.1	6.76	0.103	0.109	+5.46
2	12.7	8.07	0.127	0.111	-12.4
1	16.1	10.9	0.099	0.112	+13.0
4	43.3	38.3	0.111	0.0935	-15.7
5	50.1	44.9	0.081	0.0886	+9.46
6	62.1	54.9	0.068	0.0809	+19.0
7	77.2	63.9	0.073	0.0727	-0.44
8	101.9	88.9	0.068	0.0621	-8.63

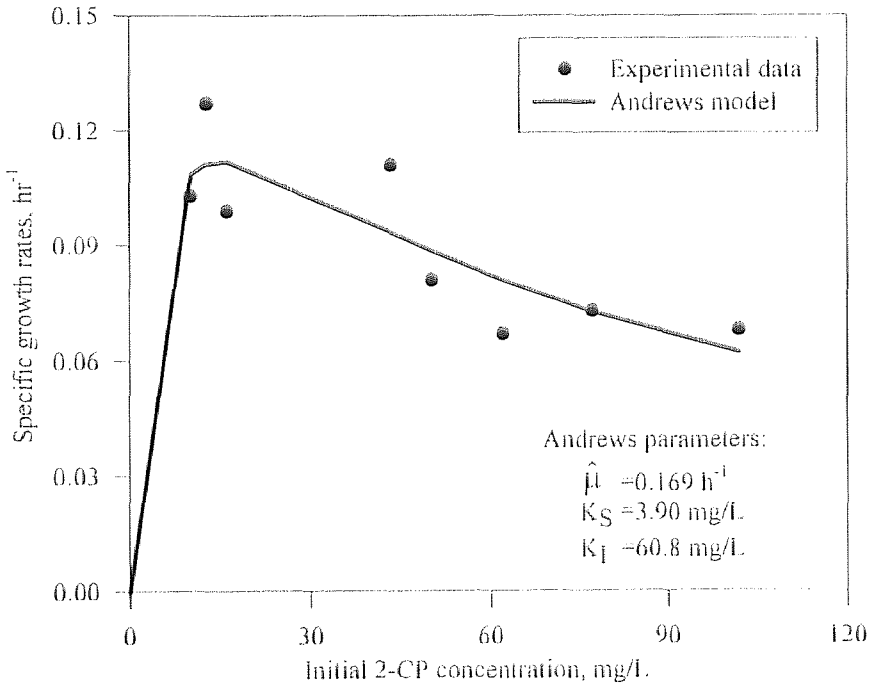

Figure 6.1 Plot of specific growth rate versus substrate concentration.

6.1.2 In Lucite Reactor

To eliminate some of the problems encountered in shake flask experiments, it was decided to carry out all the kinetic experiments in a more controllable jacketed 4.5 liter Lucite reactor. The initial biomass concentrations were maintained at a low value 5.5~10.5 ppm, which resulted in an extended exponential growth phase, allowing for sufficient data collection. A constant temperature was maintained during the entire experiment. Finally, filtered air was bubbled into the reactor via a diffuser, maintaining higher oxygen concentrations. A typical run is shown in Table 6.2. Other results are given in Tables E-1 through E-16 in Appendix E.

Table 6.2 Data obtained from batch experiment K-15.

Sample No	Time (h)	Optical density	Biomass concentration (mg/L)	Ln (biomass concentration)	2-Chlorophenol concentration (mg/L)
1	0.00	0.0200	5.47	1.70	4.950
2	0.17	0.0205	5.60	1.72	4.705
3	0.33	0.0210	5.74	1.75	4.526
4	0.50	0.0215	5.88	1.77	4.239
5	0.67	0.0220	6.01	1.79	4.002
6	0.83	0.0225	6.15	1.82	3.616
7	1.00	0.0230	6.29	1.84	3.240
8	1.20	0.0240	6.56	1.88	2.700
9	1.33	0.0245	6.70	1.90	2.501
10	1.50	0.0250	6.85	1.92	2.189
11	1.66	0.0260	7.11	1.96	1.844
12	1.86	0.0265	7.24	1.98	1.385
13	2.00	0.0270	7.38	1.99	1.071
14	2.25	0.0280	7.65	2.04	0.470
15	2.36	0.0280	7.65	2.04	0.000

The rate of biomass growth is given by the following equation (assuming μ_c =0):

$$\frac{db}{dt} = \mu \cdot b \tag{6.1}$$

And the decrease in substrate concentration is given as:

$$\frac{ds}{dt} = -r_s = \quad f(s,\mu) = \quad -\mu \cdot s = \quad -\mu \cdot \frac{b}{Y} \tag{6.2}$$

Assuming μ is constant with time: $\int \frac{db}{b} = (\mu) \int dt$ (6.3)

where, b=bo at t=0 or t_{lag}. After the integration we get the following equation:

$$\text{(a) } \mathrm{Ln}\frac{b}{b_0} = \mu\, t \text{ and also (b) } \mathrm{Ln}\frac{b}{b_0} = \mu(t - t_{lag}); \quad \text{when } t > t_{lag} \tag{6.4}$$

The specific growth rate was obtained by preparing a plot of Ln b versus time and taking the slope of the linear portion (i.e. exponential growth portion), as shown in part (a) of Figure 6.2.

The yield coefficient (Y) was obtained form the slope of biomass concentration versus 2-chlorophenol concentration [see plot (b) of Figure (6.2)]. From equations (6.1) and (6.2) we obtain the following:

$$-Y_{Expt} = \left(\frac{db}{dt}\right) \Big/ \left(-\frac{ds}{dt}\right) \quad \approx -\frac{\Delta b}{\Delta s} \tag{6.5}$$

Additional plots are shown in Figures E-1 through E-16. A list of the all the specific growth rates and respective yield coefficients are shown in Table 6.3. The average yield coefficient for *P. pickettii* on 2-CP was 0.402 with a standard deviation of 0.073. The average correlation coefficients for specific growth rate and yield coefficient plots were

0.993 (with max. 0.999, min. 0.976) and 0.980 (with max. 0.9803, min. 0.945) respectively.

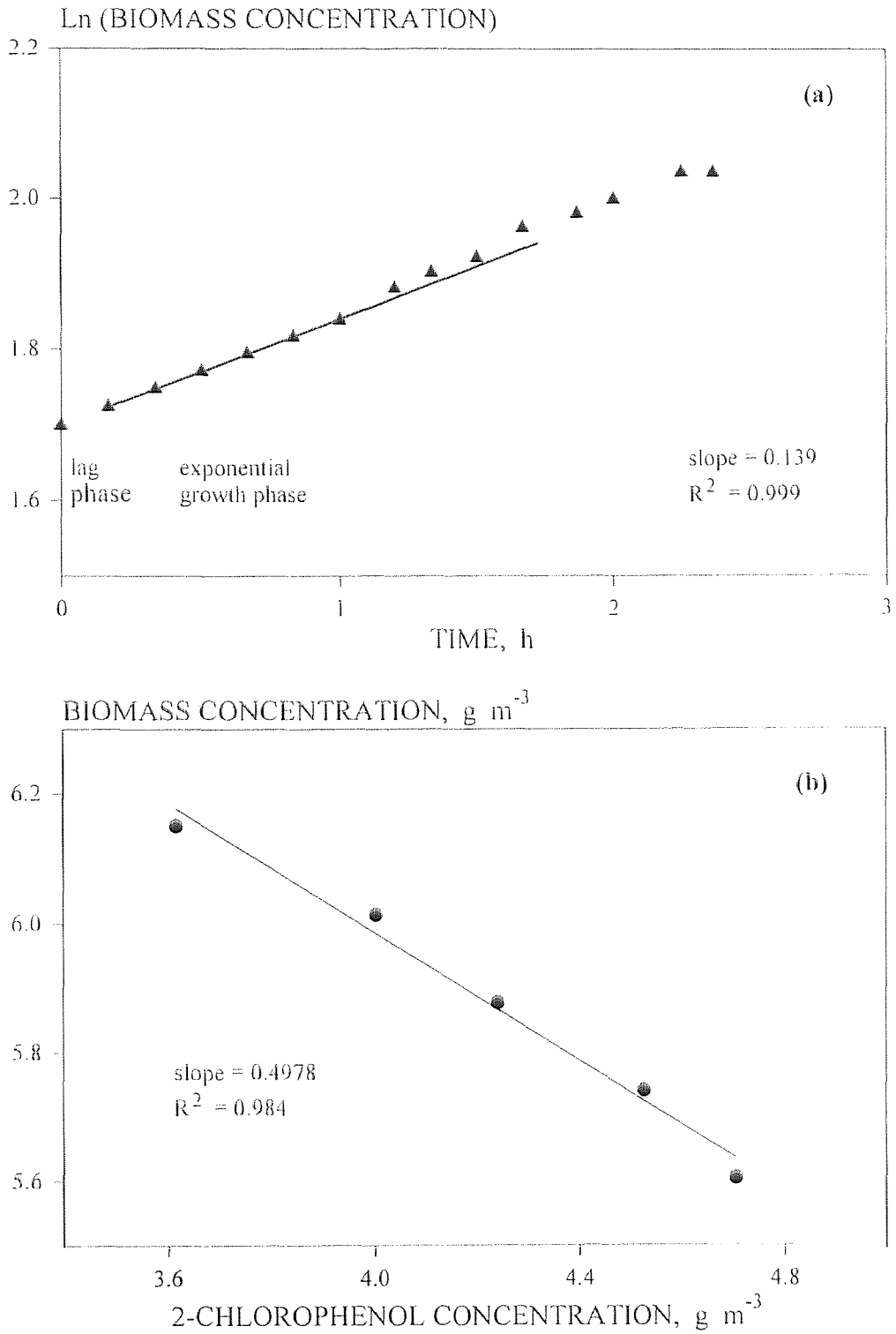

Figure 6.2 Determination of the specific growth rate (a) and yield coefficient (b) of *P. pickettii* on 2-chlorophenol.

It should be noted that the 2-CP concentrations given in Table 6.3 are the average of those on which the slopes of the specific growth rate curves were obtained (rather than the starting 2-CP concentrations). A detailed analysis of this method can be found elsewhere (Dikshitulu, 1993).

Table 6.3 Specific growth rates and yield coefficients for *Pseudomonas pickettii*.

Expt. run	Table	Specific growth rate, μ	Correlation coefficient for, μ	Specific growth rate obtained by regression	2-CP conc.	Yield coefficient Y	Correlation coefficient for, Y
k-15	E-15	0.139	0.999	0.137	4.21	0.498	0.984
k-16	E-16	0.138	0.990	0.138	4.26	0.372	0.998
k-17	E-17	0.143	0.999	0.145	5.12	0.410	0.984
k-18	E-18	0.150	0.984	0.151	6.13	0.418	0.960
k-19	E-19	0.158	0.989	0.155	7.12	0.537	0.972
k-20	E-20	0.155	0.976	0.159	8.01	0.434	0.944
k-21	E-21	0.162	0.995	0.162	13.06	0.439	0.991
k-22	E-22	0.163	0.991	0.162	15.56	0.376	0.980
k-23	E-23	0.157	0.992	0.158	20.33	0.375	0.983
k-8	E-8	0.156	0.999	0.156	22.93	0.408	0.985
k-9	E-9	0.148	0.997	0.149	28.95	0.390	0.985
k-10	E-10	0.142	0.996	0.142	35.46	0.458	0.988
k-11	E-11	0.136	0.998	0.133	43.37	0.300	0.984
k-12	E-12	0.118	0.998	0.116	63.56	0.377	0.978
k-13	E-13	0.102	0.997	0.108	74.21	0.233	0.987

In order to obtain the kinetic parameters, a plot of the specific growth rates versus 2-CP concentrations were generated as shown in Figure 6.3. Data on the plot look consistent as opposed to shake flask experiments. These data were fitted to the Andrews expression by using a nonlinear regression routine based on the Gauss-Marquardt method. The values of the Andrews parameters are given in Table 6.4. The percent error using the Lucite reactor is an order of magnitude lower than in shake flasks.

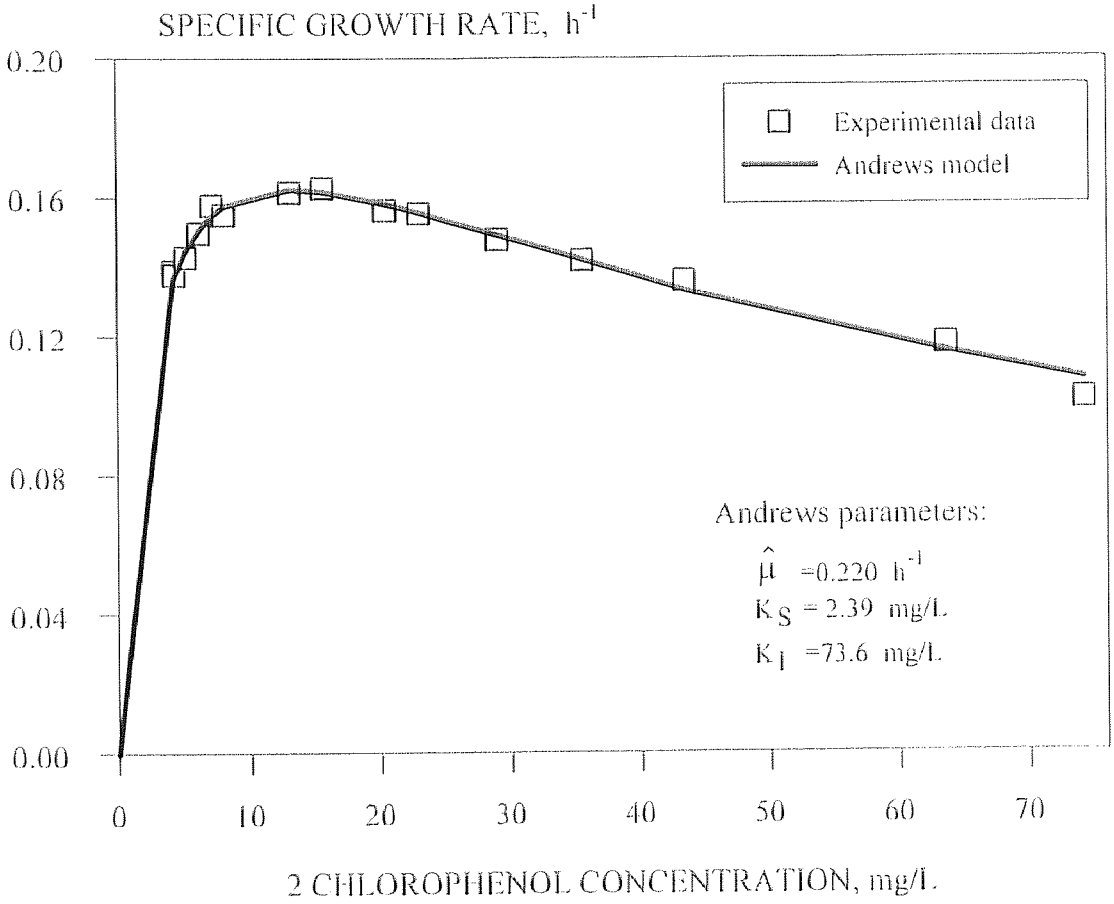

Figure 6.3 Specific growth rate of *Pseudomonas pickettii* on 2-chlorophenol.

Table 6.4 Andrews parameter for *Pseudomonas pickettii* on 2-chlorophenol.

Reactor type	$\hat{\mu}$ h^{-1}	K_s (mg/L)	K_I (mg/L)	Average % error
In Shake Flask	0.169	3.90	60.8	9.35
In Lucite Reactor	0.220	2.39	73.6	0.611

Once the biokinetic parameters were determined, biomass and 2-CP concentration profiles could be predicted for any individual experiment. From equation (6.1):

$$\frac{db}{dt} = (\mu - \mu_C)\cdot b = \left\langle \left(\frac{\hat{\mu}_S \cdot s}{K_s + s + (s^2 / K_I)} \right) - \mu_C \right\rangle \cdot b \qquad (6.6)$$

and

$$\frac{ds}{dt} = -(\mu - \mu_C)\cdot \frac{b}{Y} = -\frac{1}{Y}\cdot \left\langle \left(\frac{\hat{\mu}_s s}{K_s + s + (s^2 / K_I)} \right) - \mu_C \cdot \right\rangle \cdot b \qquad (6.7)$$

Equations (6.6) and (6.7) can be integrated numerically using a simple Runge-Kutta stepwise integration method. An average value of overall yield coefficient was used in this solution. Parameters μ_s, K_s, and K_I are already known. The value of μ_c was assumed to be zero in these batch, suspended growth, simulations. Predicted curves and experimental data are shown in Figure 6.4. The agreement is very good except toward the end of the run, which is a typical characteristic of these simulations [Dikshitulu (1993) and Wang (1995)].

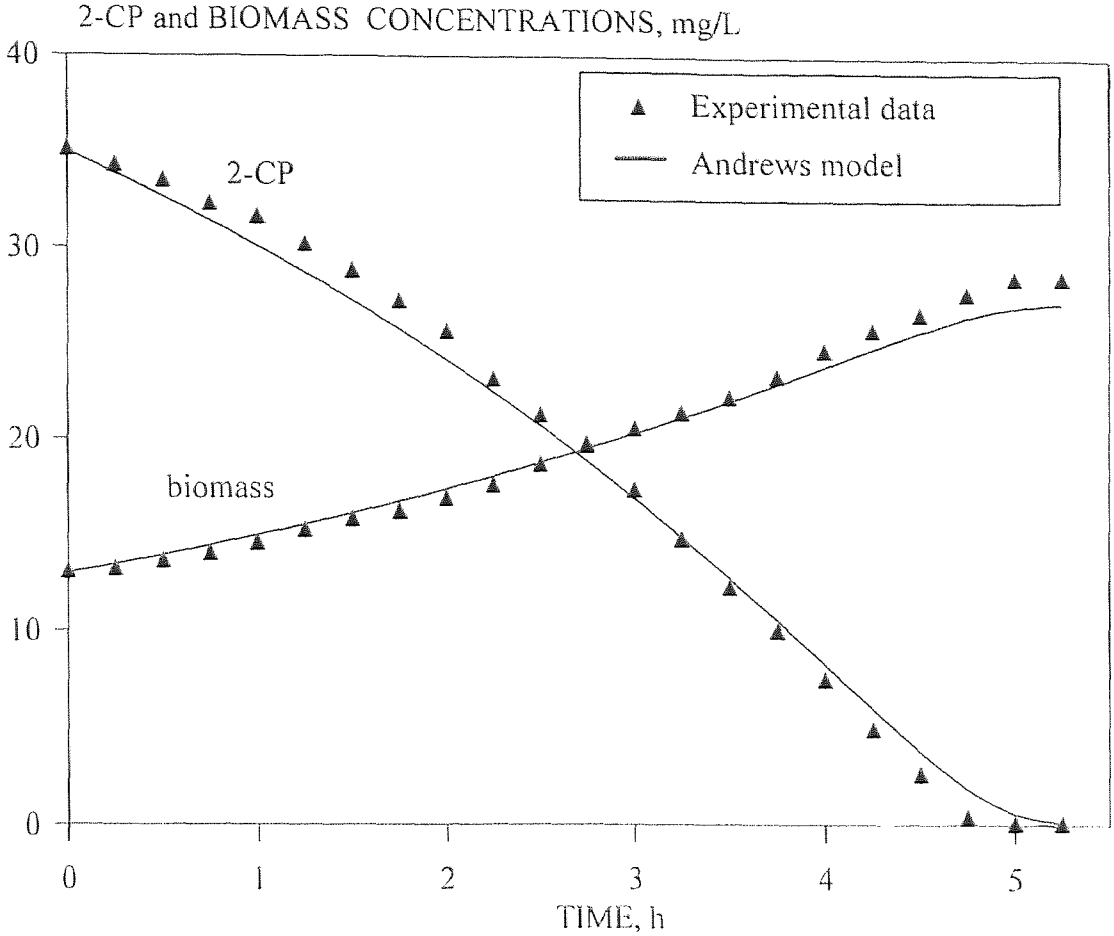

Figure 6.4 Comparison between experimentally obtained and model predicted concentration profiles for 2-chlorophenol and biomass (run # mo-k-9).

6.2 Determination of Adsorption Parameters

6.2.1 Rate of Adsorption of 2-Chlorophenol onto Pequest Soil

Two different initial concentrations (14.7 and 21.8 ppm) were used to perform these experiments. Results are given in Appendix F. Figure 6.5 shows an instantaneous initial adsorption (which is a "true" adsorption based on surface kinetics), followed by a slow adsorption which is mass transfer limited. These results are very similar to those of Bayard (1997). As a result, "true" adsorption was considered to be instantaneous in the

time scale of the processes taking place, and the soil surfaces (q) were considered to be in local equilibrium with pore aqueous phase concentration (C_a).

Due to the type of adsorption behavior observed, the rate term (A_d) in equation (5.1) was neglected.

Table 6.5 Comparison of equilibria between two sets of experiments for Pequest soil.

2-CP Concentration in the Aqueous Solution just before Addition of Soil, mg/L	Time to Attain Equilibrium, hr	Liquid/Solid Mass Ratio
14.7	40.7	3.0
21.8	44.5	3.0

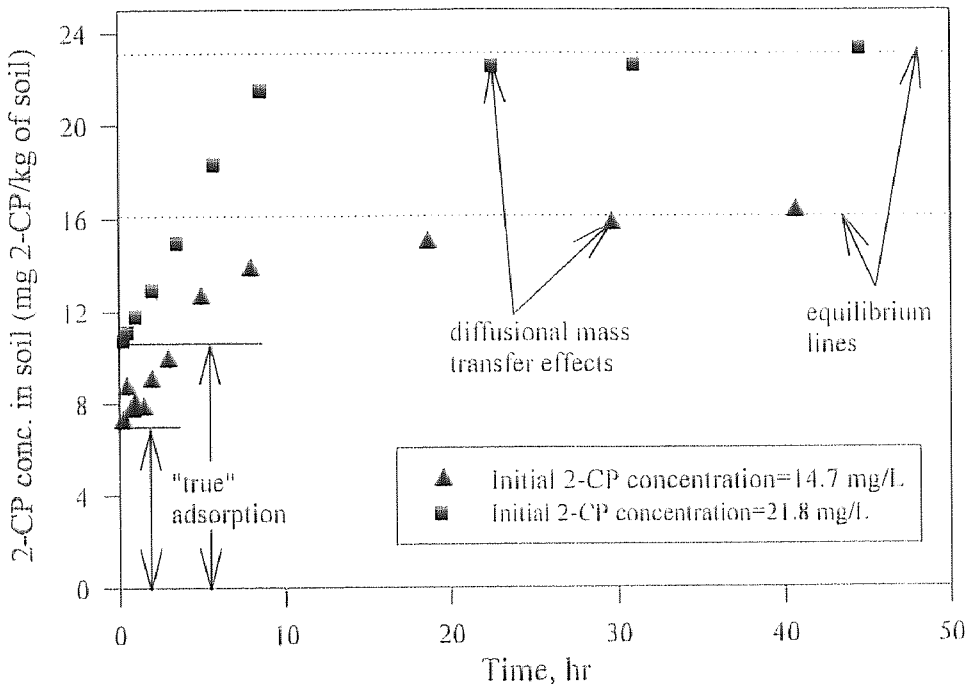

Figure 6.5 2-CP concentration in soil after adsorption from aqueous solution. (Liquid/Solid Mass Ratio=3.0; Temp.= 22 °C).

6.2.2 Adsorption Isotherm

Figure 6.6 shows adsorption equilibrium data. Results are given in Appendix F (Tables F-3 and F-4). The solid phase concentrations were calculated by mass balance from the measured aqueous phase concentrations. These data are plotted along with a Freundlich isotherm model:

$$q = k_p \cdot C_a^{1/n} \tag{6.8}$$

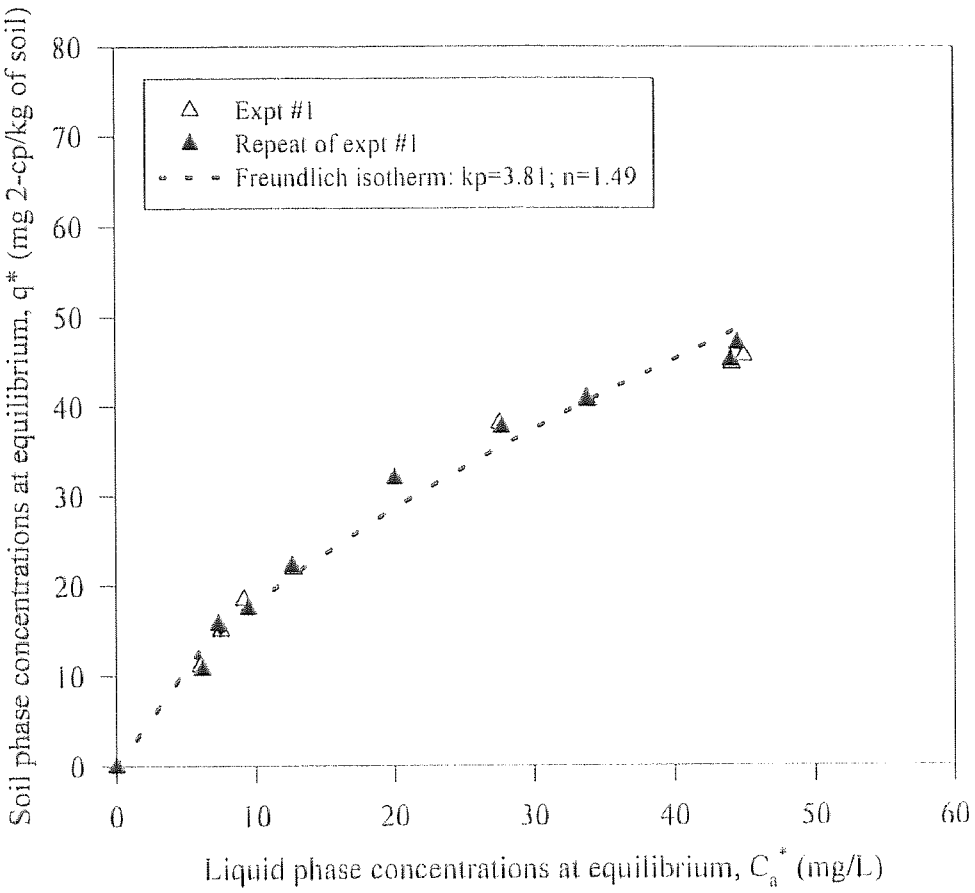

Figure 6.6 Adsorption isotherm of 2-chlorophenol onto Pequest soil. (Freundlich model)

6.3 Axial Dispersion Measurements in the Soil Column

In order to obtain the axial dispersion coefficient within the soil column, chloride tracer studies were performed at a flow rate of 1.1 mL/min. Detailed experimental procedures are discussed earlier. Data from two separate experiments are given in Tables F-5 and F-6, and plots of chloride concentrations versus time are shown in Figures 6.7 and 6.8. Following the procedure described by Levenspiel (1972), the axial dispersion coefficient (D_{le}) was estimated. Dispersion of the fluid flowing in the z-direction in the experimental soil column can be given by,

$$\frac{\partial c}{\partial t} = D_{le} \cdot \frac{\partial^2 c}{\partial z^2} \tag{6.9}$$

where, D_{le} (axial dispersion coefficient, cm^2/sec) typically characterizes the degree of backmixing during flow. In dimensionless form, equation (6.9) becomes,

$$\frac{\partial c}{\partial \tau} = \left(\frac{D_{le}}{u \cdot L}\right) \cdot \frac{\partial^2 c}{\partial x^2} - \frac{\partial c}{\partial x} \tag{6.10}$$

where $x = (u \cdot t + z)$, $\tau = (t \cdot u / L)$, and the dimensionless group $(D_{le}/u \cdot L)$, called vessel dispersion number, measures the extent of axial dispersion. Parameter $(D_{le}/u \cdot L)$ is estimated by calculating the mean and variance from the concentration versus time distribution-curve. Mean of the distribution curve (i.e. mean residence time of the chloride ion between the injection and sampling points) is given in discrete form as,

$$\bar{t} \cong \frac{\sum t_i \cdot c_i \cdot \Delta t_i}{\sum c_i \Delta t_i} \tag{6.11}$$

and the variance (σ^2) in discrete form is given by,

$$\sigma^2 \cong \frac{\sum t_i^2 \cdot c_i \cdot \Delta t_i}{\sum c_i \Delta t_i} - \bar{t}^2 \qquad (6.12)$$

For the closed vessel, the relation between dimensionless variance (σ_θ^2) and D_{le} is given as,

$$\sigma_\theta^2 = \frac{\sigma^2}{\bar{t}^2} \cong 2 \cdot \left(\frac{D_{le}}{u \cdot L} \right) \qquad (6.13)$$

Substituting by $u = L/\bar{t}$, and rearranging, equation (6.13) can be rewritten as,

$$D_{le} = \frac{\sigma^2 \cdot L^2}{2 \cdot \bar{t}^3} \qquad (6.14)$$

Values of mean and variance were obtained from the data plotted in Figures 6.7 and 6.8 and are given in Table 6.6. The axial dispersion coefficient (D_{le}) was calculated using equation (6.14) and was found to be 6.618×10^{-4} and 7.177×10^{-4} cm^2/sec for two separate runs. An average value of 6.89×10^{-4} cm^2/sec was used in subsequent simulations. Values of 0.037 and 0.040 for σ_θ^2 (dimensionless variance) indicate that the dispersion was of intermediate extent, i.e. plug flow with some back mixing [Levenspiel (1972)].

Table 6.6 Parameter values from chloride distribution curve.

	Mean, $\bar{t}$ (min)	Variance (σ^2) (min^2)	Dimensioless variance (σ_θ^2)	L (cm)	D_{le} (cm^2/sec)
Figure 6.7	228.57	1959.7	0.0370	22.0	6.618×10^{-4}
Figure 6.8	229.86	2161.4	0.0409	22.0	7.177×10^{-4}

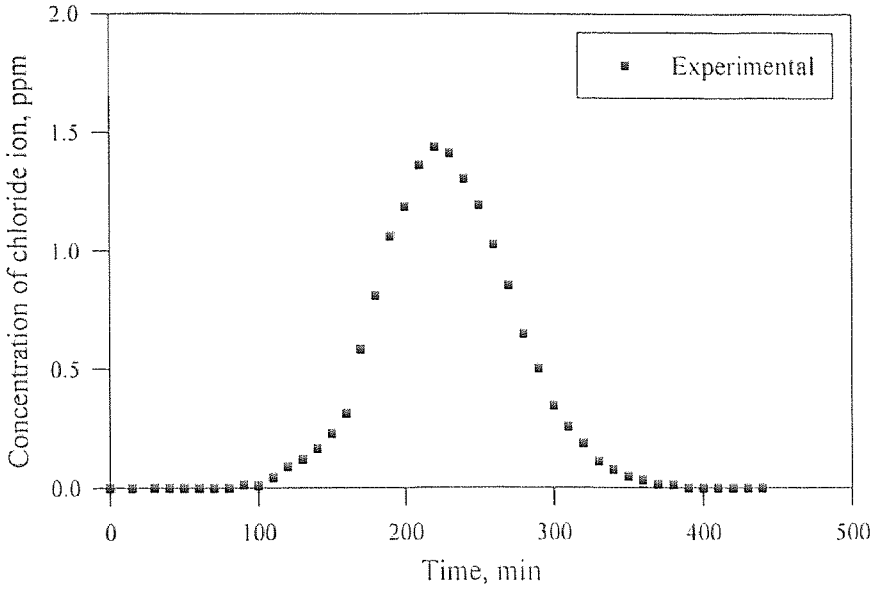

Figure 6.7 Elution data of chloride ion from the soil column (col#1). Mean residence time=228.57 min and variance=1959.7 min^2 (run#A-4)

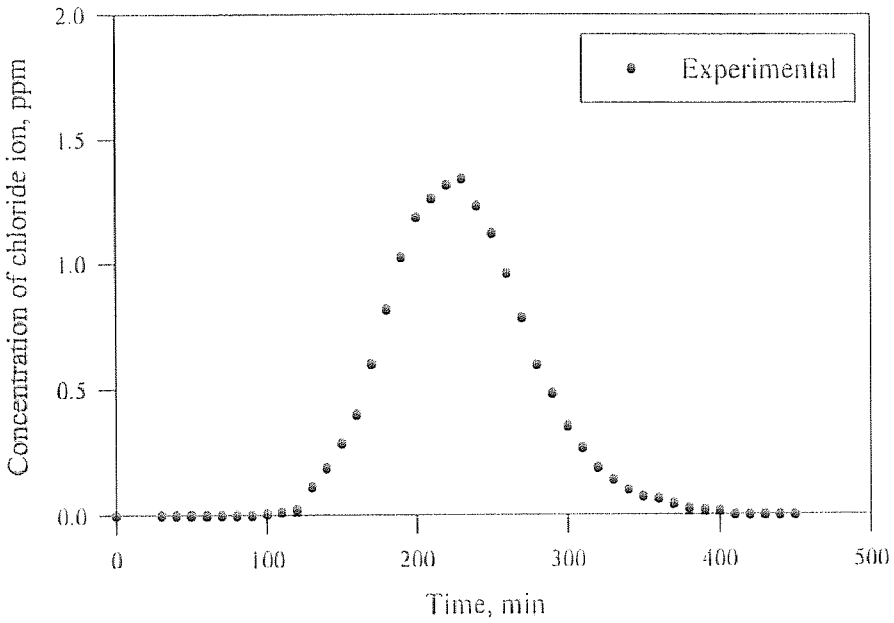

Figure 6.8 Elution data of chloride ion in the soil column (col#2). Mean residence time=229.9 min, variance=2161.4 min^2 (run# A-6)

6.4 Laboratory Soil Column Experiments and Model Simulations with Excess Oxygen

6.4.1 Experimental Results and Model Simulations

This section describes the experimental results obtained from the laboratory soil columns, as compared to the model simulations. Table G-1 and G-2 show the data for two repeat runs. The room temperature varied from 15 °C to 21 °C, and the columns were not jacketed. A steady average flow of about 1.1 mL/min was maintained during the 5-day period of each experiment. The feed solution was a sterilized synthetic medium containing 23.7 and 23.0 ppm of 2-chlorophenol, respectively, in the two experiments. During these runs, samples were taken at the same time from the inlet and the outlet of the column. Table 6.7 summarizes the results, and Figure 6.9 plots the data and the model simulations in terms of dimensionless variables.

Table G-3 and Figure 6.10 show the results of the experiment in a sterile column, during which 200 ppm $HgCl_2$ and 4 mM $CaCl_2$ solution were included in the feed solution (23.4 ppm 2-CP) to maintain sterility and soil integrity respectively. The model simulation agrees quite well with the data, although breakthrough occurs somewhat faster (14 hours rather than 30 hours in experiment). None of the parameters in this experiment were fitted to the data. All were obtained from laboratory experiments, empirical correlations, or estimations based on prior literature values.

The parameter values required for solving the equations are listed in Table 6.8. The dispersivity (D_{le}) was obtained from the tracer experiments with NaCl (section 4.5.3).

Table 6.7 Comparison of data to check the reproducibility between run#1 and run#2.

Run No.	Duration of experiment (day)	Ave. initial concentration (ppm)	Approx. final steady conc., (ppm)	% depletion at steady state
run# 1	~ 5.0	23.7	12.7	46.4
run# 2	~ 5.0	23.0	12.8	44.3

The diffusion coefficient of 2-CP in aqueous medium was estimated based on the Wilke and Chang correlation [Wilke and Chang (1955)]:

$$D_{AB} = 1.173\text{x}10^{-16} \cdot (\varphi \cdot M_B)^{0.5} \left(T/\mu_B \cdot V_A^{0.6}\right)$$

where all the parameters are in the MKS systems. The value of D_{AB} (or D_{se}) given in Table 6.9 was calculated at 18 °C.

Based on the asdorption rate data shown in Figure 6.5, the "true" (kinetic-dependent) rate of adsorption is very rapid. This was also found by other investigators [Bayard (1997), Bouchard et al. (1988), and Miller and Weber (1986)]. Therefore the term A_d in equations (5.1) and (5.36) was eliminated in the simulations.

The correlation for mass transfer coefficient was adapted from Wilson and Geankoplis (1966) and is given as,

$$k_m = 1.09 \cdot (\overline{V}_z / \varepsilon_b) \cdot (N_{Re} \cdot N_{Sc})^{-2/3}$$

where, k_m is expressed in cm/sec. This correlation is valid for $0.0016<N_{Re}<55$ and $0.35<\varepsilon_b<0.75$.

The Freundlich parameters (k_p and n) were obtained from the adsorption isotherms of 2-CP on Pequest soil.

K_i, K_s, and Y were obtained from the batch biokinetic experiments.

The value of the radius of soil aggregates (R) was taken from literature estimates [Crittenden et al. (1986) and Hutzler et al. (1986)].

The Porosity of the aggregates (ε_a) is taken from literature estimates [Crittenden et al. (1986), Hausenbuiller (1978), and Hutzler et al. (1986)].

The total bed porosity (ε_b) was obtained experimentally (section 4.5.4).

The soil density (ρ_s) was obtained experimentally (section 4.5.5).

The pore velocity ($\bar{v}_z$) in the soil column (0.00222 cm/sec, or 192 cm/day) was calculated from the feed flow rate, column dimensions and bed porosity (this velocity is somewhat higher than those encountered in "typical" groundwater flows, which range from 10 to 30 cm/day, depending on soil type and permeability).

The specific growth rate parameter ($\hat{\mu}$) was obtained from batch kinetic experiments.

Initially $\hat{\mu}_c$ was estimated as $1/10^{th}$ of $\hat{\mu}$ based on a review of the literature [Bailey and Ollis (1986), Bosma (1994), and Chen et al. (1992)]. Results are shown in Figure 6.9 (SIMU-0A). Since this was a very poor fit of the data, it was next attempted to increase $\hat{\mu}_c$ to 72% of $\hat{\mu}$ (SIMU-05). In this case $\hat{\mu}_c$ would represent a net loss of biomass, due to transport from the system as well as cell death.

For bo (the initial biomass concentration), an estimate of 24 ppm was used initially (SIMU-0A and SIMU-05), based on 34 ppm in the solution with which the column was seeded (section 4.5.2). However, 10 ppm resulted in a better data fit (SIMU-

04). The "true" value of bo would be difficult (if not impossible) to determine independently.

Table 6.8 Parameter values used in the model simulations.

Symbol	Parameters	Units	Values used in simulation
D_{le}	Dispersion coefficient of 2-CP in mobile phase	cm^2/sec	$6.89x10^{-4}$ (expt)
D_{se}	Diffusion coefficient of 2-CP in aggregates	cm^2/sec	$7.2x10^{-6}$ (correla)
k_d	Adsorption rate constant	sec^{-1}	very rapid
k_m	Mass transfer coefficient	cm/sec	$2.77x10^{-4}$ (correla)
k_p	Freundlich parameter	$(L/kg)^{1/n}$	1.71 (expt)
K_1	Andrews parameter	mg/L	73.6 (expt)
K_S	Andrews parameter	mg/L	2.4 (expt)
n	Freundlich parameter	---	1.5 (expt)
R	Aggregate radius	cm	0.10 (estimate)
Y	Yield coefficient	mg biomass per mg substrate degraded	0.40 (expt)
ε_a	Void fraction of aggregate	---	0.25 (estimate)
ε_b	Void fraction of mobile phase	---	0.42 (expt)
ρ_S	Soil density	g/cm^3	1.70 (expt)
$\hat{\mu}$	Andrews parameter	sec^{-1}	$5.55x10^{-5}$ (expt)
$\hat{\mu}_C$	Andrews parameter	sec^{-1}	$4.00x10^{-5}$ (estimate)

- Pore velocity, $\bar{v}_z$=0.00222 cm/sec (expt)
- Initial dimensionless biomass conc. in the column (bo)=4.0 (i.e. ~10mg/L)

As another model simulation, $\hat{\mu}$ was arbitrarily decreased by a factor of 5 (with $\hat{\mu}_C$ still $1/10^{th}$ of $\hat{\mu}$), as shown in Figure 6.9 (SIMU-06). In this simulation, b_o was once

again 10 ppm. The rationale was that $\hat{\mu}$ might be smaller than indicated by the suspended culture specific growth rate [Caldwell and Lawrence (1986), Doran (1985), Gordon (1983), Jeffrey and Paul (1986), Kieft and Caldwell (1984), van Loosdrecht et al. (1990), and Shreve and Vogel (1993)]. However, this did not lead to a satisfactory fit of the soil column data.

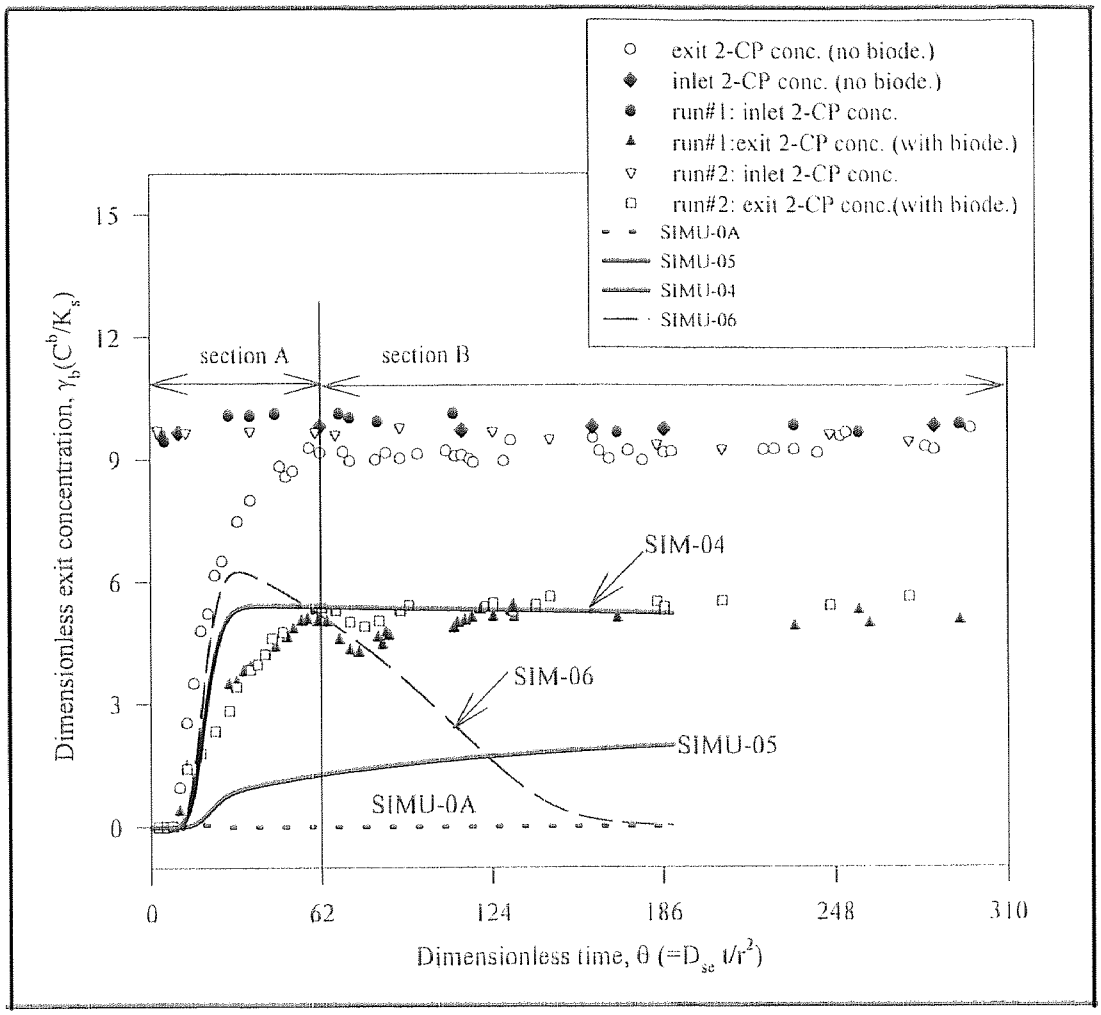

Figure 6.9 Mobile phase concentrations at the inlet and exit of the soil column. (in the time axis, 1 day is equivalent to 62).

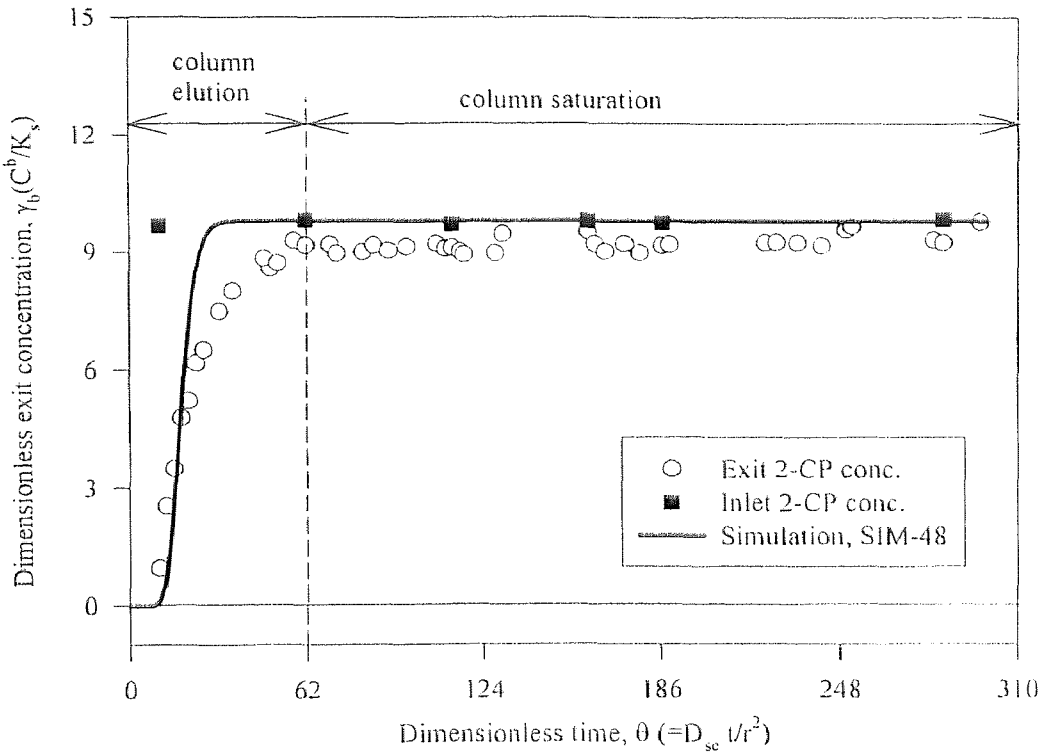

Figure 6.10 Mobile phase concentrations at the inlet and exit of the soil column in the absence of bacteria (in the time axis, 1 day is equivalent to 62).

6.4.2 Mobile Phase and Aggregate Profiles

Figure 6.11 shows "typical" pollutant concentration profiles within an aggregate located about the middle of the soil column. This is a simulation only, no measurements were possible. These profiles are flat because of diffusion into the aggregate, combined with biodegradation at the outer periphery of the aggregate where pollutant concentration (and therefore the rate of biodegradation) is highest.

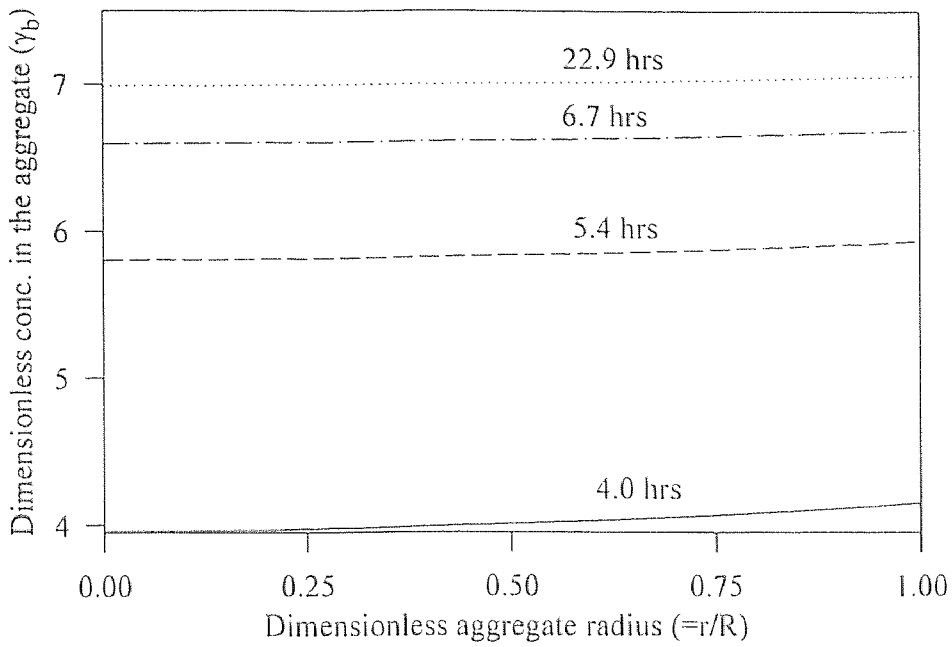

Figure 6.11 Simulated pollutant concentration profiles inside an aggregate located about the middle of the soil column (with excess oxygen).

Figure 6.12 shows the simulated pollutant concentration profiles within the soil column in the axial direction for a "new" spill (same conditions as in SIMU-04).

Figure 6.13 shows simulated biomass concentration profiles within an aggregate located about the middle of the soil column. Once again, the radial variation is small, since changes in biomass concentration follow the pollutant profile. At first, biomass at any radial point decreases, passes through minimum, and then increases. This is due to the choice of initial biomass concentration, which at first can not be sustained by the initially low pollutant concentration.

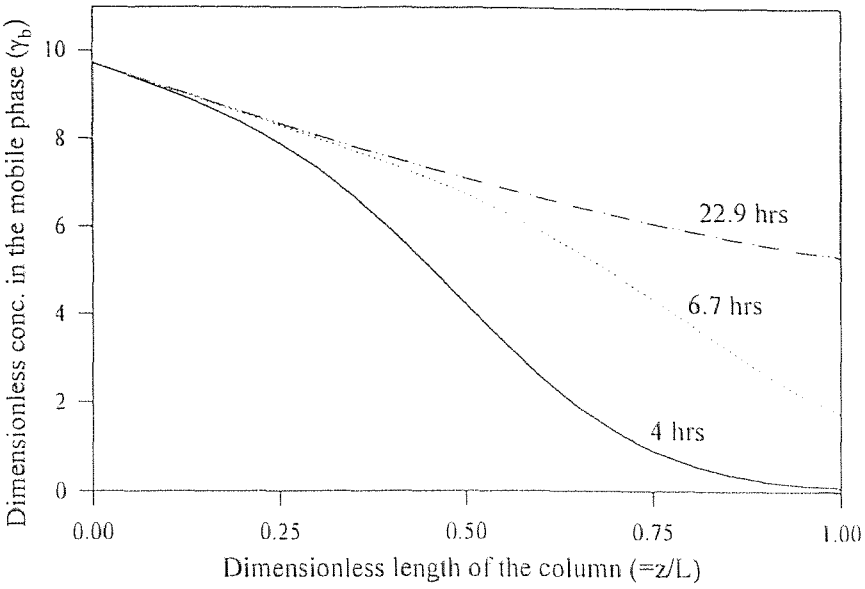

Figure 6.12 Simulated pollutant concentration profiles in the axial direction (with excess oxygen).

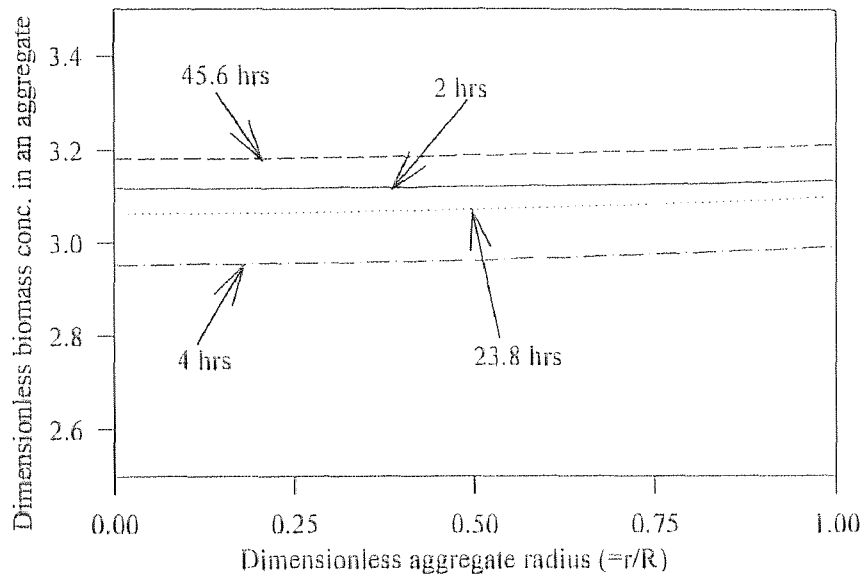

Figure 6.13 Simulated biomass concentration profiles inside an aggregate located about the middle of the soil column (with excess oxygen).

6.4.3 Sensitivity Analysis

In the previous section, the experimental results and model predictions are discussed. The plots (Figures 6.9 and 6.10) imply the model formulated in this study has the ability to account for the considered physicochemical processes encountered in an in-situ situation for a "new" spill case. This section presents the parametric sensitivity of the model based on the base values given in Table 6.8.

The parameters and variables studied for sensitivity analysis are: feed inlet concentration ($C_{z_{0^-}}$), axial dispersion coefficient (D_{le}), bed porosity (ε_b), mass transfer coefficient (k_m), Freundlich parameter (n), Peclet number (Pe), and pore velocity ($\bar{v}_z$). Table 6.9 shows the range of values chosen.

Table 6.9 Relative values of the parameters and variables.

Symbol	Units	Low Relative to Base Value	Base Value	High Relative to Base Value
$C_{z_{0^-}}$	mg/L	10	23.5	40
D_{le}	cm^2/sec	$6.89x10^{-5}$	$6.89x10^{-4}$	$6.89x10^{-3}$
ε_b	---	0.32	0.42	0.52
k_m	cm/sec	$2.77x10^{-5}$	$2.77x10^{-4}$	$2.77x10^{-3}$
n	---	0.50	1.49	2.0
Pe	---	7.7	77.0	770
$\bar{v}_z$	cm/sec	$2.22x10^{-4}$	$2.22x10^{-3}$	---

6.4.3.1 Feed Inlet Concentration ($C_{z_{0^-}}$): Figure 6.14 shows that the 2-CP concentration at the feed inlet has a strong influence on the biodegradation pattern in the column. The concentrations are 40 ppm (SIMU-11), 23.5 ppm (SIMU-04), and 10 ppm (SIMU-12). From the plot, it appears that the biomass growth pattern varies with different initial concentrations. As the 2-CP concentration increases, the percent biodegradation goes down. For example, after one day, 67.6%, 45.0%, and 19.4%, respectively, of the 2-CP is biodegraded. This is due to inhibition at higher concentrations.

6.4.3.2 Axial Dispersion Coefficient (D_{le}): Figure 6.15 shows the effect of axial dispersion on the column performance, emphasizing that hydrodynamic effects tend to have less importance than biokinetic effects.

6.4.3.3 Effect of Bed Porosity (ε_b): Bed porosity has a pronounced effect on the performance of the soil column (Figure 6.16). From the plot, it shows that higher porosity gives rise to an earlier breakthrough, with lower biodegradation. This is due to the fact that as porosity increases, the amount of soil biocatalyst decreases.

6.4.3.4 Effect of Mass Transfer Coefficient (k_m): Figure 6.17 shows the effect of mass transfer coefficient (k_m) on the pollutant concentration at the exit of the soil column, which is not very significant for the range of values tested.

6.4.3.5 Effect of Freundlich Parameter (n): Figure 6.18 shows the effect of 'n' on the contaminant distribution of the liquid inside the soil column. By changing its value from 0.5 to 2.0, no change is seen in the aqueous concentration profile (C_b). This is a result of the rapid (relatively) approach to sorption equilibrium vs. the general time scale of the process.

6.4.3.6 Peclet Number ($Pe=\bar{v}_z \cdot L/D_{le}$): Figure 6.19 shows the effect of Peclet number (Pe) on the 2-CP concentration profile in the column. A high value of Pe denotes plug flow, while a low value indicates greater axial mixing in the soil column. Again, it indicates that purely hydrodynamic effects are less important than biokinetic effects, which justifies the modelling effort.

6.4.3.7 Pore Velocity ($\bar{v}_z$): Figure 6.20 shows the effect of pore velocity. SIMU-19 (19.2 cm/day) is more "typical" of actual groundwater velocities. The plot shows (logically) that increased residence time results in increased biodegradation.

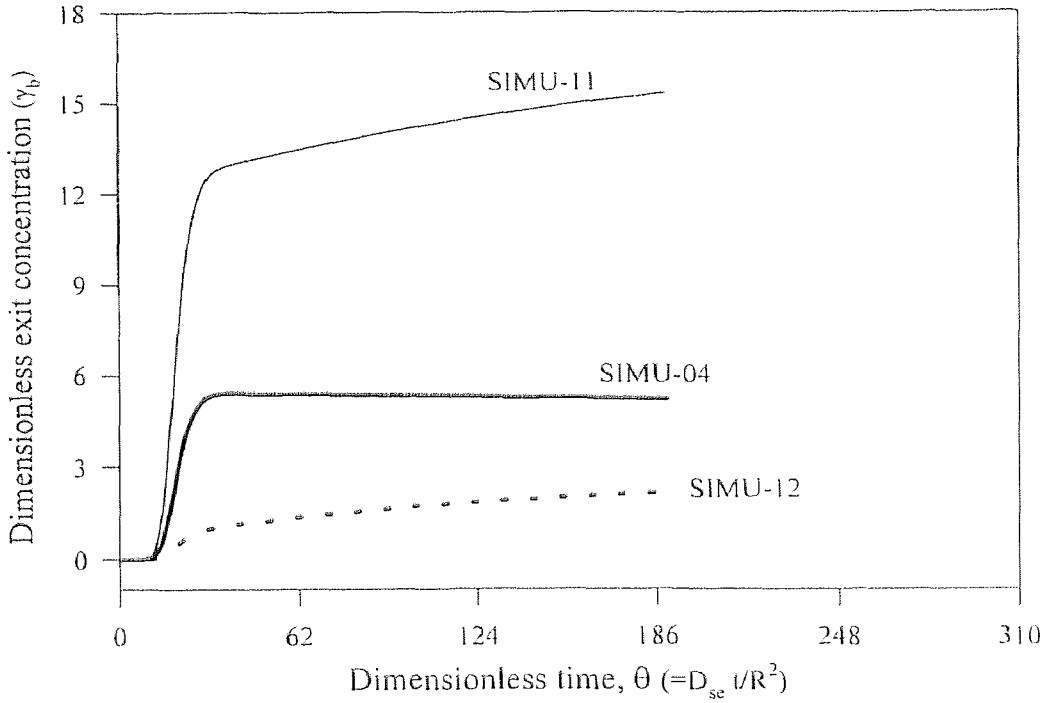

Figure 6.14 Effect of 2-CP concentration at the feed inlet (C_{z_0}). Concentrations are: 10.0 (SIMU-12), 23.5 (SIMU-04), and 40.0 mg/L (SIMU-11).

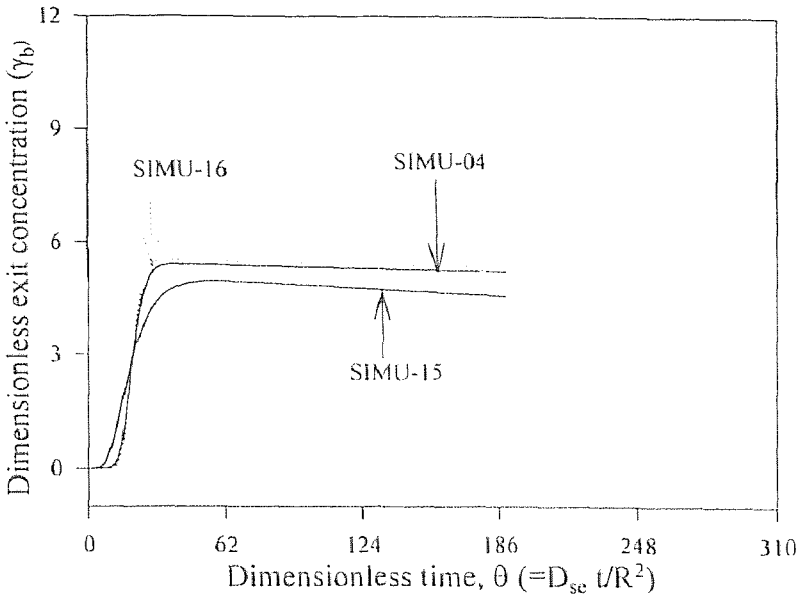

Figure 6.15 Effect of axial dispersion (D_{le}). Values are: 6.89×10^{-5} (SIMU-16), 6.89×10^{-4} (SIMU-04), and 6.89×10^{-3} cm^2/sec (SIMU-15).

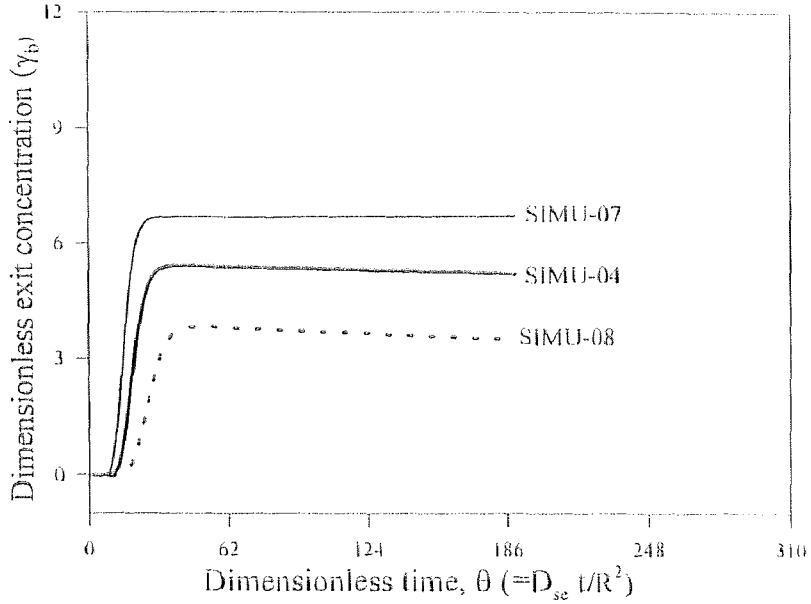

Figure 6.16 Effect of bed porosity (ε_b). Values are: 0.52 (SIMU-07), 0.42 (SIMU-04), and 0.32 (SIMU-08).

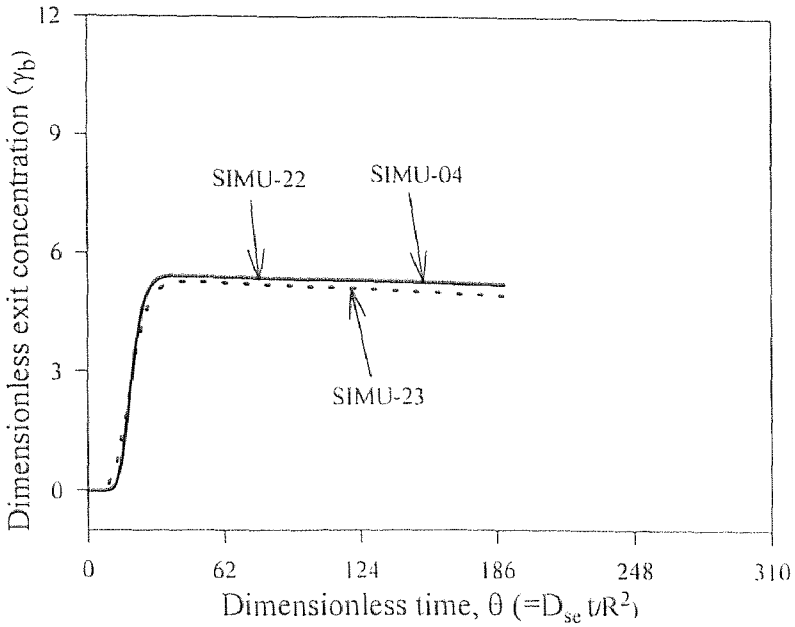

Figure 6.17 Effect of mass transfer coefficient (k_m). Values are: 2.77×10^{-5} (SIMU-22), 2.77×10^{-4} (SIMU-04), and 2.77×10^{-3} cm/sec (SIMU-23).

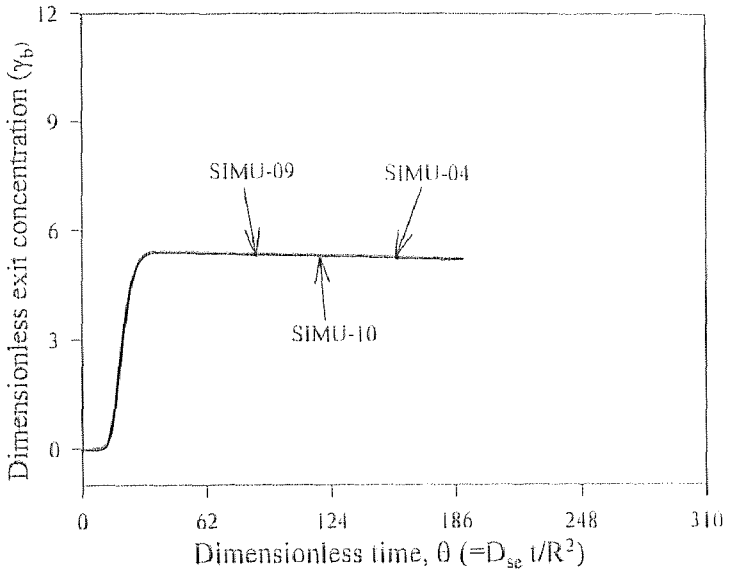

Figure 6.18 Effect of Freundlich parameter (n). Values are: 0.5 (SIMU-10), 1.49 (SIMU-04), and 2.0 (SIMU-09).

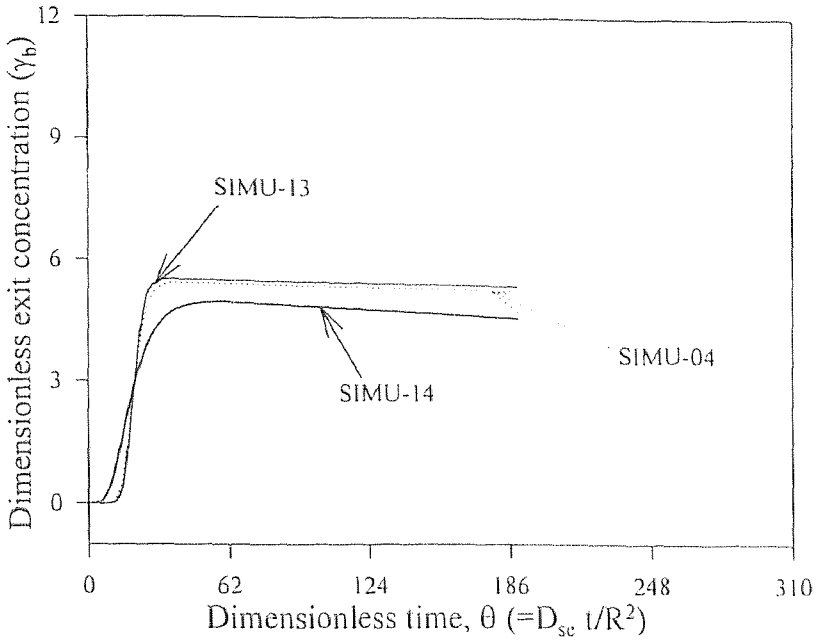

Figure 6.19 Effect of peclet number (Pe). Values are: 7.7 (SIMU-14), 77.0 (SIMU-04, base simulation), and 770 (SIMU-13).

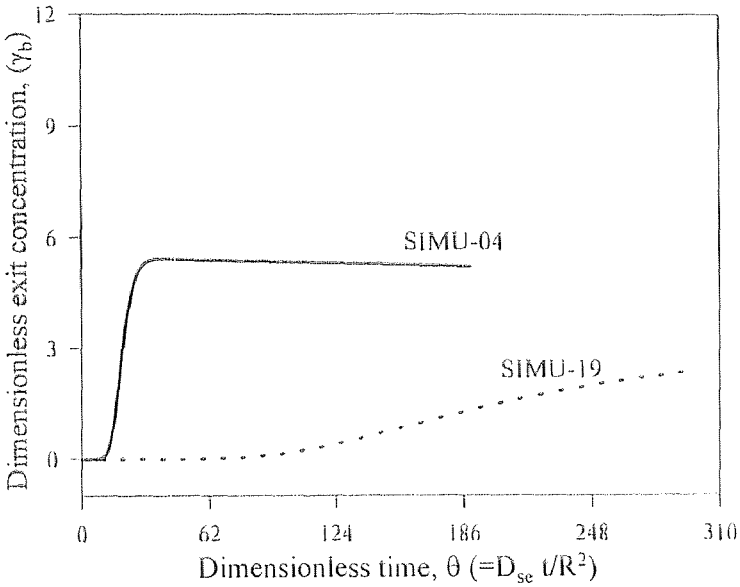

Figure 6.20 Effect of pore velocity ($\overline{v}_z$). Values are: 2.22×10^{-4} (SIMU-19) and 2.22×10^{-3} (SIMU-04) cm/sec.

6.5 Model Simulations with Oxygen Limitation

In the previous section, experimental results from soil column experiments and the model simulations including parametric sensitivity (section 6.4.2), were discussed with the assumption of an excess oxygen environment. In order to obtain simulations of the effect of oxygen in the soil column, the parameters listed in Table 6.8 and those in Table 6.10 were both utilized.

These simulations were not checked experimentally, because of difficulties encountered with oxygen measurements in the soil column (larger samples, or microelectrodes, were needed).

Table 6.10 Additional parameters required for simulation with oxygen limitation.

Symbol	Parameters	Units	Values used in simulation
D_{lo}	Dispersion coefficient of oxygen in the mobile phase	cm^2/sec	6.89×10^{-4} (expt)
D_{so}	Diffusion coefficient of oxygen in aggregates	cm^2/sec	1.86×10^{-5} (correla)
k_{so}	Mass transfer coefficient of oxygen	cm/sec	5.20×10^{-4} (correla)
K_{so}	Kinetic constant of oxygen	mg/L	0.26 (estimate)
Y_O	Yield coefficient due to oxygen	mg biomass per mg oxygen consumed	0.37 (estimate)

- Pore velocity, $\bar{v}_z$=0.00222 cm/sec (expt.)
- Initial biomass concentration in the column (b_o)=10.0 mg/L

The dispersivity (D_{le}) was obtained from the tracer experiments with NaCl (section 4.5.3), and assumed to be the same for both dissolved oxygen and pollutant.

The diffusion coefficient of oxygen in aqueous medium was estimated based on the Wilke and Chang correlation [Wilke and Chang (1955)]:

$$D_{AB} = 1.173 \times 10^{-16} \cdot (\varphi \cdot M_B)^{0.5} \left(T/\mu_B \cdot V_A^{0.6} \right)$$

where all the parameters are in the MKS systems. The value of D_{AB} (or D_{sc}) given in Table 6.9 was calculated at 18 °C.

The correlation for mass transfer coefficient was adapted from Wilson and Geankoplis (1966) and is given as,

$$k_m = 1.09 \cdot (\overline{V}_z / \varepsilon_b) \cdot (N_{Re} \cdot N_{Sc})^{-2/3}$$

where, k_m is expressed in cm/sec. This correlation is valid for $0.0016 < N_{Re} < 55$ and $0.35 < \varepsilon_b < 0.75$.

The Monod kinetic constant (K_{so}) was estimated based on a literature review [Shareefdeen (1994)].

The value of the yield coefficient (Y_o) was estimated as follows [Shuler and Khargi (1992)]. A typical cellular composition can be represented as $CH_{1.8}O_{0.5}N_{0.2}$. Assuming that $(NH_4)_2(SO_4)$ was solely used as nitrogen source, and using the value of Y (0.4 for 2-CP), the following balanced equation can be written,

$$C_6H_5OCl + 4.3\ O_2 + 0.21\ (NH4)_2\ (SO_4) \Rightarrow 2.09\ CH_{1.8}O_{0.5}N_{0.2} + 0.75\ H_2O + 3.90\ CO_2 + HCl + 0.21\ H_2SO_4 \qquad (6.15)$$

Using equation (6.15), the yield coefficient of biomass on oxygen (with 2-chlorophenol as carbon source) was calculated to be 0.37 mg biomass per mg oxygen.

With an intent to see the effect of electron acceptor (i.e. oxygen) on the laboratory column performance, simulations were performed for three scenarios: (1) under severely oxygen limited conditions (i.e. 1.2 mg/L oxygen in the feed); (2) when feed is saturated with oxygen under atmospheric air (i.e. 8.0 mg/L); and (3) when the dissolved oxygen in the feed is elevated under a pure oxygen atmosphere (to 23 mg/L). *For each simulation, the designated amount of oxygen was initially assumed to be present everywhere in the column, and the subsequent oxygen entree to the column was with the feed only.*

Simulation results are shown in Figure 6.21 and 6.22, which represent the dimensionless exit concentrations of pollutant and oxygen, respectively. Figure 6.21 indeed shows that oxygen has a strong influence on the column behavior. Simulation corresponding to 1.2 mg/L oxygen in the feed shows almost no biodegradation (POLLU-26). Simulation corresponding to saturation (8.0 mg/L) in the feed shows some biodegradation. However, an examination of the oxygen profile (OXY-25) shows that the concentration drops rapidly and remains below 3 mg/L in the effluent. Finally, simulation corresponding to an elevated oxygen concentration in the feed (23 mg/L) under a pure oxygen atmosphere (saturation is about 40 mg/L in water) results in nearly the same effluent as that assuming excess oxygen. This is because the oxygen concentration remains above 9 mg/L in the column effluent (OXY-27).

Figure 6.23 shows the oxygen concentration profiles inside an aggregate located at the exit of the column. The conditions for this simulation corresponds to POLLU-25

(Figure 6.21) and OXY-25 (Figure 6.22). Once again, the profiles are flat. The oxygen concentration at any particular radial point initially decreases (because of consumption of the initial O_2 in the column) and then rises as O_2 enters with the feed.

Figure 6.24 shows oxygen concentration profiles within the soil column in the axial direction for a "new" spill (once again corresponding to the conditions of POLLU-25).

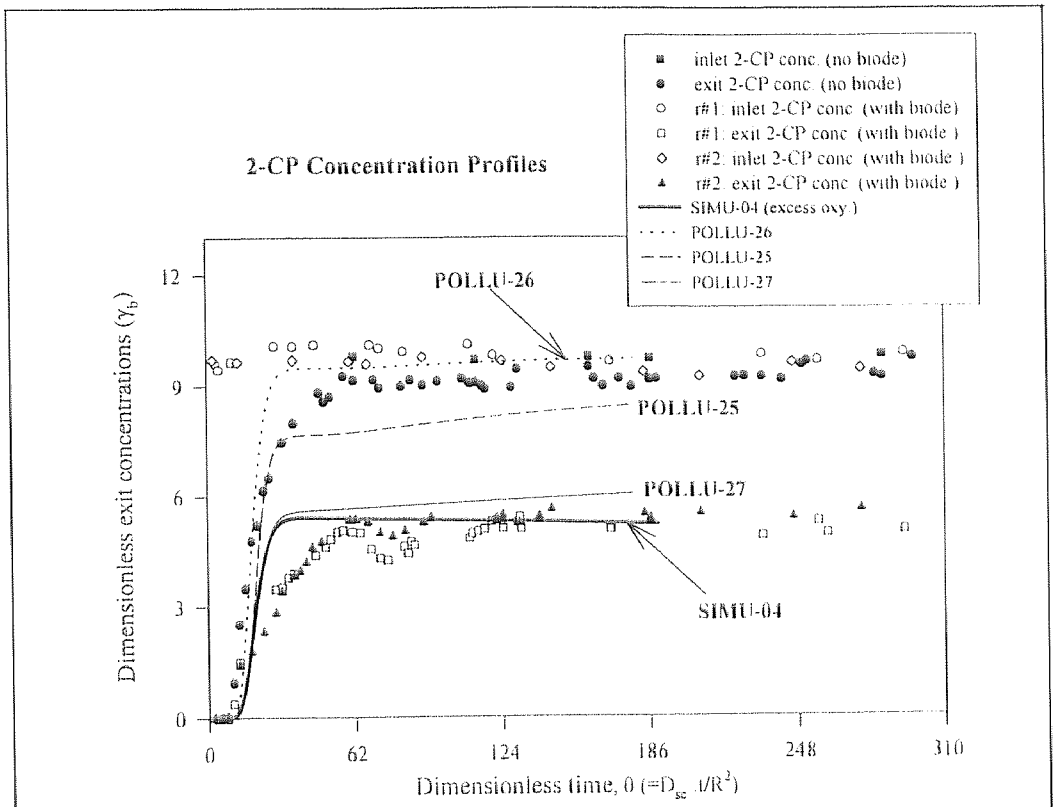

Figure 6.21 Effect of electron acceptor (oxygen) on the column performance. Inlet oxygen concentrations are: 1.2 (POLLU-26), 8.0 (POLLU-25), and 23 ppm (POLLU-27). Inlet 2-CP concentration=23.5 ppm.

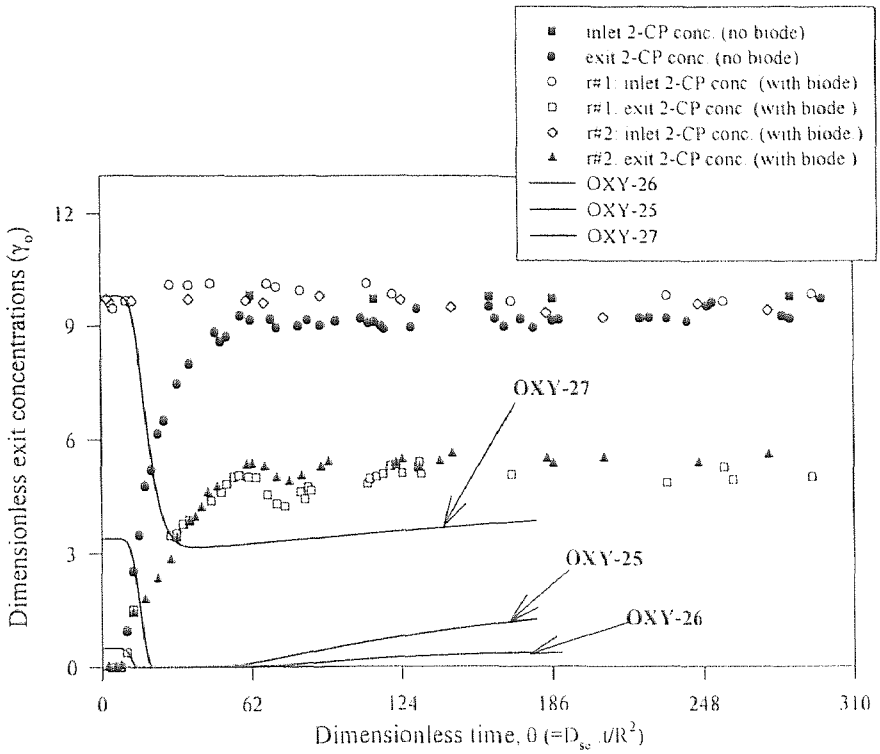

Figure 6.22 Simulated oxygen concentration profiles. Inlet oxygen concentrations are: 1.2 (OXY-26), 8.0 (OXY-25), and 23 ppm (OXY-27). Inlet 2-CP conc.=23.5 ppm.

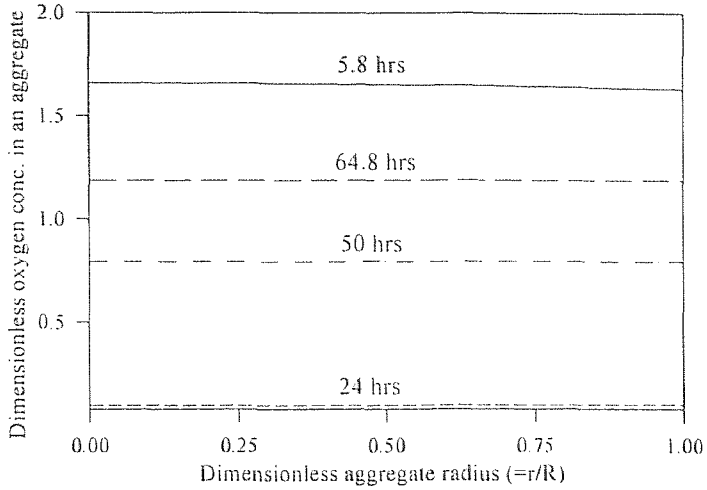

Figure 6.23 Simulated oxygen concentration profiles inside an aggregate located at the exit of the column.

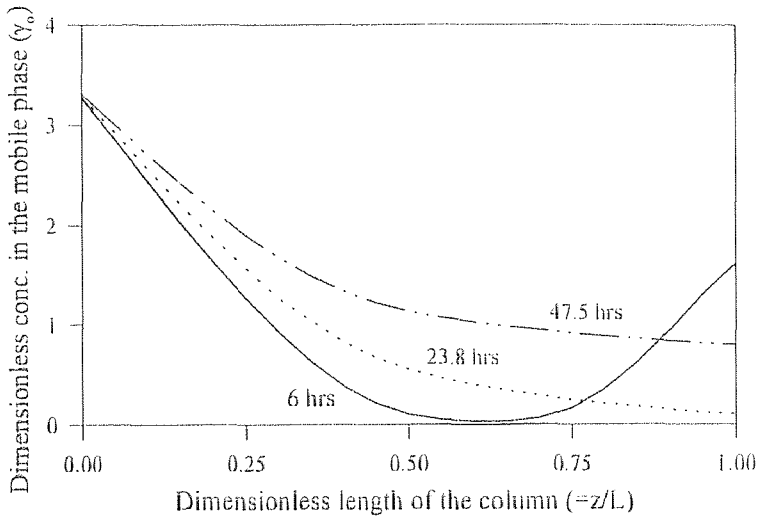

Figure 6.24 Simulated oxygen concentration profiles in the axial direction.

Figure 6.25 shows the sensitivity of the simulations to changes in K_{so} and Y_o. For all these simulations, an inlet oxygen concentration of 8.0 mg/L was used. Again, the simulations are sensitive to changes in the biokinetic parameters, with K_{so} being more sensitive than Y_o.

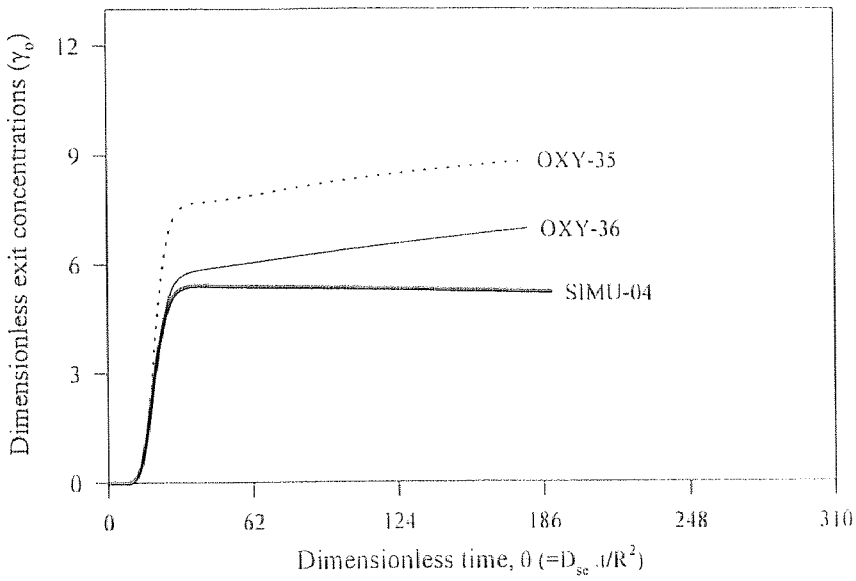

Figure 6.25 Effect of K_{SO} and Y_O on column performance. Values are: K_{SO}=0.50 and Y_O=0.37 (OXY-35); K_{SO}=0.26 and Y_O=1.2 (OXY-36). Inlet conc. of 2-CP=23.5 ppm.

CHAPTER 7

CONCLUSIONS AND FUTURE WORK

7.1 Conclusions

In-situ bioremediation in its entirety is a very complex process, which depends on the physical system (soil geology, soil chemistry, hydrology, distribution of nutrients and electron acceptors, etc.) and on the microbial ecology.

In order to predict and quantify the fate of pollutants in an in-situ bioremediation system, currently there are many existing models which typically place greater emphasis on hydraulic and physical parameters, such as the "true" diffusivity, or permeability, of the soil structure, and much less emphasis on kinetic effects. When biodegradation is included at all, it is generally assumed to be in equilibrium with the bulk liquid concentration, and biodegradation is assumed to follow a first-order or Monod (non-inhibitory) model. Quite often, these models also assume constant biomass; thereby neglecting biomass growth, which can have a profound impact on the performance of a bioremediation system. They also neglect the effect of oxygen limiting situations, which again has an important effect on performance.

In this dissertation, a mathematical model was developed of in-situ bioremediation in the saturated zone which is analogous to a packed-bed of catalyst particles. The model considers diffusion, sorption, and biodegradation in the "catalyst" (namely, soil aggregates); and convection, diffusion, and mass transfer from the aggregates into the surrounding groundwater. The soil aggregates are considered to be

agglomerated soil particles with relatively stagnant fluid in the interstices. Biomass is attached to the individual soil particles which are considered to be small compared to the overall aggregate diameter. Thus, mathematically, the interior of the aggregates is treated as a case of homogeneous catalysis.

In order to solve the set of resulting non-linear, coupled PDEs, the following parameters had to be determined by a combination of laboratory experiments, empirical correlations, or estimates based on prior work:

Parameters	**Symbol**	**Method of determination**
Dispersion coefficient of 2-CP in mobile phase	D_{le}	Experiment
Dispersion coefficient of oxygen in the mobile phase	D_{lo}	Experiment
Diffusion coefficient of 2-CP in aggregates	D_{se}	Correlation
Diffusion coefficient of oxygen in aggregates	D_{so}	Correlation
Adsorption rate constant	k_d	Experiment
Mass transfer coefficient	k_m	Correlation
Freundlich parameter	k_p	Experiment
Andrews parameter	K_i	Experiment
Andrews parameter	K_S	Experiment
Mass transfer coefficient of oxygen	k_{so}	Correlation
Kinetic constant of oxygen	K_{so}	Estimate
Freundlich parameter	n	Experiment
Aggregate radius	R	Estimate
Yield coefficient	Y	Experiment
Yield coefficient due to oxygen	Y_O	Estimate
Void fraction of aggregate	ε_a	Estimate
Void fraction of mobile phase	ε_b	Experiment
Soil density	ρ_S	Experiment
Andrews parameter	$\hat{\mu}$	Experiment
Andrews parameter	$\hat{\mu}_C$	Estimate

The resulting equations were solved using the "Method of Lines", and a stable numerical solution was obtained. Sensitivity analyses showed the biokinetic parameters ($\hat{\mu}$ and $\hat{\mu}_C$), initial biomass concentration, feed inlet concentration, average pore velocity, and bed porosity have strong effects on the system results. Other parameters (e.g. axial dispersion coefficient, Peclet number, mass transfer coefficient, and Freundlich parameters) had little effect on column performance (for the ranges of parameter values tested).

The model was compared against experiments, using a 24 cm long, 5 cm inside diameter laboratory soil column packed with soil from a site in Pequest, NJ. The method of column packing was an important step in column preparation to maintain consistency, avoid channeling and non-uniform flow distribution. Column packing was tested by axial dispersivity measurements. The column was seeded with a pure culture of *Pseudomonas pickettii*, and 2-chlorophenol was the test pollutant. Two successful biodegradation runs were made on one packed column. A separate set of experiments on another column was performed without any biomass present. Sterility was maintained by including 200 ppm mercuric chloride in the feed. Calculated dispersivities (using NaCl tracer) were nearly the same for both columns.

Three interrelated microbial parameters: $\hat{\mu}$, $\hat{\mu}_C$, and the initial biomass concentration (b_o), have a strong influence on the exit concentration profiles. The first simulation, with $\hat{\mu}_C$ estimated as $1/10^{th}$ of $\hat{\mu}$, resulted in a poor fit of the data. For b_o (the initial biomass concentration), an estimate of 24 ppm was used initially, based on 34 ppm in the solution with which the column was seeded. When $\hat{\mu}_C$ was increased to 72%

of $\hat{\mu}$, and b_o was decreased from 24 to 10 ppm, a good fit of the soil column data was obtained. The "true" value of b_o would be difficult (if not impossible) to determine independently (presumably, as a steady-state is approached, the initial choice of b_o should become less importanct). Such a high value of $\hat{\mu}_C$ would represent the net loss of microorganisms from the system, including not only cell death, but losses due to transport as well.

The effects of oxygen limitation are also quite pronounced. Even when the column is saturated with atmospheric oxygen (8 mg/L), bioremediation is severely limited by oxygen availability. Only when oxygen in the feed reached 23 mg/L (possible with a pure oxygen atmosphere) did the results approach those assuming no oxygen limitation.

These results clearly emphasize the paramount importance of the biokinetic parameters in the modelling results, in the laboratory soil column, and presumably in the field as well. Biomass growth and loss, and the effects of oxygen limitation, overwhelmed any effects due to transport or flow.

7.2 Future Work

Future work would benefit greatly by having an independent measure of biomass in the soil columns. This is a difficult problem to solve, but biochemical (e.g. lipid profiles) and fluorescent techniques hold some promise.

Microbial consortia and mixed substrates can also be examined (rather than a pure culture and single substrate, such as used in this dissertation).

Finally, field tests of the model are already planned at former sites of manufactured gas plants, in which the electron acceptors are most likely Fe^{+3} and $SO_4^{=}$.

APPENDIX A

DETAILED TREATMENT OF BOUNDARY CONDITIONS [EQUATIONS (5.13) AND (5.15)] FOR THE MOBILE PHASE AT THE EXIT AND ENTRANCE POINTS OF THE LABORATORY SOIL COLUMN

In the following, a detailed treatment has been given by performing mass balance considering fundamental principles for obtaining the exit and entrance boundary conditions [e.g. equations (5.13) and (5.15) in Chapter 5] in the mobile phase.

At the entrance of the bed (i.e. at z=0 in the Figure A-1), molar flow rate of the pollutant must be the same between upstream section of the column ($z=0^-$) and bed entrance point (z=0). Therefore, it can be expressed as,

$$F_b\Big|_{z=0^-} = F_b\Big|_{z=0} \qquad (A1.1)$$

where $F_b\Big|_{z=0}$ is the sum of convection due to superficial liquid velocity and molecular dispersion at $z=0^-$; and $F_b\Big|_{z=0}$ is the sum of convection due to liquid pore velocity and molecular dispersion at z=0. Now, $F_b\Big|_{z=0}$ can be written as,

$$F_b\Big|_{z=0^-} = Q \cdot C\Big|_{z=0^-} - A \cdot D_b \cdot \frac{\partial C}{\partial z}\Big|_{z=0^-} \qquad (A1.2)$$

where, Q is the volumetric flow rate. A is the empty bed cross-sectional area ($= \frac{\pi}{4} d^2$). C is the inlet concentration at $z=0^-$. D_b is the dispersion coefficient. Also defining v_z as the superficial liquid velocity (= Q/A), equation (A1.2) can be written as,

$$F_b\Big|_{z=0} = (\frac{\pi}{4} d^2) \cdot v_z \cdot C\Big|_{z=0^-} - (\frac{\pi}{4} d^2) \cdot D_b \cdot \frac{\partial C}{\partial z}\Big|_{z=0^-} \qquad (A1.3)$$

Now, just at the entrance point to the bed i.e. z=0, right hand side of equation (A1.1) can be expressed as,

$$F_b\Big|_{z=0} = (\frac{\pi}{4} d^2) \cdot \varepsilon_b \cdot \overline{v}_z \cdot C\Big|_{z=0} - (\frac{\pi}{4} d^2) \cdot \varepsilon_b \cdot D_b \cdot \frac{\partial C}{\partial z}\Big|_{z=0} \qquad (A1.4)$$

where, $\bar{v}_z$ is the liquid pore velocity and is defined by ($\bar{v}_z = v_z/\varepsilon_b$) and $(\frac{\pi}{4}d^2 \cdot \varepsilon_b)$ is the cross sectional area just after the entrance into the column.

It is now assumed that, in the upstream section ($z=0^-$) the liquid is well mixed and hence concentration gradient is assumed to be zero. Then equation (A1.3) yields,

$$F_b\Big|_{z=0^-} = (\frac{\pi}{4}d^2) \cdot v_z \cdot C\Big|_{z=0^-} \qquad (A1.5)$$

Combining equations (A1.4) and (A1.5) it can be written as,

$$(\frac{\pi}{4}d^2) \cdot \varepsilon_b \cdot \bar{v}_z \cdot C\Big|_{z=0^-} = (\frac{\pi}{4}d^2) \cdot \varepsilon_b \cdot \bar{v}_z \cdot C\Big|_{z=0} - (\frac{\pi}{4}d^2) \cdot \varepsilon_b \cdot D_b \cdot \left.\frac{\partial C}{\partial z}\right|_{z=0} \qquad (A1.6)$$

After rearrangement equation (A1.6) gives rise to,

$$\bar{v}_z \cdot \left(C\Big|_{z=0^-}\right) = \bar{v}_z \cdot C\Big|_{z=0} - D_b \cdot \left.\frac{\partial C}{\partial z}\right|_{z=0} \qquad (A1.6)$$

Redefining some of the variables as $C\Big|_{z=0^-} = C_{z_{0^-}}$; and also $D_b = D_{le}$, it is obtained as,

$$\bar{v}_z \cdot C_{z_{0^-}} = \bar{v}_z \cdot C_b - D_b \cdot \left.\frac{\partial C}{\partial z}\right|_{z=0} \qquad (A1.7)$$

This is the boundary equation (termed as Danckwerts boundary condition) at the entrance of the column (z=0), which is essentially equation (5.13) in Chapter 5.

In a similar manner, another boundary condition at the exit of the bed (z=L) can be written. At the exit of the bed (z=L), molar flow rate of the pollutant is the same between bed exit point (z=L) and downstream point ((z=L$^+$). Therefore,

$$F_b\Big|_{z=L} = F_b\Big|_{z=L^+} \qquad (A1.8)$$

The F-terms in equation (A1.8) are expressed as,

$$F_b\big|_{z=L} = \left(\frac{\pi}{4}d^2\right)\cdot\varepsilon_b\cdot\bar{v}_Z\cdot C\big|_{z=L} - \left(\frac{\pi}{4}d^2\right)\cdot\varepsilon_b\cdot D_b\cdot\left.\frac{\partial C}{\partial z}\right|_{z=L} \qquad (A1.9)$$

$$F_b\big|_{z=L^+} = \left(\frac{\pi}{4}d^2\right)\cdot v_Z\cdot C\big|_{z=L^+} - \left(\frac{\pi}{4}d^2\right)\cdot D_b\cdot\left.\frac{\partial C}{\partial z}\right|_{z=L^+} \qquad (A1.10)$$

where the parameters are described earlier.

It is assumed that the concentrations just outside the bed ($z=L^+$) were equal to the exit concentrations, therefore,

$$C_b\big|_{z=L} = C_b\big|_{z=L^+} \qquad (A1.10)$$

$$\text{and } \left.\frac{\partial C_b}{\partial z}\right|_{z=L^+} = 0 \qquad (A1.11)$$

Substituting expressions (A1.9) and (A1.10) in (A1.8) and applying (A1.11), and rearranging, the equation (A1.8) can be written as,

$$\varepsilon_b\cdot\bar{v}_Z\cdot C\big|_{z=L} - \varepsilon_b\cdot D_b\cdot\left.\frac{\partial C}{\partial z}\right|_{z=L} = v_Z\cdot C\big|_{z=L^+} \qquad (A1.12)$$

Now, applying condition from equation (A1.10) and substituting $v_z = \bar{v}_z\cdot\varepsilon_b$, the equation (A1.12) can be given as,

$$-D_b\cdot\left.\frac{\partial C_b}{\partial z}\right|_{z=L} = 0 \qquad (A1.13)$$

$$\text{This finally gives rise to: } \left.\frac{\partial C_b}{\partial z}\right|_{z=L} = 0 \qquad (A1.14)$$

This is the boundary condition at the exit of the bed ($z=L$), which is equation (5.15).

APPENDIX B

COMPUTER CODES

B-1 Computer Code for Solving Equations without Oxygen Limitation.

B-2 Computer Code for Solving Equations with Oxygen Limitation.

APPENDIX B-1

Computer Code for Solving Equations without Oxygen Limitation

```
C     ****************************************************************
C
C     Solution of the Model Equations "without" Oxygen Limitation
C
C     This code is written in FORTRAN for VAX/VMS environment
C     by Dilip Kumar Mandal
C
C     Method used:  Method of lines (MOL)
C
C     The ODEs are written in the subroutine "FCN" and then integrated using
C     standard IMSL subroutine named "DIVPAG' (Double Precision Version
C     of Initial Value Problem Utilizing Adams-Moulton or Gear Method)
C
C     ****************************************************************
C
C                         MAIN PROGRAM
C
C     EXTERNAL and COMMON LINKS to IMSL ROUTINE "DIVPAG" &"FCN"
C     MB=NB=discretized points in z-direction (X)
C     MR=NR=discretized points in r-direction (ETA)
C     MEQ=NEQ= total no. of equations
C     NEQ=MB+3*MB*MR
C     A(1,1)= parameter for the subroutine used
C     RWKSP and IWKIN are for workspace specification
C     NSTEP=Total number of steps
      parameter (NB=30, NR=20, NEQ=NB+3*NB*NR, NSTEP=1000000)
      implicit  real*8(A-H, O-Z)
      dimension ETA(NR), C(NEQ), X(NB), PARAM(50)
      dimension A(1,1)
      external FCN, FCNJ
      real *8 NDASH
      common /LIST1/ DSE,DLE,VOIDA,VOIDB,XMU,XMUC,XKP,XKD,XKM,
     $  DELT,TMAX,C1ZERO,GAMMAZO
     $  /LIST2/ PHIA, PHIB, PHIC, SHERA, SHERB,PSI,PEC,
     $  DELETA,DELX,NDASH,RHOS,XKS,XK1,XY,CONST1
     $  /LIST3/ETA
      common /WORKSP/RWKSP
      real RWKSP(600000)
      OPEN(UNIT=24,FILE='KUMAR.IN', STATUS='OLD')
      OPEN(UNIT=6,FILE='KUMAR.OUT',STATUS='NEW')
      call IWKIN (600000)
C
C     Reading of Input Data
C
C     V=Velocity
C     R=Radius of the particle
C     DSE=Effective diffusivity in the aggregate
C     DLE=Dispersion coefficient in mobile phase
```

```
C       VOIDA=Void fraction in the aggregates
C       VOIDB=Void fraction in the mobile phase
C       XMU=Specific growth rate
C       XMUC=Specific growth constant
C       XKS=Kinetic constant
C       XKI=Kinetic inhibitory constant
C       XKP=kp of Freundlich Isotherm
C       XY=Yield coefficient
C       XKD=Adsorption rate constant
C       XKM=Mass transfer coefficient
C       XL=Length of the column
C       RHOS=Density of solid
C       NDASH=Power n-dash in equilm relation
C       CONSTAN1=Constant already defined
C       DELT= IMSL directive parameter
C       TMAX= Maximum run time of the program.
C
        Read(24,*) ,XL,R,DSE,DLE,VOIDA,VOIDB,XMU,XMUC,XKS,XKI,XY,XKM,
     $   XKD,XKP,NDASH,RHOS,DELT,TMAX
C
C       Locations of discretized points
C       DELX= Length step in z-direction
C       DELETA=Length step in r-direction
C
        DELX = 1.0/(DFLOAT(NB))
        DELETA = 1.0/(DFLOAT(NR-1))
        DO 10 I=1,NB
                X(I) = DFLOAT(I)*DELX
                WRITE(85,123) X(I)
123             FORMAT(1X,'X=',1X,12(1X,F5.3)/)
10              CONTINUE
        DO  12  I=1,NR
                ETA(I) = (DFLOAT(I)*DELETA) - DELETA
                WRITE(85,119) ETA(I)
119             FORMAT(1X,'R=',F5.3,1X,12(1X,F5.3)/)
12              CONTINUE
C
C       Calculation of parameters
C       PHIA=Dimensionless thiele modulus
C       PHIB=Dimensionless thiele modulus
C       PHIC=Dimensionless thiele modulus
C       SHERA=Sherwood number
C       SHERB=Modified sherwood number
C       PEC=Dimensionless peclet number
C       PSI=Dimensionless peclet number
C       CONST1=Constant term in Freundlich relation after dimensionless
C       GAMMAZO [=(C_Z_0-)/Ks] is just before entrance into bed
C
        PHIA  = ((R**2.0)*XKD)/DSE
        PHIB  = ((R**2.0)*XMU)/DSE
        PHIC  = ((R**2.0)*XMUC)/DSE
        SHERA = (XKM*R)/DSE
        SHERB = ((3.0*(1-VOIDB)/VOIDB)*(XKM*R))/DSE
        PEC   = (V*XL)/DLE
        PSI   = (V*(R**2.0))/(XL*DSE)
```

```
      CONST1= (XKS**(NDASH-1))/((XKP**NDASH)*(RHOS**NDASH))
      GAMMAZO=9.8
C
C     Output of INPUT DATA and CALCULATED parameters
C
      write(85,5) NB,NR,V,XL,R,DSE,DLE,VOIDA,VOIDB,XMU,XMUC,XKS,
     $ XKI,XY,XKM,XKD,XKP,XKP,RHOS,DELT,TMAX,DELX,DELETA,CONST1,
     $ PHIA,PHIB,PHIC,SHERA,SHERB,PEC,PSI
C
    5 FORMAT(///,T5,'NB=',I5,T30,'NR=',I5,T55,'V=',D12.5,/,
     $ T5,'XL=',D12.5,T30,'R=',D12.5,T55,'DSE=',D12.5,/,
     $ T5,'DLE=',D12.5,T30,'VOIDA=',D12.5,T55,'VOIDB=',D12.5,/,
     $ T5,'XMU=',D12.5,T30,'XMUC=',D12.5,T55,'XKS=',D12.5,/,
     $ T5,'XKI=',D12.5,T30,'XY=',D12.5,T55,'XKM=',D12.5,/,
     $ T5,'XKD=',D12.5,T30,'XKP=',D12.5,T55,'XKP=',D12.5,/,
     $ T5,'RHOS=',D12.5,T30,'DELT=',D12.5,T55,'TMAX=',D12.5,/,
     $ T5,'DELX=',D12.5,T30,'DELETA=',D12.5,T55,'CONST1=',D12.5,/,
     $ T5,'PHIA=',D12.5,T30,'PHIB=',D12.5,T55,'PHIC=',D12.5,/,
     $ T5,'SHERA=',D12.5,T30,'SHERB=',D12.5,T55,'PEC=',D12.5,/,
     $ T5,'PSI=',D12.5,////)
C
C     Initializations
C
      DO 29 I=1,NB
       C(I)=0.0
29    CONTINUE
      NEQ1=NB
      NEQ2=NEQ1+NB*NR
      DO 30 I=NEQ1+1,NEQ2
       C(I)=0.0
30    CONTINUE
      NEQ3=NEQ2+NB*NR
      DO 31 I=NEQ2+1,NEQ3
       C(I)=0.0
31    CONTINUE
      NEQ4=NEQ3+NB*NR
      DO 32 I=NEQ3+1,NEQ4
       C(I)= 4.05
32    CONTINUE
C
C     SET UP PARAMETERS FOR CALL TO  "DIVPAG"
C
      T = 0.0
      TOL = 1.0D-6
      MXSTEP= 60000000
      METH = 2
      MITER = 3
      IATYPE = 0.0
      PARAM(4) = MXSTEP
      PARAM(12) = METH
      PARAM(13) = MITER
      PARAM(19) = IATYPE
      IDO = 1
C
      TOLD=1.0
```

```
      DO 111 ISTEP = 1,NSTEP
      TEND = TMAX*DFLOAT(ISTEP)/DFLOAT(NSTEP)
C
      call DIVPAG (IDO,NEQ,FCN,FCNJ,A,T,TEND,TOL,PARAM,C)
C     PRINT *,'C=',C
C
C     Integration at updated times and controlled output
C
      if (TOLD .eq. ISTEP) then
      TOLD=TOLD+1000.0
C
      WRITE(6,59) T
      WRITE(25,59) T
59    FORMAT(//,T5,'T=',F9.3,/)
      WRITE(6,113) (X(I), I=1,NB)
      WRITE(25,113) (X(I), I=1,NB)
113   FORMAT(1X,'X=',1X,'0.000',12(1X,F5.3),/)
C
C     OUTPUT for Cb
      WRITE(6,114) C1ZERO,(C(I),I=1,NB)
      WRITE(25,114) C1ZERO,(C(I),I=1,NB)
114   FORMAT ('C1=', 13 (1X,F5.3))
C
C     OUTPUT for Ca
C
      DO 115  I=1,NR
         NSTART = NB+I
         NLAST = NB+NB*NR-NR+I
      WRITE(6,116) ETA(I),(C(K),K=NSTART,NLAST,NR)
      WRITE(25,116) ETA(I),(C(K),K=NSTART,NLAST,NR)
116   FORMAT (1X,'R=',F6.2,1X,12(1X,F6.2))
115   continue
C
C     WRITE(6,217)
C     WRITE(25,217)
C
C     OUTPUT for q
      DO 215  I=1,NR
         NSTART = NB+NB*NR+I
         NLAST = NB+2*NB*NR-NR+I
      WRITE(6,106) ETA(I),(C(K),K=NSTART,NLAST,NR)
      WRITE(25,106) ETA(I),(C(K),K=NSTART,NLAST,NR)
106   FORMAT (1X,'R=',F6.2,1X,12(1X,F6.2))
215   continue
C
C     OUTPUT for b
      DO 315  I=1,NR
         NSTART = NB+2*NB*NR+I
         NLAST = NB+3*NB*NR-NR+I
      WRITE(6,108) ETA(I),(C(K),K=NSTART,NLAST,NR)
      WRITE(25,108) ETA(I),(C(K),K=NSTART,NLAST,NR)
108   FORMAT (1X,'R=',F6.2,1X,12(1X,F6.2))
315   continue
217   FORMAT(//)
      WRITE(41,137)T,C(NB)
```

```
137     FORMAT (1X, 'T=',1X,F10.3,1X,'C1=',1X,F7.4)
C
        else
        end if
111     continue
C
C       Final call to release workspace
        IDO=3
        call DIVPAG (IDO,NEQ,FCN,FCNJ,A,T,TEND,TOL,PARAM,C)
        STOP
        END
```

APPENDIX B-2

Computer Code for Solving Equations with Oxygen Limitation

```
C     ****************************************************************
C     Solution of the Model Equations "with" Oxygen Limitation
C     This code is written in FORTRAN for VAX/VMS environment
C     by Dilip K. Mandal
C
C     Method used:  Method of lines (MOL)
C
C     The ODEs are written in the subroutine "FCN" and then integrated using
C     standard IMSL subrioutine named "DIVPAG' (Double Precision Version
C     of Initial Value Problem Utilizing Adamson Gear Technique).
C     ****************************************************************
C
C                         MAIN PROGRAM
C
C     EXTERNAL and COMMON LINKS to IMSL ROUTINE DIVPAG and FCN
C
C     MB=NB=discretized points in z-direction (X)
C     MR=NR=discretized points in r-direction (ETA)
C     MEQ=NEQ= total no. of equations
C     NEQ=2*MB+4*MB*MR
C     A(1,1)= parameter for the subroutine used
C     RWKSP, IWKIN are for workspace specification
C     NSTEP=total number of steps
C
      parameter (NB=30, NR=20, NEQ=2*NB+4*NB*NR, NSTEP=1200000)
      implicit  real*8(A-H, O-Z)
      dimension ETA(NR), C(NEQ), X(NB), PARAM(50)
      dimension A(1,1)
      external FCN, FCNJ
      real *8 NDASH
      common /LIST1/ DSE,DSO,DLE,DLO,VOIDA,VOIDB,XMU,XMUC,XKP,
     $ XKD,XKM,XKMO,DELT,TMAX,C1ZERO,C2ZERO,GAMMAZO,GAMMAOO
     $ /LIST2/ PHIA,PHIB,PHIC,PHIK,SHERA,SHERB,PSI,PEC,PECO,
     $ SHAO,SHBO,
     $ DELETA,DELX,NDASH,RHOS,XKS,XKSO,XKI,XY,XYO,CONST1
     $ /LIST3/ETA

      common /WORKSP/RWKSP
      real RWKSP(600000)
      OPEN(UNIT=24,FILE='OXYF.IN', STATUS='OLD')
c     OPEN(UNIT=6,FILE='OXYF.OUT',STATUS='NEW')
      call IWKIN (600000)
C
C     Reading of Input Data
C     V=Velocity
C     R=Radius of the particle
C     DSE=Effective diffusivity in the aggregate phase
C     DLE=Dispersion co-efficient in mobile phase
```

```
C       VOIDA=Void fraction in the aggregate phase
C       VOIDB=Void fraction in the in the mobile phase
C       XMU=Specific growth rate
C       XMUC=Specific growth constant
C       XKS=Kinetic constant
C       XKI=Kinetic inhibitory constant
C       XKP=kp of Freundlich Isotherm
C       XY=Yield coefficient
C       XKD=KD=Adsorption rate constant
C       XKM=KM=Mass transfer coefficient
C       XL=Length of the column
C       RHOS=Density of solid
C       NDASH=Power n-dash in equilibrium relation
C       DSO=Diffusivity of oxygen in the aggre. phase
C       DLO=Dispersion co-effi. of oxy in the mobile phase
C       XKSO=Kinetic constant of Oxygen
C       XYO=Yield coeffi w.r.t. oxy
C       XKMO=mass transfer coeff of oxy
C
        Read(24,*) V,XL,R,DSE,DLE,VOIDA,VOIDB,XMU,XMUC,XKS,XKI,XY,XKM,
     $  XKD,XKP,NDASH,RHOS,DSO,DLO,XKMO,XKSO,XYO,DELT,TMAX
C
C       Locations of discretization points
C
        DELX = 1.0/(DFLOAT(NB))
        DELETA = 1.0/(DFLOAT(NR-1))
        DO 10 I=1,NB
                X(I) = DFLOAT(I)*DELX
                WRITE(46,123) X(I)
123             FORMAT(1X,'X=',1X,12(1X,F5.3)/)
10              CONTINUE
C
        DO  12  I=1,NR
                ETA(I) = (DFLOAT(I)*DELETA) - DELETA
                WRITE(46,119) ETA(I)
119             FORMAT(1X,'R=',F5.3,1X,12(1X,F5.3)/)
12              CONTINUE
C
C       Calculation of parameters
C       PHIA=Dimensionless thiele modulus
C       PHIB=Dimensionless thiele modulus
C       PHIC=Dimensionless thiele modulus
C       SHERA=Sherwood number
C       SHERB=Modified sherwood number
C       PEC=Dimensionless peclet number
C       PSI=Dimensionless peclet number
C       PHIK=Dimensionless thiele modulus for oxygen
C       SHAO=Sherwood number for oxygen
C       SHBO=Modified sherwood number for oxygen
C       PECO=Dimensionless peclet number for oxygen
C       CONST1=Constant term in Freundlich relation after dimensionless
C       GAMMAZO [=(C_Z_0-)/Ks] is just before entrance into bed, pollutant
C       GAMMAOO is (Cm_O_0-)/KS just before entrance into bed, oxygen
C
        PHIA  = ((R**2.0)*XKD)/DSE
```

```
      PHIB  = ((R**2.0)*XMU)/DSE
      PHIC  = ((R**2.0)*XMUC)/DSE
      SHERA = (XKM*R)/DSE
      SHERB = ((3.0*(1-VOIDB)/VOIDB)*(XKM*R))/DSE
      PEC   = (V*XL)/DLE
      PSI   = (V*(R**2.0))/(XL*DSE)
      PHIK  = (XKSO/XKS)
      SHAO  = (XKMO*R)/DSO
      SHBO  = ((3.0*(1-VOIDB)/VOIDB)*(XKMO*R))/DSE
      PECO  = (V*XL)/DLO
      CONST1= (XKS**(NDASH-1))/((XKP**NDASH)*(RHOS**NDASH))
C
      GAMMAZO= 9.8
      GAMMAOO= 3.3
C
C     Output of INPUT DATA and CALCULATED parameters
C
      write(6,5) NB,NR,V,XL,R,DSE,DLE,VOIDA,VOIDB,XMU,XMUC,XKS,
     $ XKI,XY,XKM,XKD,XKP,XKP,RHOS,DELT,TMAX,DELX,DELETA,CONST1,
     $ PHIA,PHIB,PHIC,SHERA,SHERB,PEC,DSO,DLO,XKSO,XYO,XKMO,
     $ PHIK,PECO,SHAO,SHBO,PSI
C
      write(46,5) NB,NR,V,XL,R,DSE,DLE,VOIDA,VOIDB,XMU,XMUC,XKS,
     $ XKI,XY,XKM,XKD,XKP,XKP,RHOS,DELT,TMAX,DELX,DELETA,CONST1,
     $ PHIA,PHIB,PHIC,SHERA,SHERB,PEC,DSO,DLO,XKSO,XYO,XKMO,
     $ PHIK,PECO,SHAO,SHBO,PSI
C
   5  FORMAT(///,T5,'NB=',I5,T30,'NR=',I5,T55,'V=',D12.5,/,
     $ T5,'XL=',D12.5,T30,'R=',D12.5,T55,'DSE=',D12.5,/,
     $ T5,'DLE=',D12.5,T30,'VOIDA=',D12.5,T55,'VOIDB=',D12.5,/,
     $ T5,'XMU=',D12.5,T30,'XMUC=',D12.5,T55,'XKS=',D12.5,/,
     $ T5,'XKI=',D12.5,T30,'XY=',D12.5,T55,'XKM=',D12.5,/,
     $ T5,'XKD=',D12.5,T30,'XKP=',D12.5,T55,'XKP=',D12.5,/,
     $ T5,'RHOS=',D12.5,T30,'DELT=',D12.5,T55,'TMAX=',D12.5,/,
     $ T5,'DELX=',D12.5,T30,'DELETA=',D12.5,T55,'CONST1=',D12.5,/,
     $ T5,'PHIA=',D12.5,T30,'PHIB=',D12.5,T55,'PHIC=',D12.5,/,
     $ T5,'SHERA=',D12.5,T30,'SHERB=',D12.5,T55,'PEC=',D12.5,/,
     $ T5,'DSO=',D12.5,T30,'DLO=',D12.5,T55,'XKSO=',D12.5,/,
     $ T5,'XYO=',D12.5,T30,'XKMO=',D12.5,T55,'PHIK=',D12.5,/,
     $ T5,'PECO=',D12.5,T30,'SHAO=',D12.5,T55,'SHBO=',D12.5,/,
     $ T5,'PSI=',D12.5,////)
C
C     Initializations
C
C     For Cb
      DO 27 I=1,NB
        C(I)=0.0
27    CONTINUE
C
C     For Cmo
      NEQ1=NB
      NEQ2=2*NB
      DO 28 I=NEQ1+1,NEQ2
        C(I)= 3.4
28    CONTINUE
```

```
C
C       For Ca
        NEQ3=NEQ2+NB*NR
        DO 29 I=NEQ2+1,NEQ3
         C(I)=0.0
29      CONTINUE
C
C       For q
        NEQ4=NEQ3+NB*NR
        DO 30 I=NEQ3+1,NEQ4
         C(I)= 0.0
30      CONTINUE
C
C       For b
        NEQ5=NEQ4+NB*NR
        DO 31 I=NEQ4+1,NEQ5
         C(I)= 4.05
31      CONTINUE
C       For Co
        NEQ6=NEQ5+NB*NR
        DO 32 I=NEQ5+1,NEQ6
         C(I)= 3.4
32      CONTINUE
C
C       SET UP PARAMETERS FOR CALL TO  "DIVPAG"
C
        T = 0.0
        TOL = 1.0D-6
        MXSTEP= 60000000
        METH = 2
        MITER = 3
        IATYPE = 0.0
        PARAM(4) = MXSTEP
        PARAM(12) = METH
        PARAM(13) = MITER
        PARAM(19) = IATYPE
        IDO = 1
C
        TOLD=1.0
        DO 111 ISTEP = 1,NSTEP
        TEND = TMAX*DFLOAT(ISTEP)/DFLOAT(NSTEP)
C
        call DIVPAG (IDO,NEQ,FCN,FCNJ,A,T,TEND,TOL,PARAM,C)
C       PRINT *,'C=',C
C
C       Integration at updated times
C       And output at selected steps
C
        if (TOLD .eq. ISTEP) then
        TOLD=TOLD + 1000.0
C
        WRITE(6,59) T
        WRITE(31,59) T
59      FORMAT(//,T5,'T=',F9.3,/)
C       WRITE(6,113) (X(I), I=1,NB)
```

```
      WRITE(31,113) (X(I), I=1,NB)
113   FORMAT(1X,'X=',1X,'0.000',12(1X,F5.3),/)
C
C     Ooutput for Cb
C
      WRITE(6,114) C1ZERO,(C(I),I=1,NB)
      WRITE(31,114) C1ZERO,(C(I),I=1,NB)
114   FORMAT ('C1=', 13 (1X,F5.3))
C
C     Output for oxygen (axial)
C
      NST=NB+1
      NLAST=2*NB
      WRITE(6,117) C2ZERO,(C(I),I=NST,NLAST)
      WRITE(31,117) C2ZERO,(C(I),I=NST,NLAST)
117   FORMAT (/,'C2=', 13 (1X,F5.3))
C
C     Output for Ca
C
      DO 115  I=1,NR
         NSTART = 2*NB+1
         NLAST = 2*NB+NB*NR-NR+1
C
      WRITE(6,116) ETA(I),(C(K),K=NSTART,NLAST,NR)
      WRITE(31,116) ETA(I),(C(K),K=NSTART,NLAST,NR)
115   continue
C
C     Output for q
C
      DO 215  I=1,NR
         NSTART = 2*NB+NB*NR+1
         NLAST = 2*NB+2*NB*NR-NR+1
C
      WRITE(6,116) ETA(I),(C(K),K=NSTART,NLAST,NR)
      WRITE(31,116) ETA(I),(C(K),K=NSTART,NLAST,NR)
215   continue
C
C     Output for b
C
      DO 315  I=1,NR
         NSTART = 2*NB+2*NB*NR+1
         NLAST = 2*NB+3*NB*NR-NR+1
      WRITE(6,126) ETA(I),(C(K),K=NSTART,NLAST,NR)
      WRITE(25,116) ETA(I),(C(K),K=NSTART,NLAST,NR)
315   continue
C
C     Output for oxygen (in aggregate)
C
      DO 415  I=1,NR
         NSTART = 2*NB+3*NB*NR+1
         NLAST = 2*NB+4*NB*NR-NR+1
C
      WRITE(6,116) ETA(I),(C(K),K=NSTART,NLAST,NR)
      WRITE(31,116) ETA(I),(C(K),K=NSTART,NLAST,NR)
415   continue
```

```
C
116     FORMAT (1X,'R=',F6.3,1X,12(1X,F6.3))
217     FORMAT(//)
C
        WRITE(6,137)T,C(NB),C(2*NB)
        WRITE(64,137)T,C(NB),C(2*NB)
137     FORMAT(1X,'T=',1X,F8.3,1X,'C1=',1X,F6.3,1X,'C2=',1X,F6.3)
C
        else
        end if
111     continue
C
C       Final call to release workspace
C
        IDO=3
        call DIVPAG (IDO,NEQ,FCN,FCNJ,A,T,TEND,TOL,PARAM,C)
        STOP
        END
```

APPENDIX C

CALIBRATION CURVES

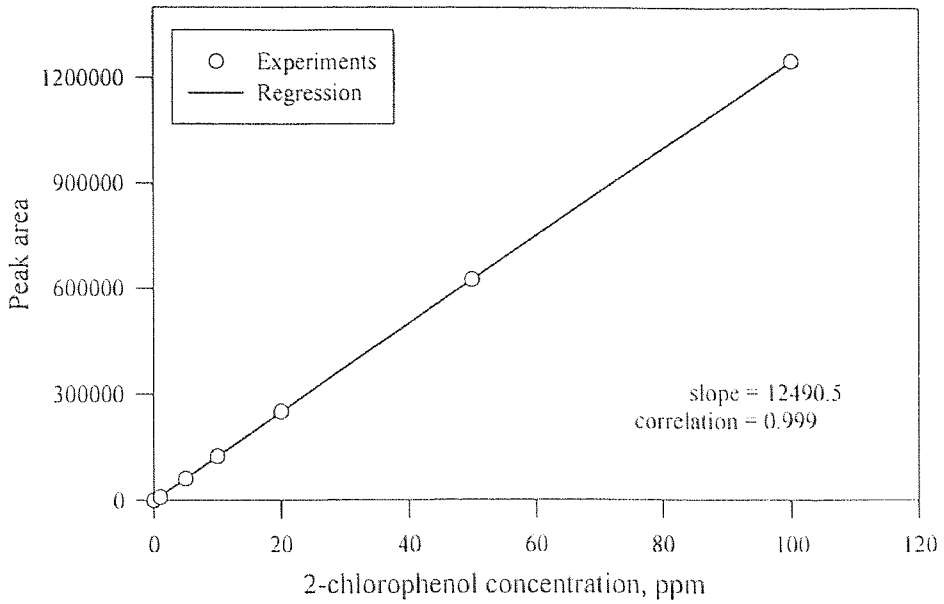

Figure C-1 Calibration curve for 2-chlorophenol concentration measurements.

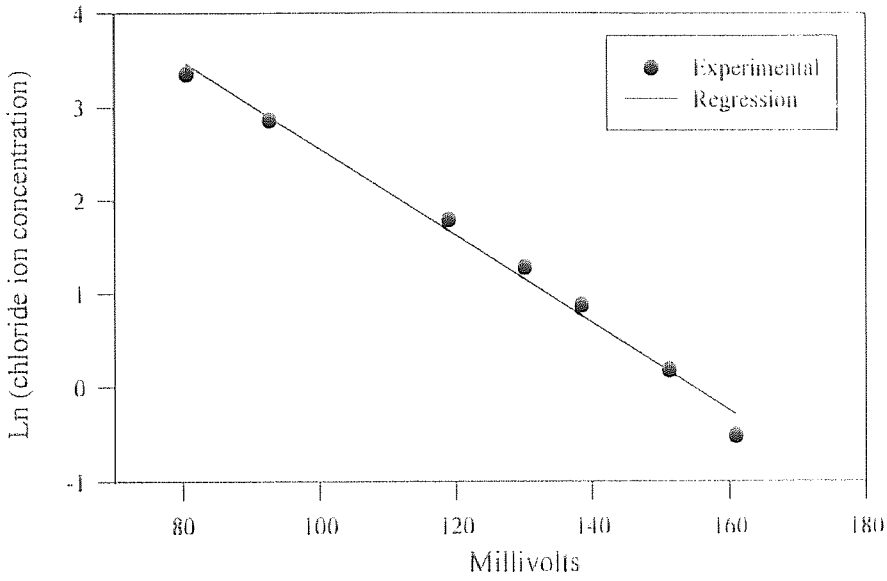

Figure C-2 Calibration curve for chloride concentration measurement using Ionplus chloride electrode.

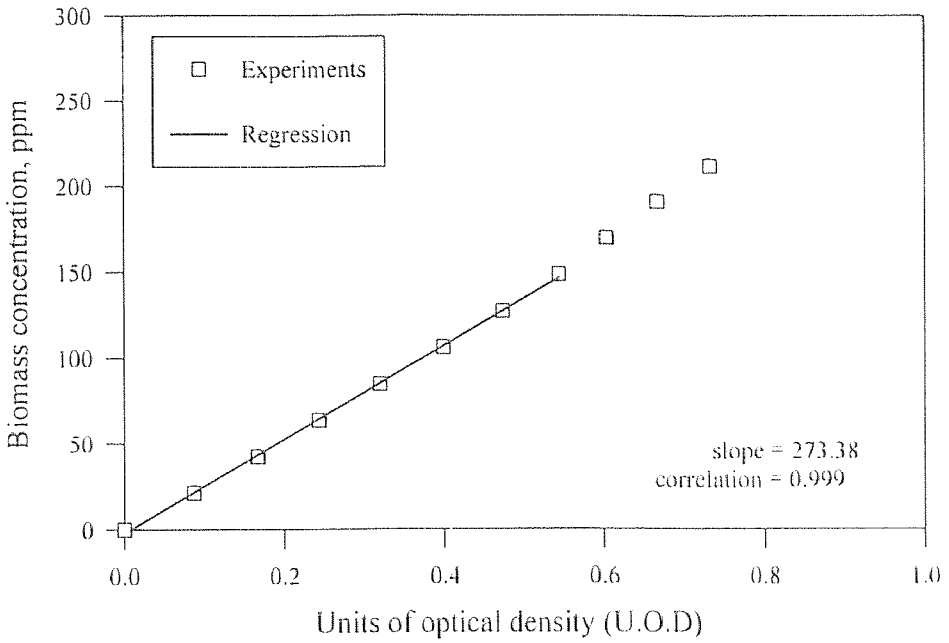

Figure C-3 Calibration curve for determination of biomass concentration from optical density readings [taken from Dishitulu (1993)].

APPENDIX D

TABLES AND FIGURES OF EXPERIMENTAL RESULTS OBTAINED IN SHAKE FLASKS FOR KINETICS PARAMETER EVALUATION

Table D-1 Experimental data obtained from batch experiment run-1.

Sample No	Time (h)	Optical density	Biomass concentration (mg/L)	Ln (biomass concentration)	2-Chlorophenol concentration (mg/L)
1	0.00	0.069	18.9	2.94	19.22
2	1.33	0.077	21.0	3.05	16.05
3	2.83	0.090	24.6	3.20	9.80
4	3.37	0.094	25.7	3.25	6.83
5	4.20	0.105	28.7	3.36	1.60

Table D-2 Experimental data obtained from batch experiment run-2.

Sample No	Time (h)	Optical density	Biomass concentration (mg/L)	Ln (biomass concentration)	2-Chlorophenol concentration (mg/L)
1	0.00	0.031	8.48	2.14	14.27
2	0.83	0.033	9.02	2.20	12.69
3	1.33	0.035	9.57	2.26	11.45
4	1.83	0.037	10.12	2.31	10.08
5	2.33	0.040	10.94	2.40	8.36
6	2.83	0.043	11.76	2.46	6.33
7	3.33	0.045	12.30	2.51	4.74
8	3.83	0.048	13.12	2.57	2.86
9	4.08	0.050	13.67	2.62	2.00
10	4.33	0.053	14.49	2.68	0.90

Table D-3 Experimental data obtained from batch experiment run-9.

Sample No	Time (h)	Optical density	Biomass concentration (mg/L)	Ln (biomass concentration)	2-Chlorophenol concentration (mg/L)
1	0.00	0.033	9.02	2.20	11.25
2	0.50	0.034	9.30	2.23	10.10
3	1.00	0.036	9.84	2.29	9.00
4	1.50	0.038	10.39	2.34	7.60
5	2.00	0.040	10.94	2.39	6.10
6	2.50	0.042	11.48	2.44	4.40
7	3.00	0.044	12.03	2.49	3.40
8	3.50	0.048	13.12	2.57	2.00
9	4.00	0.051	13.94	2.63	1.00
10	4.50	0.053	14.49	2.67	0.20

Table D-4 Experimental data obtained from batch experiment run-4.

Sample No	Time (h)	Optical density	Biomass concentration (mg/L)	Ln (biomass concentration)	2-Chlorophenol concentration (mg/L)
1	0.00	0.039	10.7	2.37	46.8
2	0.50	0.039	10.7	2.37	46.6
3	0.75	0.039	10.7	2.37	47.4
4	1.00	0.040	10.9	2.39	47.4
5	1.50	0.041	11.2	2.41	43.2
6	2.00	0.043	11.8	2.46	41.2
7	2.50	0.045	12.3	2.51	43.1
8	3.00	0.048	13.1	2.57	41.0
9	3.50	0.050	13.7	2.61	37.0
10	4.00	0.053	14.5	2.67	35.7
11	4.50	0.058	15.9	2.76	33.9
12	5.00	0.060	16.4	2.80	31.1
13	5.50	0.064	17.5	2.86	27.7
14	6.50	0.072	19.7	3.00	21.2
15	7.50	0.083	22.7	3.12	13.3
16	8.50	0.099	27.1	3.30	3.27

Table D-5 Experimental data obtained from batch experiment run-5.

Sample No	Time (h)	Optical density	Biomass concentration (mg/L)	Ln (biomass concentration)	2-Chlorophenol concentration (mg/L)
1	0.00	0.042	11.5	2.44	63.0
2	0.33	0.042	11.5	2.44	62.1
3	0.50	0.042	11.5	2.44	63.0
4	0.83	0.042	11.5	2.44	61.1
5	1.50	0.042	11.5	2.44	60.0
6	2.00	0.042	11.5	2.44	59.0
7	2.58	0.042	11.5	2.44	59.6
8	3.00	0.042	11.5	2.44	55.0
9	3.50	0.042	11.5	2.44	56.3
10	4.00	0.043	11.8	2.46	54.5
11	4.50	0.045	12.3	2.51	52.2
12	5.00	0.050	13.7	2.61	50.1
13	5.50	0.052	14.2	2.65	48.7
14	6.00	0.055	15.0	2.71	45.5
15	7.00	0.059	16.1	2.78	42.0
16	8.00	0.064	17.5	2.86	38.1
17	9.00	0.066	18.0	2.89	32.8

Table D-6 Experimental data obtained from batch experiment run-6.

Sample No	Time (h)	Optical density	Biomass concentration (mg/L)	Ln (biomass concentration)	2-Chlorophenol concentration (mg/L)
1	0.00	0.118	32.3	3.47	65.1
2	0.50	0.119	32.5	3.48	66.6
3	1.00	0.122	33.3	3.51	62.1
4	1.50	0.125	34.2	3.53	60.0
5	2.00	0.131	35.8	3.58	57.5
6	2.50	0.133	36.3	3.59	54.7
7	3.00	0.140	38.3	3.64	49.4
8	3.50	0.144	39.4	3.67	45.8
9	4.50	0.161	44.0	3.78	33.7
10	5.00	0.166	45.4	3.81	28.1
11	5.50	0.177	48.4	3.88	21.1
12	6.00	0.187	51.1	3.93	12.2
13	7.00	0.210	57.4	4.05	0.0

Table D-7 Experimental data obtained from batch experiment run-7.

Sample No	Time (h)	Optical density	Biomass concentration (mg/L)	Ln (biomass concentration)	2-Chlorophenol concentration (mg/L)
1	0.00	0.127	34.7	3.55	81.4
2	0.50	0.128	35.0	3.55	80.1
3	1.00	0.131	35.8	3.58	77.2
4	1.50	0.134	36.6	3.60	74.9
5	2.00	0.140	38.3	3.64	73.7
6	2.50	0.144	39.4	3.67	70.3
7	3.00	0.150	41.0	3.71	65.7
8	3.50	0.155	42.4	3.75	57.4
9	4.50	0.168	45.9	3.83	49.9
10	5.00	0.175	47.8	3.87	42.3
11	5.50	0.183	50.0	3.91	35.0
12	6.00	0.196	53.6	3.98	24.5
13	7.00	0.225	61.5	4.12	7.16
14	7.50	0.242	66.1	4.19	0.0

Table D-8 Experimental data obtained from batch experiment run-8.

Sample No	Time (h)	Optical density	Biomass concentration (mg/L)	Ln (biomass concentration)	2-Chlorophenol concentration (mg/L)
1	0.00	0.102	27.9	3.33	109.3
2	0.50	0.103	28.1	3.34	107.1
3	1.00	0.106	29.0	3.37	106.4
4	1.50	0.108	29.5	3.38	107.4
5	2.00	0.110	30.1	3.40	101.9
6	2.50	0.114	31.2	3.44	101.0
7	3.00	0.117	32.0	3.47	99.47
8	3.50	0.120	32.8	3.49	91.03
9	4.50	0.129	35.3	3.56	87.41
10	5.00	0.134	36.6	3.60	85.45
11	5.50	0.140	38.3	3.64	74.54
12	6.00	0.145	39.6	3.68	70.11
13	7.00	0.155	42.4	3.75	61.74
14	7.50	0.160	43.7	3.78	57.35
15	8.00	0.170	46.5	3.84	49.00
16	8.50	0.176	48.1	3.87	42.16
17	9.00	0.184	50.3	3.92	37.41
18	9.50	0.193	52.7	3.97	30.42

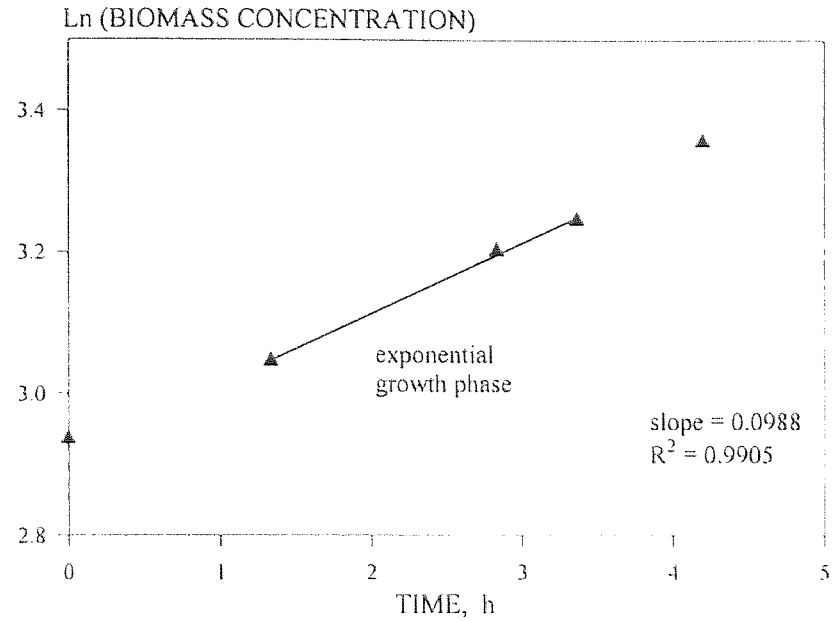

Figure D-1 Determination of the specific growth rate of *P. pickettii* on 2-chlorophenol (run#1 in shake flask).

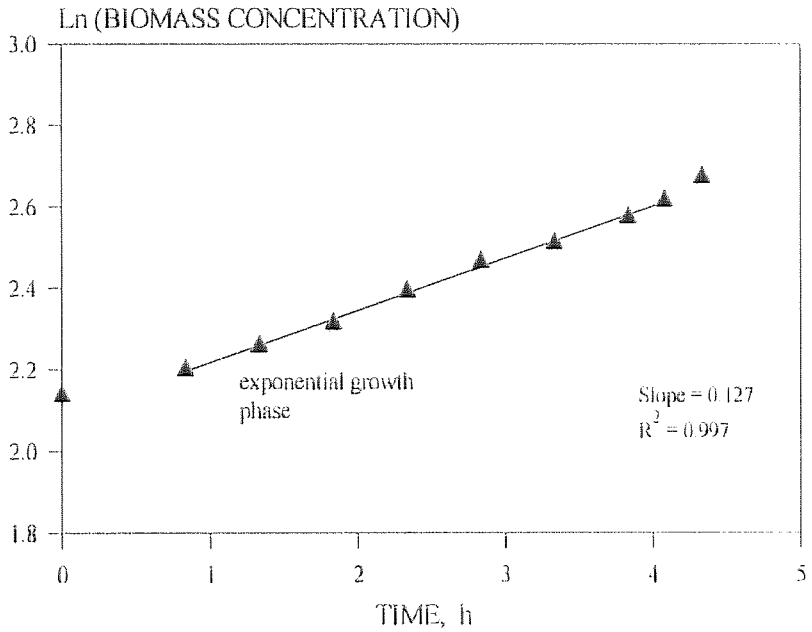

Figure D-2 Determination of the specific growth rate of *P. pickettii* on 2-chlorophenol (run#2 in shake flask).

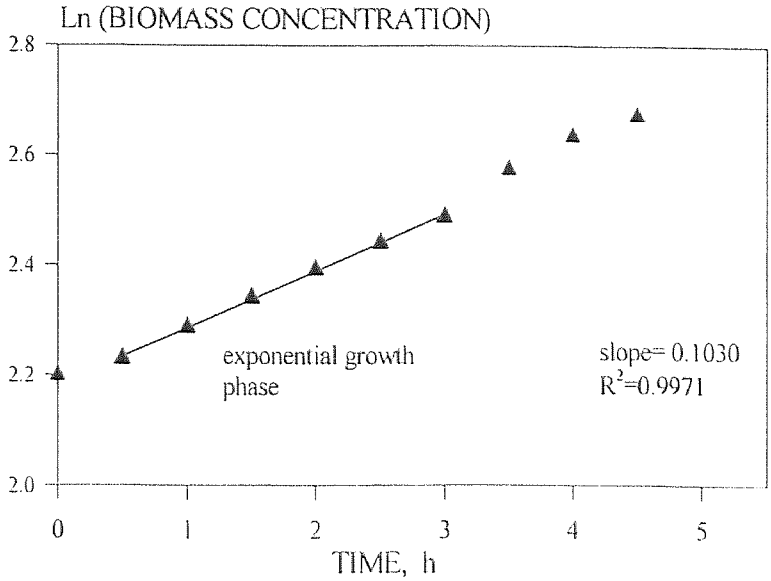

Figure D-3 Determination of the specific growth rate of *P. pickettii* on 2-chlorophenol (run#9 in shake flask).

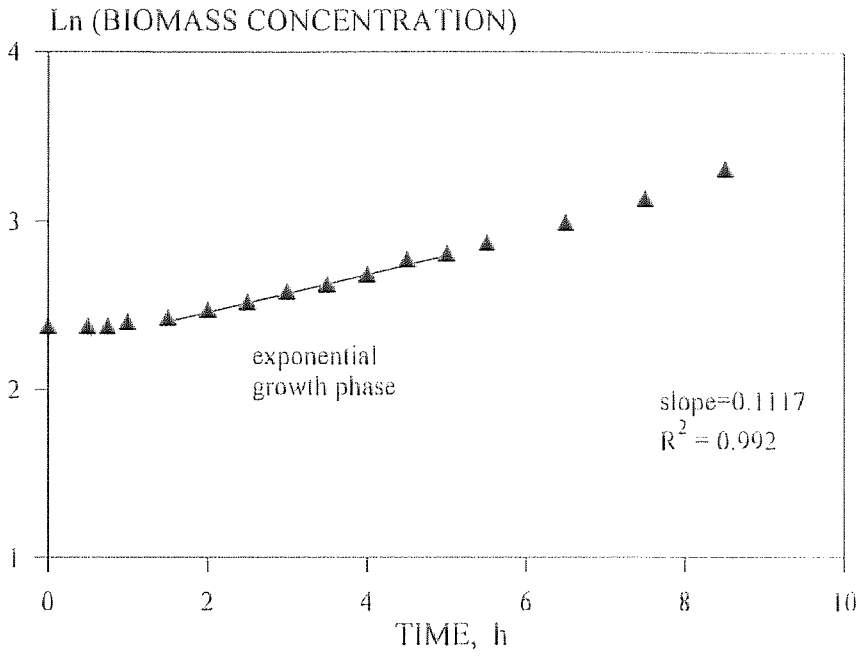

Figure D-4 Determination of the specific growth rate of *P. pickettii* on 2-chlorophenol (run#4 in shake flask).

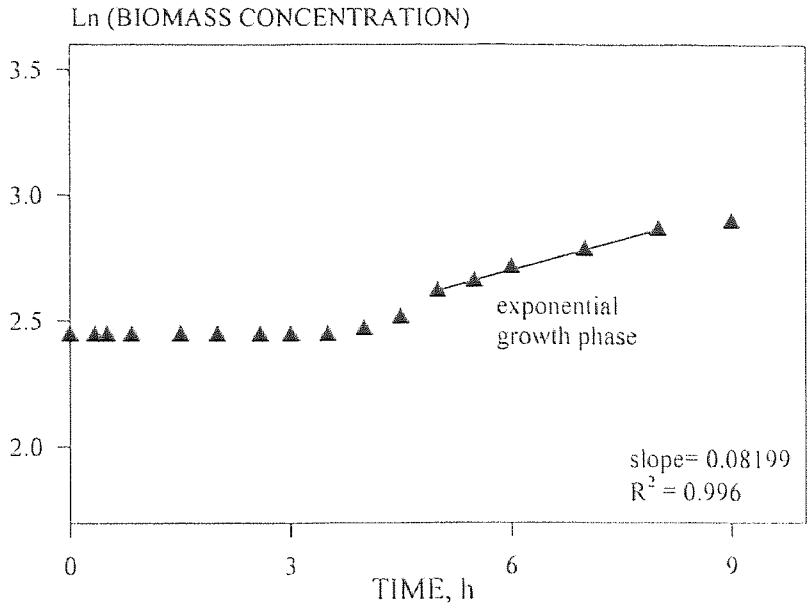

Figure D-5 Determination of the specific growth rate of *P. pickettii* on 2-chlorophenol (run#5 in shake flask).

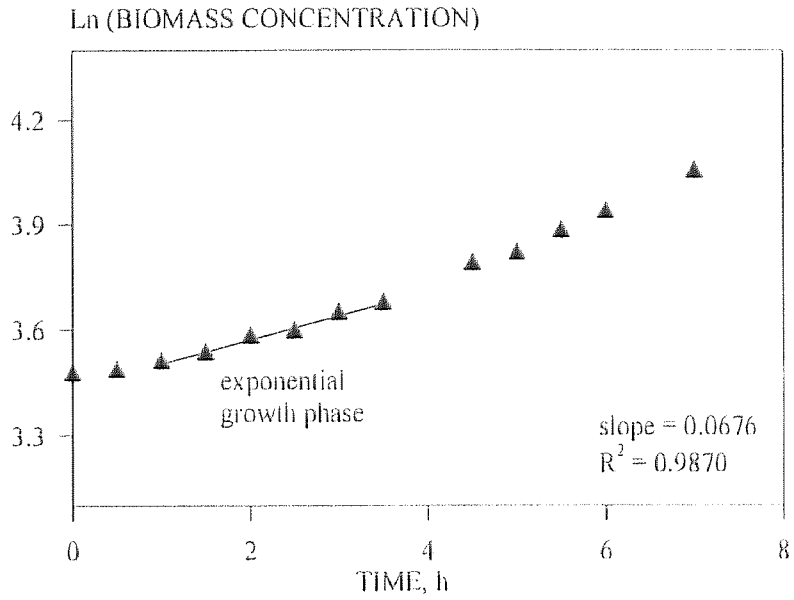

Figure D-6 Determination of the specific growth rate of *P. pickettii* on 2-chlorophenol (run#6 in shake flask).

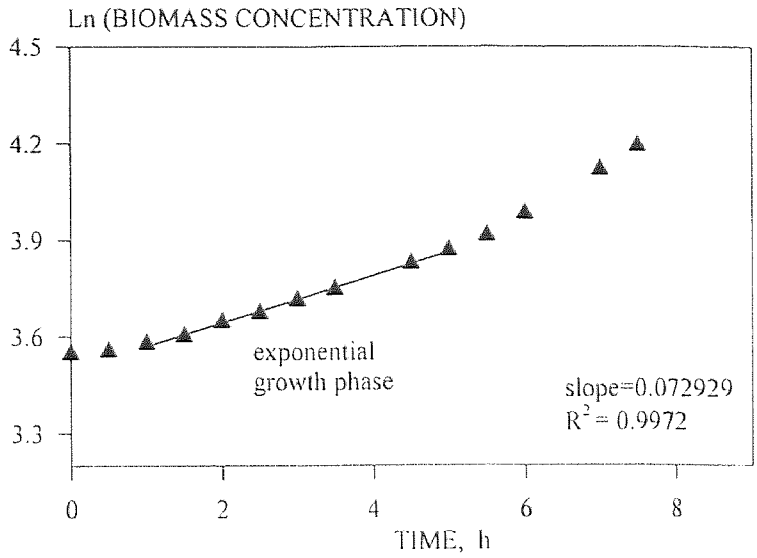

Figure D-7 Determination of the specific growth rate of *P. pickettii* on 2-chlorophenol (run#7 in shake flask).

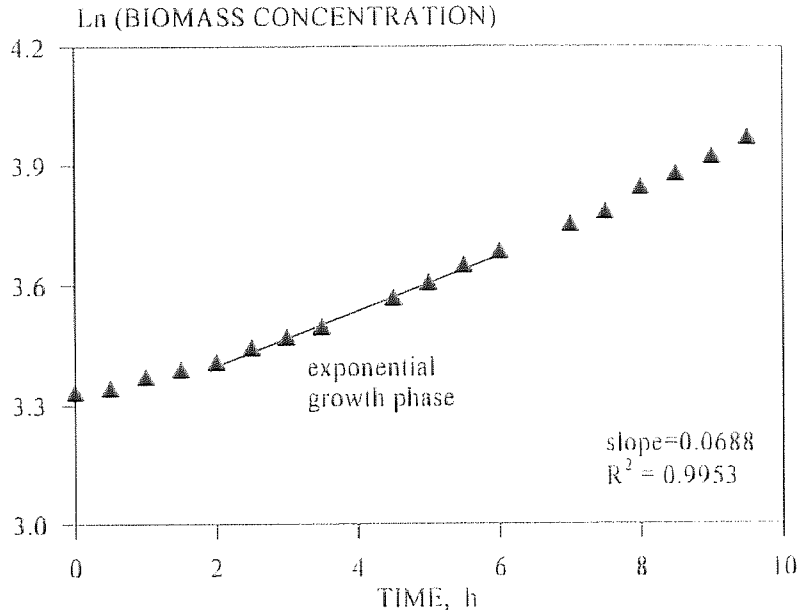

Figure D-8 Determination of the specific growth rate of *P. pickettii* on 2-chlorophenol (run#8 in shake flask).

APPENDIX E

TABLES AND FIGURES OF EXPERIMENTAL RESULTS OBTAINED IN JACKETTED BATCH REACTOR FOR KINETICS PARAMETER EVALUATION

Table E-1 Experimental data obtained from batch experiment K-8.

Sample No	Time (h)	Optical density	Biomass concentration (mg/L)	Ln (biomass concentration)	2-Chlorophenol concentration (mg/L)
1	0.00	0.0430	11.8	2.46	28.8
2	0.25	0.0435	11.9	2.48	27.5
3	0.50	0.0445	12.2	2.50	26.8
4	0.75	0.0460	12.6	2.53	25.4
5	1.00	0.0480	13.1	2.57	24.2
6	1.25	0.0500	13.7	2.62	23.4
7	1.50	0.0520	14.2	2.65	21.1
8	1.75	0.0540	14.8	2.69	20.6
9	2.00	0.0560	15.3	2.73	19.1
10	2.25	0.0580	15.9	2.76	17.4
11	2.50	0.0600	16.4	2.80	15.2
12	2.75	0.0620	16.9	2.83	14.3
13	3.00	0.0640	17.5	2.86	13.1
14	3.25	0.0660	18.0	2.89	11.2
15	3.42	0.0680	18.6	2.92	10.3
16	3.50	0.0695	19.0	2.94	9.23
17	3.75	0.0720	19.7	2.98	7.74
18	4.00	0.0740	20.2	3.01	5.89
19	4.25	0.0760	20.8	3.03	3.90
20	4.50	0.0790	21.6	3.07	2.60
21	4.75	0.0820	22.4	3.11	0.98
22	5.00	0.0850	23.2	3.15	0.00
23	5.25	0.0850	23.2	3.15	0.00

Table E-2 Experimental data obtained from batch experiment K-9.

Sample No	Time (h)	Optical density	Biomass concentration (mg/L)	Ln (biomass concentration)	2-Chlorophenol concentration (mg/L)
1	0.00	0.0475	13.0	2.56	35.0
2	0.25	0.0480	13.1	2.57	34.2
3	0.50	0.0495	13.5	2.61	33.4
4	0.75	0.0510	13.9	2.63	32.2
5	1.00	0.0530	14.5	2.67	31.5
6	1.25	0.0555	15.2	2.72	30.1
7	1.50	0.0575	15.7	2.75	28.7
8	1.67	0.0590	16.1	2.78	27.1
9	2.00	0.0615	16.8	2.82	25.5
10	2.25	0.0640	17.5	2.86	23.1
11	2.50	0.0680	18.6	2.92	21.2
12	2.75	0.0720	19.7	2.98	19.6
13	3.00	0.0750	20.5	3.02	17.3
14	3.25	0.0780	21.3	3.06	14.7
15	3.50	0.0810	22.1	3.10	12.2
16	3.75	0.0850	23.2	3.15	9.92
17	4.00	0.0900	24.6	3.20	7.38
18	4.25	0.0940	25.7	3.25	4.80
19	4.50	0.0970	26.5	3.28	2.50
20	4.75	0.1010	27.6	3.32	0.30
21	5.00	0.1040	28.4	3.35	0.00
22	5.25	0.1040	28.4	3.35	0.00

Table E-3 Experimental data obtained from batch experiment K-10.

Sample No	Time (h)	Optical density	Biomass concentration (mg/L)	Ln (biomass concentration)	2-Chlorophenol concentration (mg/L)
1	0.00	0.0430	11.8	2.46	42.9
2	0.25	0.0430	11.8	2.46	41.8
3	0.50	0.0440	12.0	2.49	41.3
4	0.75	0.0445	12.2	2.50	40.6
5	1.00	0.0455	12.4	2.52	39.1
6	1.25	0.0470	12.8	2.55	38.2
7	1.50	0.0490	13.4	2.59	37.0
8	1.75	0.0510	13.9	2.63	36.5
9	2.00	0.0530	14.5	2.67	34.6
10	2.25	0.0545	14.9	2.70	33.8
11	2.50	0.0565	15.4	2.74	33.0
12	2.75	0.0580	15.9	2.76	31.5
13	3.00	0.0600	16.4	2.80	30.5
14	3.25	0.0620	16.9	2.83	29.4
15	3.50	0.0630	17.2	2.85	28.3
16	3.75	0.0645	17.8	2.87	27.3
17	4.00	0.0670	18.5	2.91	25.7
18	4.25	0.0690	19.1	2.94	24.6
19	4.50	0.0710	19.7	2.97	23.4
20	4.75	0.0735	20.2	3.00	21.5
21	5.00	0.0750	20.8	3.02	20.1
22	5.25	0.0770	21.3	3.05	17.9
23	5.50	0.0790	22.0	3.07	16.0
24	5.75	0.0810	22.7	3.10	14.0
25	6.00	0.0850	23.5	3.15	12.1

Table E-3 (continued)

Sample No	Time (h)	Optical density	Biomass concentration (mg/L)	Ln (biomass concentration)	2-Chlorophenol concentration (mg/L)
26	6.25	0.0880	24.3	3.18	10.6
27	6.50	0.0900	25.2	3.20	8.50
28	6.75	0.0940	25.7	3.25	6.58
29	7.00	0.0960	26.5	3.27	4.70
30	7.25	0.0980	27.3	3.29	2.67
31	7.50	0.1010	28.2	3.32	0.85
32	7.75	0.1050	29.0	3.36	0.00
33	8.00	0.1060	29.3	3.37	0.00

Table E-4 Experimental data obtained from batch experiment K-11.

Sample No	Time (h)	Optical density	Biomass concentration (mg/L)	Ln (biomass concentration)	2-Chlorophenol concentration (mg/L)
1	0.00	0.0370	10.1	2.31	51.8
2	0.25	0.0370	10.1	2.31	51.0
3	0.50	0.0380	10.4	2.34	50.4
4	0.75	0.0385	10.5	2.35	49.3
5	0.83	0.0390	10.7	2.37	48.8
6	1.00	0.0400	10.9	2.39	47.8
7	1.25	0.0415	11.3	2.43	45.5
8	1.50	0.0430	11.8	2.46	44.5
9	1.75	0.0445	12.2	2.50	43.4
10	2.00	0.0460	12.6	2.53	42.5
11	2.25	0.0470	12.8	2.55	40.5
12	2.50	0.0490	13.4	2.59	39.0
13	2.75	0.0510	13.9	2.63	38.5
14	3.00	0.0525	14.4	2.66	37.0
15	3.25	0.0540	14.8	2.69	35.3
16	3.50	0.0560	15.3	2.73	33.4
17	3.75	0.0570	15.6	2.75	32.1
18	4.00	0.0590	16.1	2.78	30.1
19	4.25	0.0610	16.7	2.81	27.3
20	4.50	0.0620	16.9	2.83	24.5
21	4.75	0.0640	17.5	2.86	21.9
22	5.00	0.0660	18.0	2.89	21.4
23	5.25	0.0680	18.6	2.92	20.7
24	5.50	0.0700	19.1	2.95	18.1
25	5.75	0.0720	19.7	2.98	17.4

Table E-4 (continued)

Sample No	Time (h)	Optical density	Biomass concentration (mg/L)	Ln (biomass concentration)	2-Chlorophenol concentration (mg/L)
26	6.00	0.0740	20.2	3.01	15.0
27	6.25	0.0770	21.1	3.05	13.0
28	6.50	0.0790	21.6	3.07	10.7
29	6.75	0.0820	22.4	3.11	8.10
30	7.00	0.0840	23.0	3.13	6.05
31	7.25	0.0870	23.8	3.17	4.60
32	7.50	0.0895	24.5	3.20	2.25
34	7.75	0.0920	25.2	3.22	1.00
35	8.00	0.0950	26.0	3.26	0.15
36	8.25	0.0980	26.8	3.29	0.00
37	8.50	0.0980	26.8	3.29	0.00

Table E-5 Experimental data obtained from batch experiment K-12.

Sample No	Time (h)	Optical density	Biomass concentration (mg/L)	Ln (biomass concentration)	2-Chlorophenol concentration (mg/L)
1	0.00	0.0470	12.8	2.55	73.1
2	0.25	0.0470	12.8	2.55	72.3
3	0.50	0.0480	13.1	2.57	71.5
4	0.75	0.0485	13.3	2.58	69.8
5	1.00	0.0495	13.5	2.61	69.0
6	1.25	0.0510	13.9	2.63	68.2
7	1.50	0.0520	14.2	2.65	67.1
8	1.75	0.0540	14.8	2.69	66.4
9	2.00	0.0560	15.3	2.73	65.0
10	2.25	0.0570	15.6	2.75	63.8
11	2.50	0.0590	16.1	2.78	62.4
12	2.75	0.0610	16.7	2.81	61.5
13	3.00	0.0630	17.2	2.85	60.8
14	3.25	0.0645	17.6	2.87	58.9
15	3.50	0.0660	18.0	2.89	56.2
16	3.75	0.0680	18.6	2.92	53.5
17	4.00	0.0700	19.1	2.95	51.9
18	4.25	0.0720	19.7	2.98	49.3
19	4.50	0.0740	20.2	3.01	48.0
20	4.75	0.0760	20.8	3.03	46.6
21	5.00	0.0780	21.3	3.06	44.1
22	5.25	0.0800	21.9	3.09	41.3
23	5.50	0.0820	22.4	3.11	38.3
24	5.75	0.0840	23.0	3.13	36.6
25	6.00	0.0870	23.8	3.17	33.7

Table E-5 (continued)

Sample No	Time (h)	Optical density	Biomass concentration (mg/L)	Ln (biomass concentration)	2-Chlorophenol concentration (mg/L)
26	6.25	0.0900	24.6	3.20	31.8
27	6.50	0.0930	25.4	3.24	27.6
28	6.75	0.0970	26.5	3.28	25.8
29	7.00	0.1000	27.3	3.31	23.4
30	7.25	0.1030	28.2	3.34	21.0
31	7.50	0.1070	29.3	3.38	16.9
32	7.75	0.1120	30.6	3.42	13.2
34	8.00	0.1170	32.0	3.47	9.43
35	8.25	0.1220	33.4	3.51	6.40
36	8.50	0.1260	34.4	3.54	2.86
37	8.75	0.1290	35.3	3.56	0.34
38	9.00	0.1320	36.1	3.59	0.00
39	9.25	0.1330	36.4	3.59	0.00

Table E-6 Experimental data obtained from batch experiment K-13.

Sample No	Time (h)	Optical density	Biomass concentration (mg/L)	Ln (biomass concentration)	2-Chlorophenol concentration (mg/L)
1	0.00	0.0380	10.4	2.34	88.6
2	0.25	0.0380	10.4	2.34	88.2
3	0.50	0.0390	10.7	2.37	87.8
4	0.75	0.0390	10.7	2.37	86.5
5	1.00	0.0395	10.8	2.38	85.6
6	1.25	0.0400	10.9	2.39	83.7
7	1.50	0.0410	11.2	2.42	82.3
8	1.75	0.0420	11.5	2.44	81.0
9	2.00	0.0430	11.8	2.46	80.4
10	2.33	0.0445	12.2	2.50	79.2
11	2.58	0.0460	12.6	2.53	78.7
12	2.75	0.0470	12.8	2.55	77.7
13	3.00	0.0475	13.0	2.56	76.0
14	3.25	0.0490	13.4	2.59	74.9
15	3.50	0.0500	13.7	2.62	73.0
16	3.75	0.0510	13.9	2.63	71.5
17	4.00	0.0525	14.4	2.66	69.5
18	4.25	0.0545	14.9	2.70	67.9
19	4.50	0.0555	15.2	2.72	65.8
20	4.75	0.0570	15.6	2.75	63.8
21	5.00	0.0590	16.1	2.78	62.0
22	5.25	0.0600	16.4	2.80	60.2
23	5.50	0.0610	16.7	2.81	58.0
24	5.75	0.0630	17.2	2.85	55.9

Table E-6 (continued)

Sample No	Time (h)	Optical density	Biomass concentration (mg/L)	Ln (biomass concentration)	2-Chlorophenol concentration (mg/L)
25	6.00	0.0650	17.8	2.88	53.9
26	6.25	0.0660	18.0	2.89	52.0
27	6.50	0.0670	18.3	2.91	49.9
28	6.75	0.0690	18.9	2.94	47.7
29	7.00	0.0710	19.4	2.97	45.6
30	7.25	0.0730	20.0	2.99	43.7
31	7.50	0.0750	20.5	3.02	41.7
32	7.75	0.0760	20.8	3.03	39.2
34	8.00	0.0780	21.3	3.06	37.8
35	8.25	0.0800	21.9	3.09	35.0
36	8.50	0.0810	22.1	3.10	32.1
37	8.75	0.0825	22.6	3.12	31.1
38	9.00	0.0850	23.2	3.15	29.7
39	9.25	0.0875	23.9	3.17	27.2
40	9.50	0.0900	24.6	3.20	25.4
41	9.75	0.0930	25.4	3.24	23.5
42	10.00	0.0960	26.2	3.27	19.1
43	10.25	0.0990	27.1	3.30	18.4
44	10.50	0.1020	27.9	3.33	15.6
45	10.75	0.1060	29.0	3.37	12.6
46	11.00	0.1100	30.1	3.40	10.6
47	11.25	0.1150	31.4	3.45	7.25
48	11.50	0.1190	32.5	3.48	4.82
49	11.75	0.1240	33.9	3.52	2.66

Table E-6 (continued)

Sample No	Time (h)	Optical density	Biomass concentration (mg/L)	Ln (biomass concentration)	2-Chlorophenol concentration (mg/L)
50	12.00	0.1270	34.7	3.55	0.81
51	12.25	0.1300	35.5	3.57	0.00
52	12.50	0.1310	35.8	3.58	0.00

Table E-7 Experimental data obtained from batch experiment K-15.

Sample No	Time (h)	Optical density	Biomass concentration (mg/L)	Ln (biomass concentration)	2-Chlorophenol concentration (mg/L)
1	0.00	0.0200	5.47	1.70	4.95
2	0.17	0.0205	5.60	1.72	4.71
3	0.33	0.0210	5.74	1.75	4.53
4	0.50	0.0215	5.88	1.77	4.24
5	0.67	0.0220	6.01	1.79	4.00
6	0.83	0.0225	6.15	1.82	3.62
7	1.00	0.0230	6.29	1.84	3.24
8	1.20	0.0240	6.56	1.88	2.70
9	1.33	0.0245	6.70	1.90	2.50
10	1.50	0.0250	6.83	1.92	2.19
11	1.67	0.0260	7.11	1.96	1.84
12	1.87	0.0265	7.24	1.98	1.39
13	2.00	0.0270	7.38	2.00	1.07
14	2.25	0.0280	7.65	2.04	0.47
15	2.37	0.0280	7.65	2.04	0.00

Table E-8 Experimental data obtained from batch experiment K-16.

Sample No	Time (h)	Optical density	Biomass concentration (mg/L)	Ln (biomass concentration)	2-Chlorophenol concentration (mg/L)
1	0.00	0.0200	5.47	1.70	5.89
2	0.17	0.0200	5.47	1.70	5.28
3	0.33	0.0205	5.60	1.72	5.16
4	0.50	0.0210	5.74	1.75	4.85
5	0.67	0.0215	5.88	1.77	4.47
6	0.83	0.0220	6.01	1.79	4.04
7	1.00	0.0225	6.15	1.82	3.72
8	1.17	0.0230	6.29	1.84	3.35
9	1.33	0.0240	6.56	1.88	2.90
10	1.50	0.0245	6.70	1.90	2.54
11	1.67	0.0250	6.83	1.92	2.09
12	1.83	0.0260	7.11	1.96	1.67
13	2.00	0.0265	7.24	1.98	1.27
14	2.17	0.0270	7.38	2.00	0.89
15	2.42	0.0280	7.65	2.04	0.12
16	2.67	0.0290	7.93	2.07	0.00
17	2.92	0.0290	7.93	2.07	0.00

Table E-9 Experimental data obtained from batch experiment K-17.

Sample No	Time (h)	Optical density	Biomass concentration (mg/L)	Ln (biomass concentration)	2-Chlorophenol concentration (mg/L)
1	0.00	0.0200	5.47	1.70	6.36
2	0.17	0.0200	5.47	1.70	6.03
3	0.33	0.0205	5.60	1.72	5.51
4	0.50	0.0210	5.74	1.75	5.28
5	0.67	0.0215	5.88	1.77	5.01
6	0.83	0.0220	6.01	1.79	4.55
7	1.00	0.0225	6.15	1.82	4.36
8	1.17	0.0230	6.29	1.84	3.91
9	1.33	0.0235	6.42	1.86	3.55
10	1.50	0.0240	6.56	1.88	3.07
11	1.67	0.0245	6.70	1.90	2.72
12	1.83	0.0250	6.83	1.92	2.33
13	2.00	0.0260	7.11	1.96	1.95
14	2.25	0.0270	7.38	2.00	1.37
15	2.50	0.0280	7.65	2.04	0.69
16	2.75	0.0285	7.79	2.05	0.00
17	3.00	0.0280	7.65	2.04	0.00

Table E-10 Experimental data obtained from batch experiment K-18.

Sample No	Time (h)	Optical density	Biomass concentration (mg/L)	Ln (biomass concentration)	2-Chlorophenol concentration (mg/L)
1	0.00	0.0390	10.7	2.37	8.14
2	0.17	0.0400	10.9	2.39	7.57
3	0.33	0.0405	11.1	2.40	6.67
4	0.50	0.0420	11.5	2.44	6.19
5	0.67	0.0430	11.8	2.46	5.46
6	0.83	0.0440	12.0	2.49	4.80
7	1.00	0.0445	12.2	2.50	4.17
8	1.17	0.0465	12.7	2.54	3.50
9	1.33	0.0470	12.8	2.55	2.97
10	1.50	0.0480	13.1	2.57	2.33
11	1.67	0.0490	13.4	2.59	1.59
12	1.83	0.0505	13.8	2.63	1.01
13	2.00	0.0510	13.9	2.63	0.03
14	2.17	0.0510	13.9	2.63	0.00

Table E-11 Experimental data obtained from batch experiment K-19.

Sample No	Time (h)	Optical density	Biomass concentration (mg/L)	Ln (biomass concentration)	2-Chlorophenol concentration (mg/L)
1	0.00	0.0290	7.93	2.07	9.55
2	0.17	0.0295	8.06	2.09	8.74
3	0.33	0.0305	8.34	2.12	8.03
4	0.50	0.0310	8.47	2.14	7.92
5	0.67	0.0320	8.75	2.17	7.30
6	0.83	0.0330	9.02	2.20	6.96
7	1.00	0.0340	9.30	2.23	6.55
8	1.17	0.0345	9.43	2.24	5.93
9	1.33	0.0360	9.84	2.29	5.54
10	1.50	0.0375	10.3	2.33	4.84
11	1.67	0.0380	10.4	2.34	4.20
12	1.83	0.0400	10.9	2.39	3.70
13	2.00	0.0410	11.2	2.42	3.07
14	2.17	0.0420	11.5	2.44	2.55
15	2.33	0.0435	11.9	2.48	1.99
16	2.50	0.0440	12.0	2.49	1.34
17	2.67	0.0450	12.3	2.51	0.78
18	2.83	0.0460	12.6	2.53	0.12
19	3.00	0.0460	12.6	2.53	0.00

Table E-12 Experimental data obtained from batch experiment K-20.

Sample No	Time (h)	Optical density	Biomass concentration (mg/L)	Ln (biomass concentration)	2-Chlorophenol concentration (mg/L)
1	0.00	0.0210	5.74	1.75	10.0
2	0.20	0.0215	5.88	1.77	9.53
3	0.33	0.0220	6.01	1.79	8.83
4	0.50	0.0230	6.29	1.84	8.24
5	0.67	0.0230	6.29	1.84	7.90
6	0.83	0.0240	6.56	1.88	7.58
7	1.00	0.0245	6.70	1.90	7.03
8	1.17	0.0250	6.83	1.92	6.71
9	1.33	0.0260	7.11	1.96	6.43
10	1.50	0.0265	7.24	1.98	6.08
11	1.70	0.0270	7.38	2.00	5.43
12	1.83	0.0285	7.79	2.05	5.14
13	2.00	0.0290	7.93	2.07	4.55
14	2.17	0.0300	8.20	2.10	3.80
15	2.33	0.0310	8.47	2.14	3.56
16	2.58	0.0320	8.75	2.17	2.69
17	2.83	0.0330	9.02	2.20	1.99
18	3.08	0.0350	9.57	2.26	1.19
19	3.33	0.0360	9.84	2.29	0.57
20	3.58	0.0360	9.84	2.29	0.00

Table E-13 Experimental data obtained from batch experiment K-21.

Sample No	Time (h)	Optical density	Biomass concentration (mg/L)	Ln (biomass concentration)	2-Chlorophenol concentration (mg/L)
1	0.00	0.0300	8.20	2.10	15.8
2	0.25	0.0310	8.47	2.14	15.2
3	0.50	0.0320	8.75	2.17	14.3
4	0.75	0.0335	9.16	2.21	13.4
5	1.00	0.0350	9.57	2.26	12.8
6	1.25	0.0360	9.84	2.29	11.8
7	1.50	0.0380	10.4	2.34	10.9
8	1.77	0.0390	10.7	2.37	10.1
9	2.00	0.0410	11.2	2.42	8.90
10	2.25	0.0420	11.5	2.44	8.00
11	2.50	0.0435	11.9	2.48	6.82
12	2.75	0.0450	12.3	2.51	5.41
13	3.00	0.0470	12.8	2.55	4.16
14	3.25	0.0490	13.4	2.59	2.90
15	3.50	0.0510	13.9	2.63	1.73
16	3.75	0.0530	14.5	2.67	0.75
17	4.00	0.0550	15.0	2.71	0.02
18	4.25	0.0550	15.0	2.71	0.00

Table E-14 Experimental data obtained from batch experiment K-22.

Sample No	Time (h)	Optical density	Biomass concentration (mg/L)	Ln (biomass concentration)	2-Chlorophenol concentration (mg/L)
1	0.00	0.0390	10.7	2.37	20.3
2	0.17	0.0390	10.7	2.37	19.4
3	0.33	0.0400	10.9	2.39	18.2
4	0.50	0.0410	11.2	2.42	17.2
5	0.67	0.0420	11.5	2.44	16.8
6	0.83	0.0435	11.9	2.48	15.2
7	1.00	0.0440	12.0	2.49	14.7
8	1.17	0.0460	12.6	2.53	13.8
9	1.33	0.0470	12.8	2.55	13.1
10	1.50	0.0485	13.3	2.58	11.8
11	1.67	0.0500	13.7	2.62	10.9
12	1.83	0.0520	14.2	2.65	10.0
13	2.03	0.0540	14.8	2.69	8.96
14	2.17	0.0550	15.0	2.71	8.18
15	2.33	0.0565	15.4	2.74	6.89
16	2.50	0.0580	15.9	2.76	5.85
17	2.75	0.0610	16.7	2.81	4.21
18	3.00	0.0630	17.2	2.85	2.71
19	3.25	0.0660	18.0	2.89	1.11
20	3.50	0.0690	18.9	2.94	0.22
21	3.75	0.0700	19.1	2.95	0.00

Table E-15 Experimental data obtained from batch experiment K-23.

Sample No	Time (h)	Optical density	Biomass concentration (mg/L)	Ln (biomass concentration)	2-Chlorophenol concentration (mg/L)
1	0.00	0.0390	10.7	2.37	25.2
2	0.17	0.0390	10.7	2.37	24.8
3	0.33	0.0400	10.9	2.39	23.6
4	0.50	0.0410	11.2	2.42	22.8
5	0.67	0.0420	11.5	2.44	21.9
6	0.83	0.0435	11.9	2.48	21.1
7	1.00	0.0450	12.3	2.51	20.7
8	1.17	0.0460	12.6	2.53	19.6
9	1.33	0.0470	12.8	2.55	18.7
10	1.50	0.0480	13.1	2.57	17.9
11	1.67	0.0490	13.4	2.59	16.8
12	1.83	0.0505	13.8	2.63	16.0
13	2.00	0.0520	14.2	2.65	15.4
14	2.17	0.0535	14.6	2.68	14.1
15	2.33	0.0550	15.0	2.71	12.9
16	2.50	0.0560	15.3	2.73	11.9
17	2.67	0.0580	15.9	2.76	11.0
18	2.83	0.0590	16.1	2.78	9.87
19	3.00	0.0605	16.5	2.81	8.76
20	3.25	0.0630	17.2	2.85	7.02
21	3.50	0.0660	18.0	2.89	5.24
22	3.75	0.0680	18.6	2.92	3.42
23	4.00	0.0710	19.4	2.97	1.73
24	4.25	0.0730	20.0	2.99	0.56
25	4.50	0.0750	20.5	3.02	0.00
26	4.75	0.0760	20.8	3.03	0.00

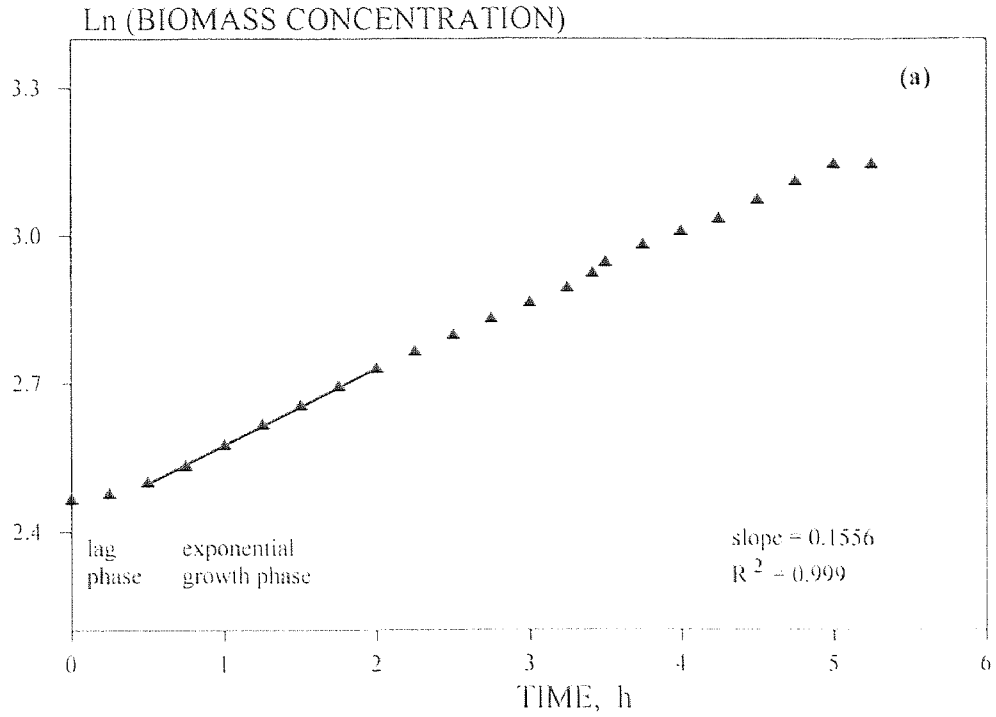

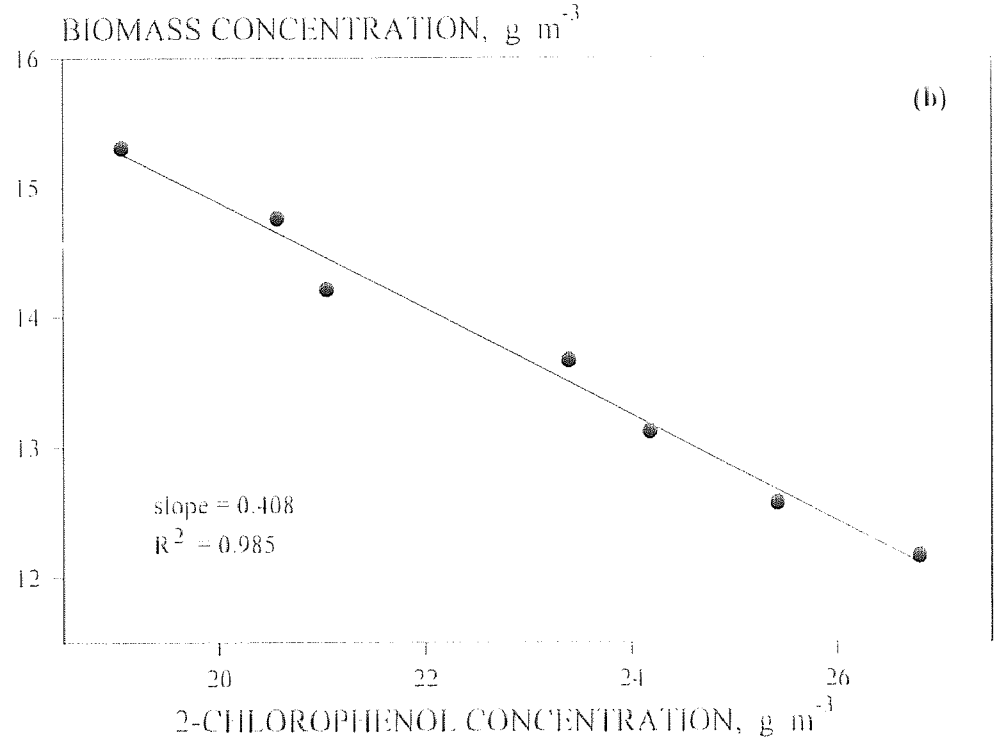

Figure E-1 Determination of the specific growth rate (a) and yield coefficient (b) of *P. pickettii* on 2-chlorophenol (Expt. K-8).

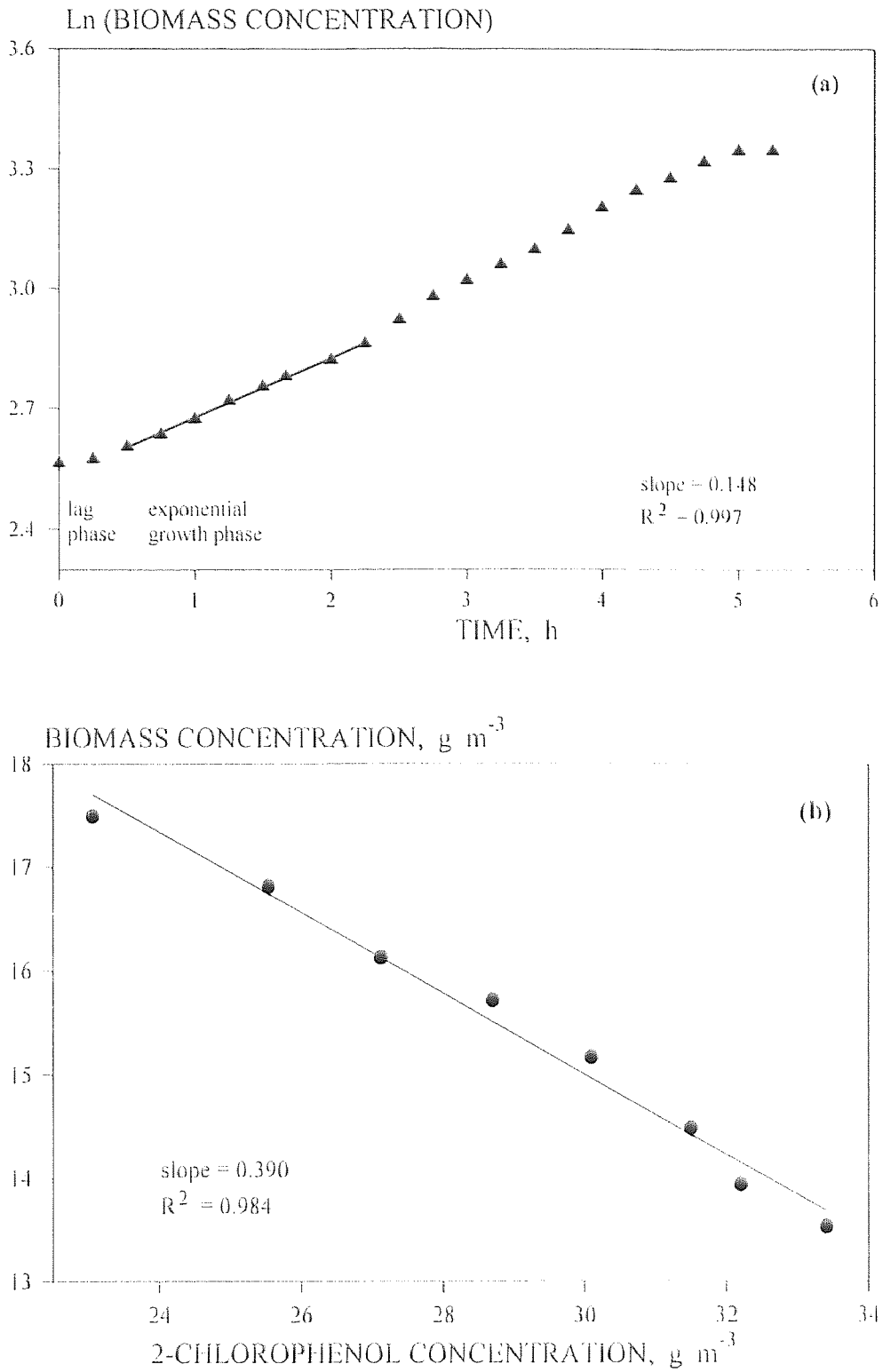

Figure E-2 Determination of the specific growth rate (a) and yield coefficient (b) of *P. pickettii* on 2-chlorophenol (Expt. K-9).

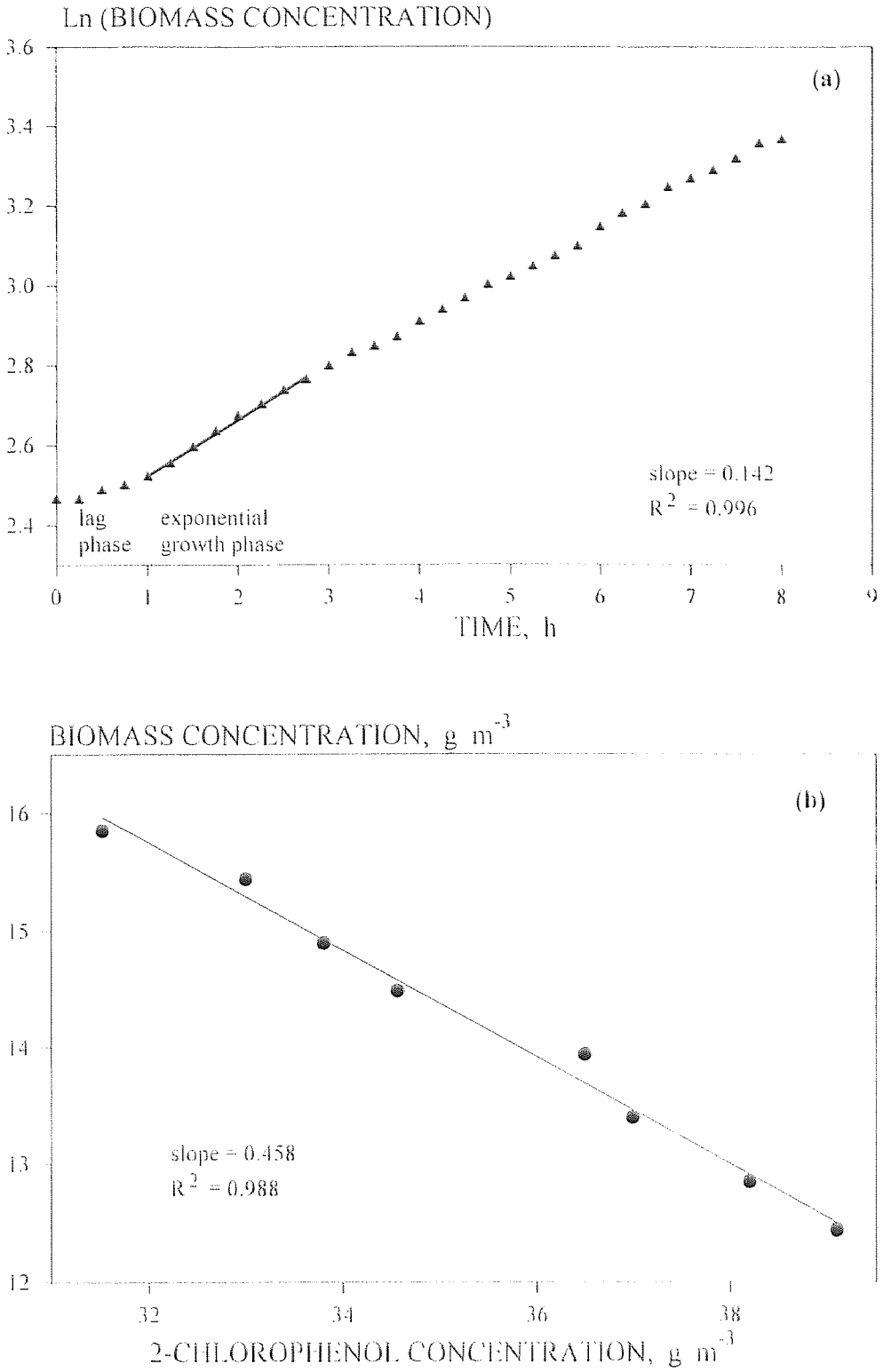

Figure E-3 Determination of the specific growth rate (a) and yield coefficient (b) of *P. pickettii* on 2-chlorophenol (Expt. K-10).

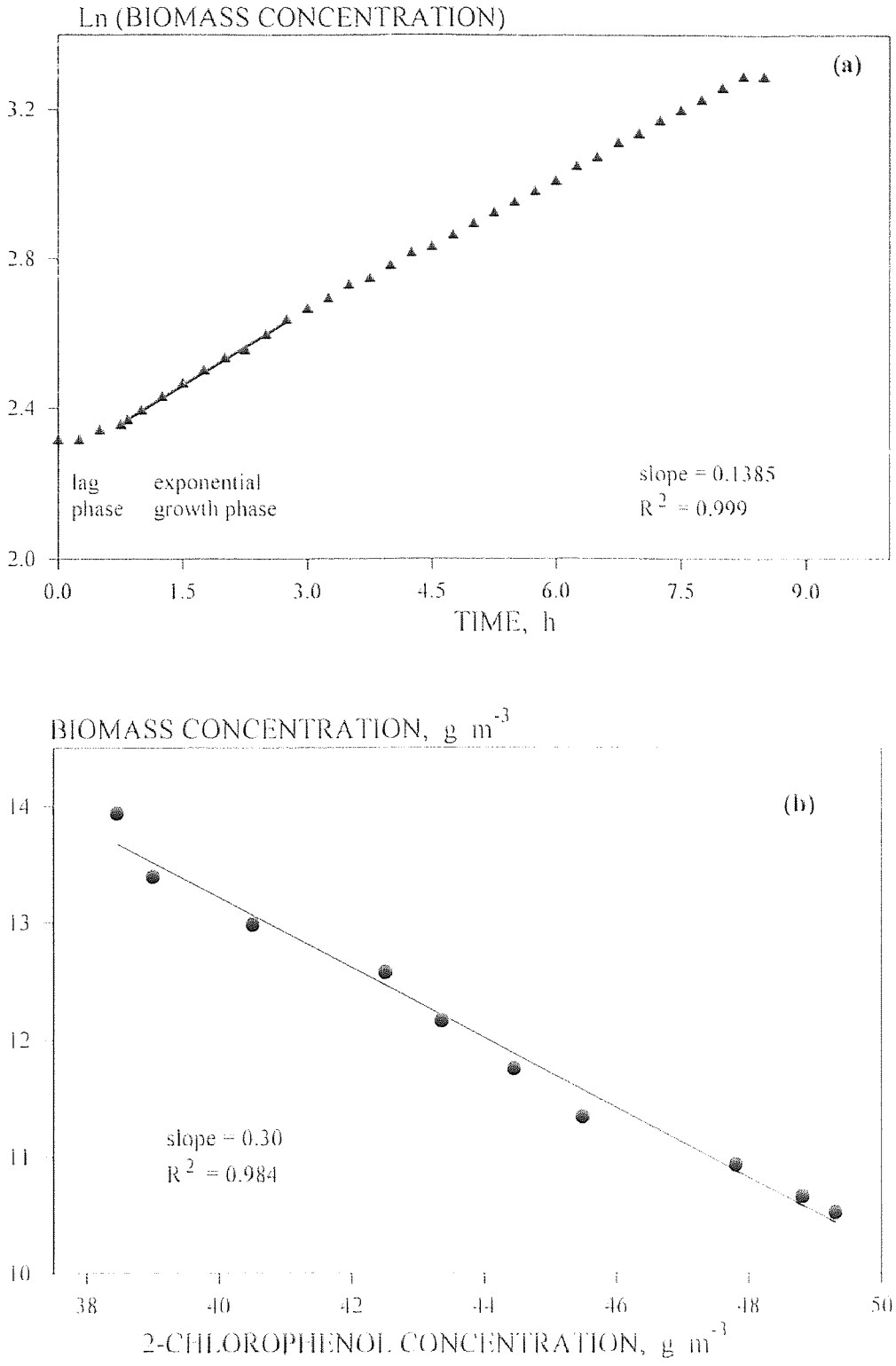

Figure E-4 Determination of the specific growth rate (a) and yield coefficient (b) of *P. pickettii* on 2-chlorophenol (Expt. K-11).

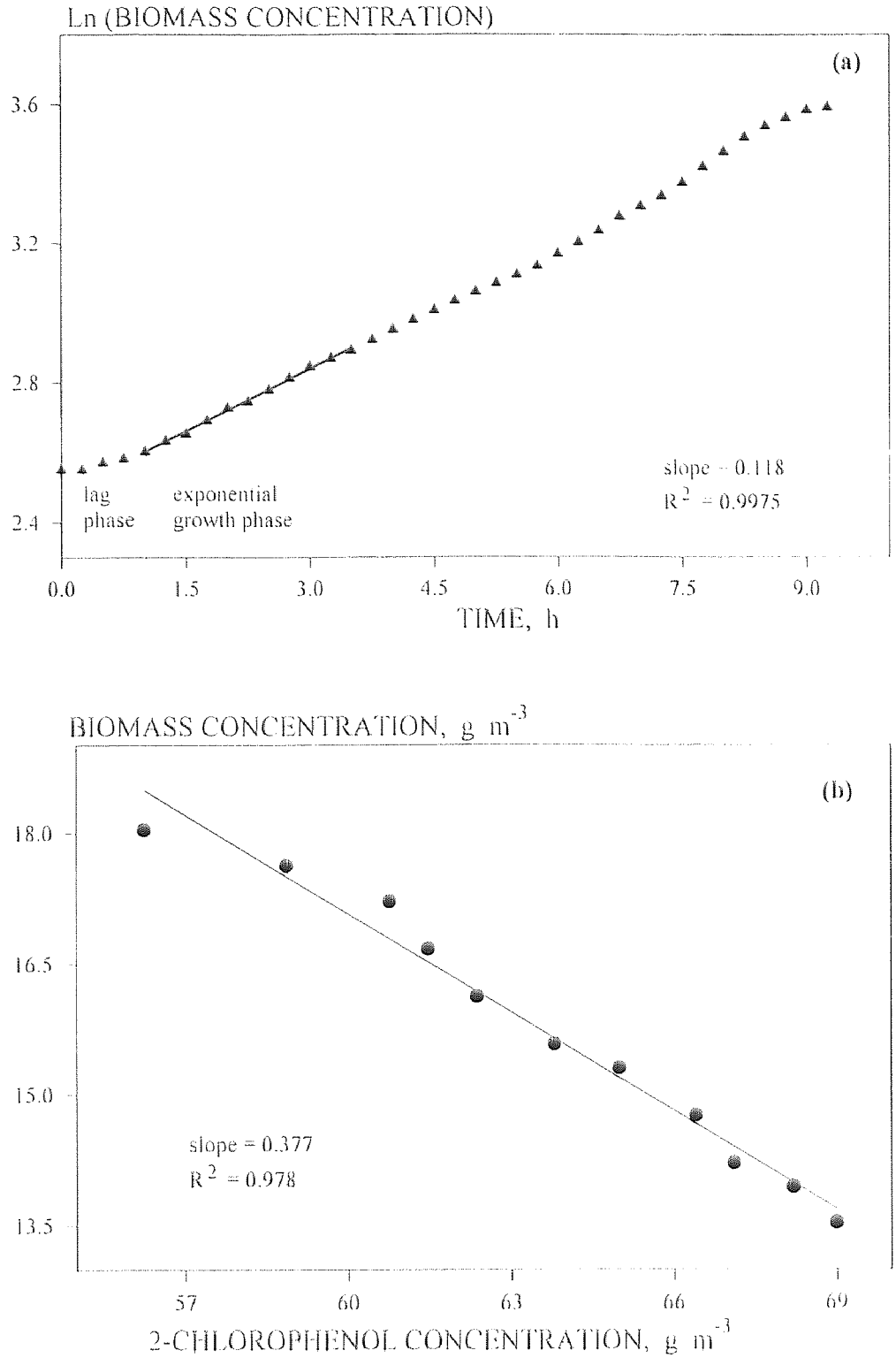

Figure E-5 Determination of the specific growth rate (a) and yield coefficient (b) of *P. pickettii* on 2-chlorophenol (Expt. K-12).

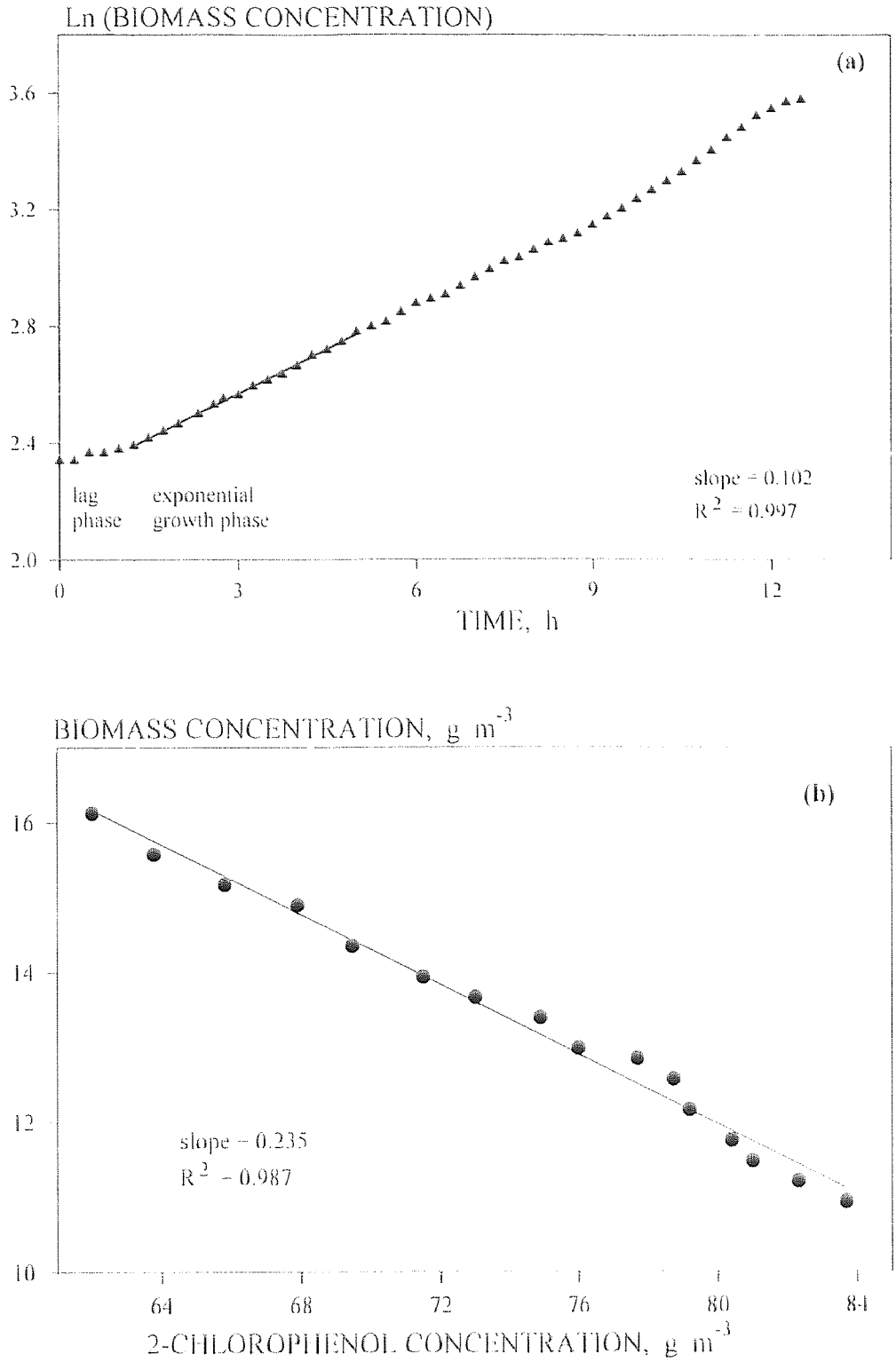

Figure E-6 Determination of the specific growth rate (a) and yield coefficient (b) of *P. pickettii* on 2-chlorophenol (Expt. K-13).

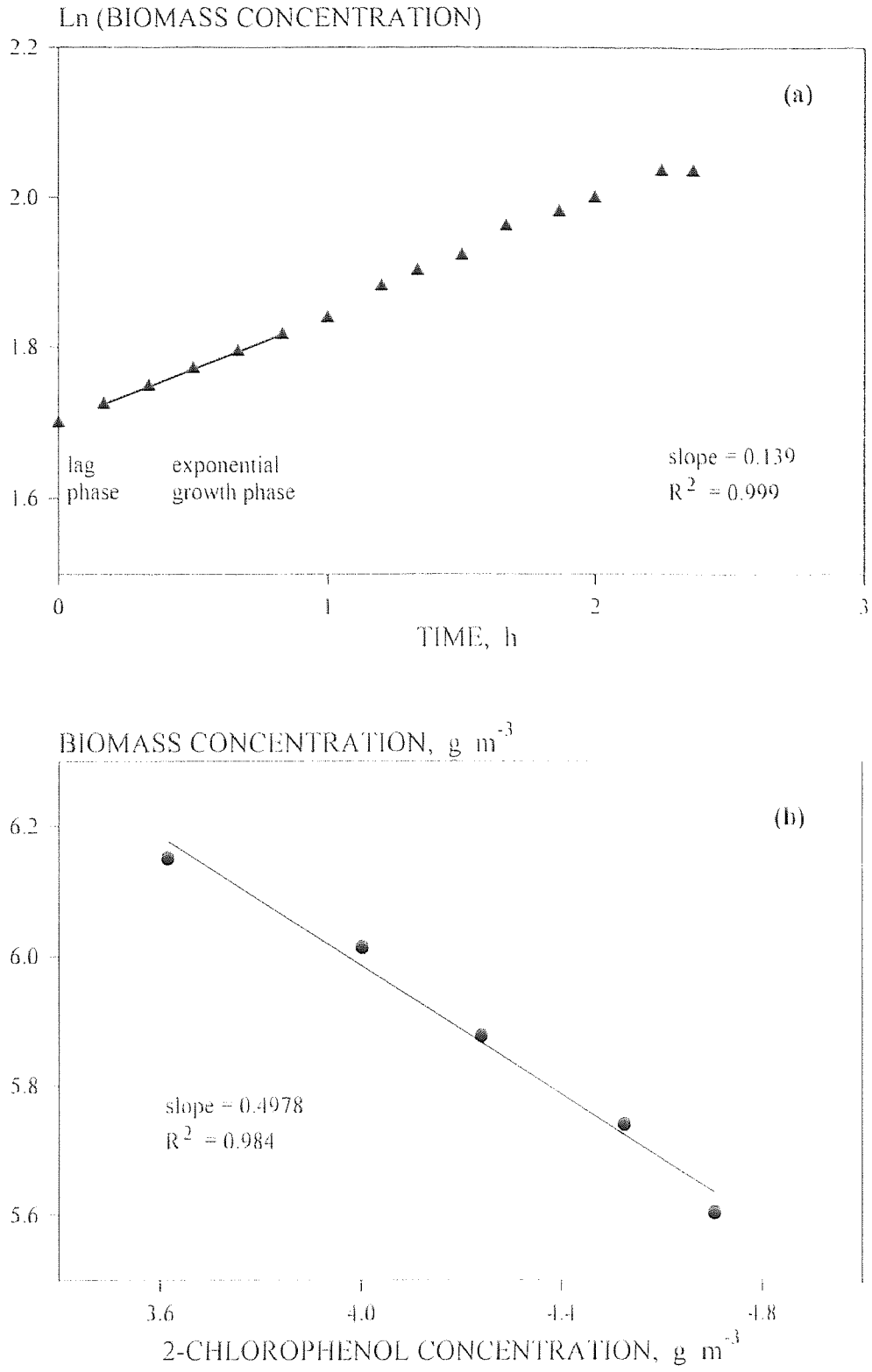

Figure E-7 Determination of the specific growth rate (a) and yield coefficient (b) of *P. pickettii* on 2-chlorophenol (Expt. K-15).

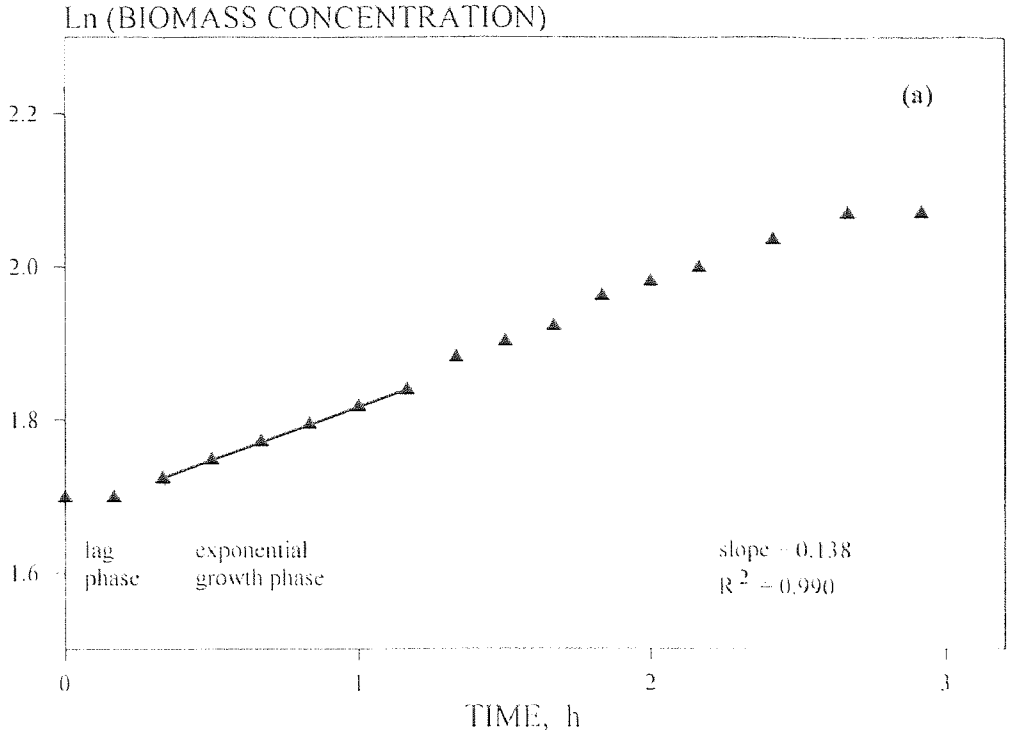

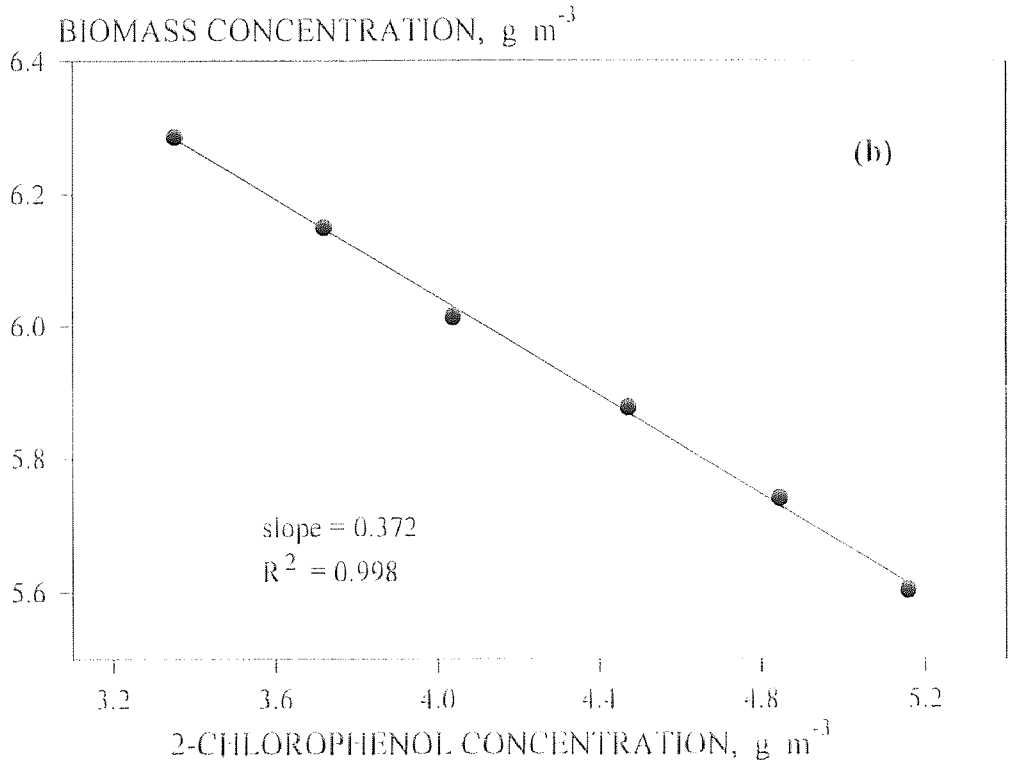

Figure E-8 Determination of the specific growth rate (a) and yield coefficient (b) of *P. pickettii* on 2-chlorophenol (Expt. K-16).

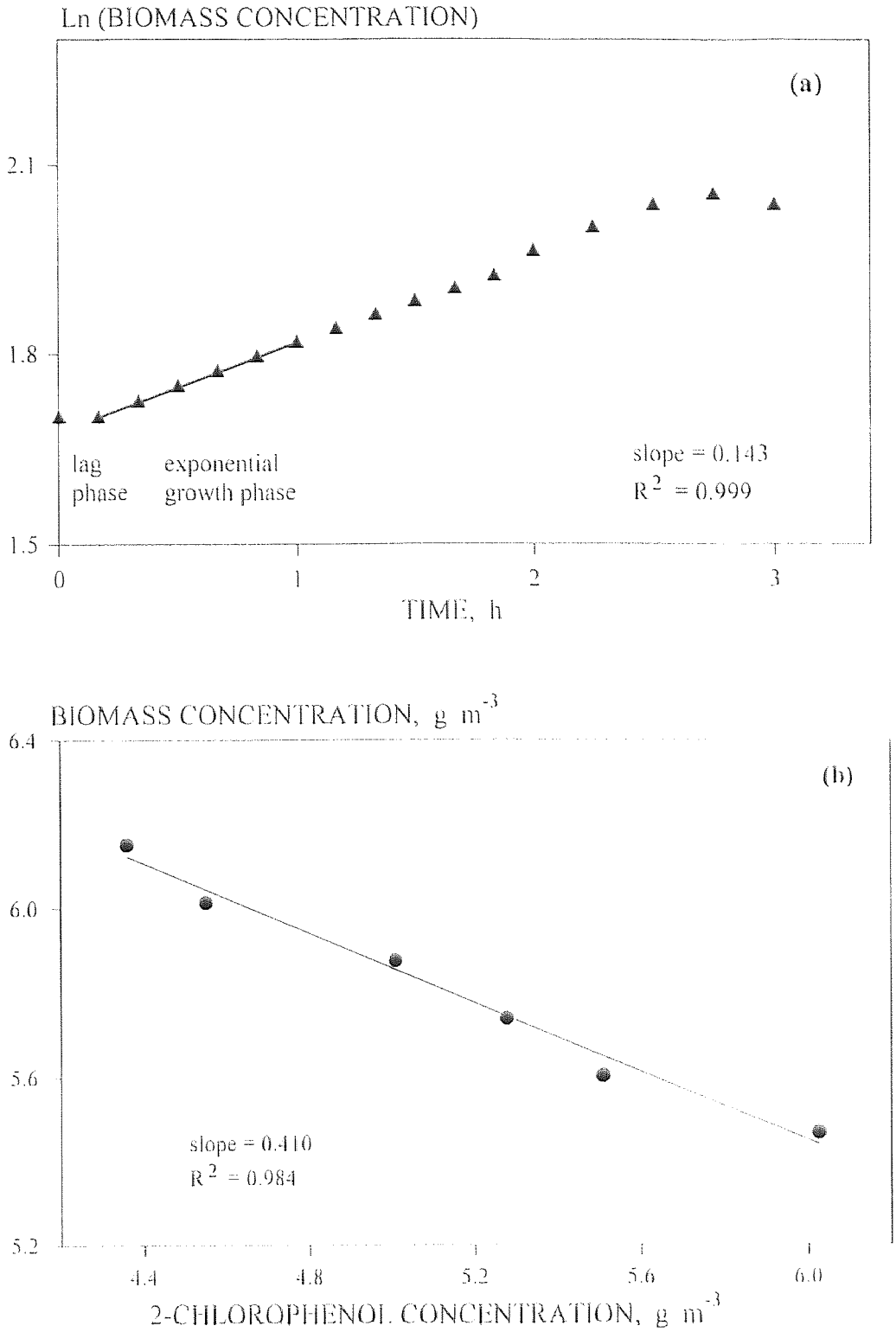

Figure E-9 Determination of the specific growth rate (a) and yield coefficient (b) of *P. pickettii* on 2-chlorophenol (Expt. K-17).

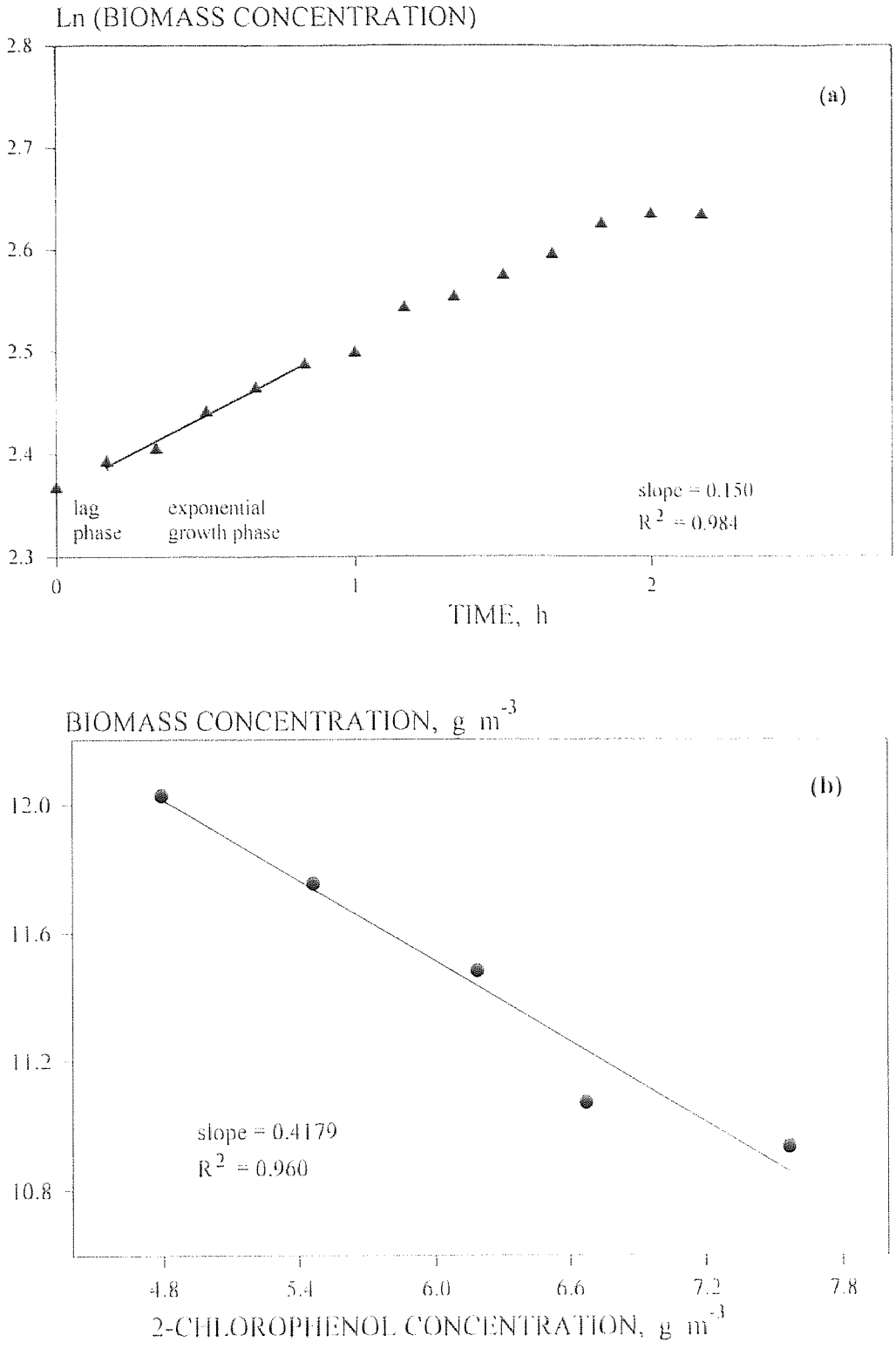

Figure E-10 Determination of the specific growth rate (a) and yield coefficient (b) of *P. pickettii* on 2-chlorophenol (Expt. K-18).

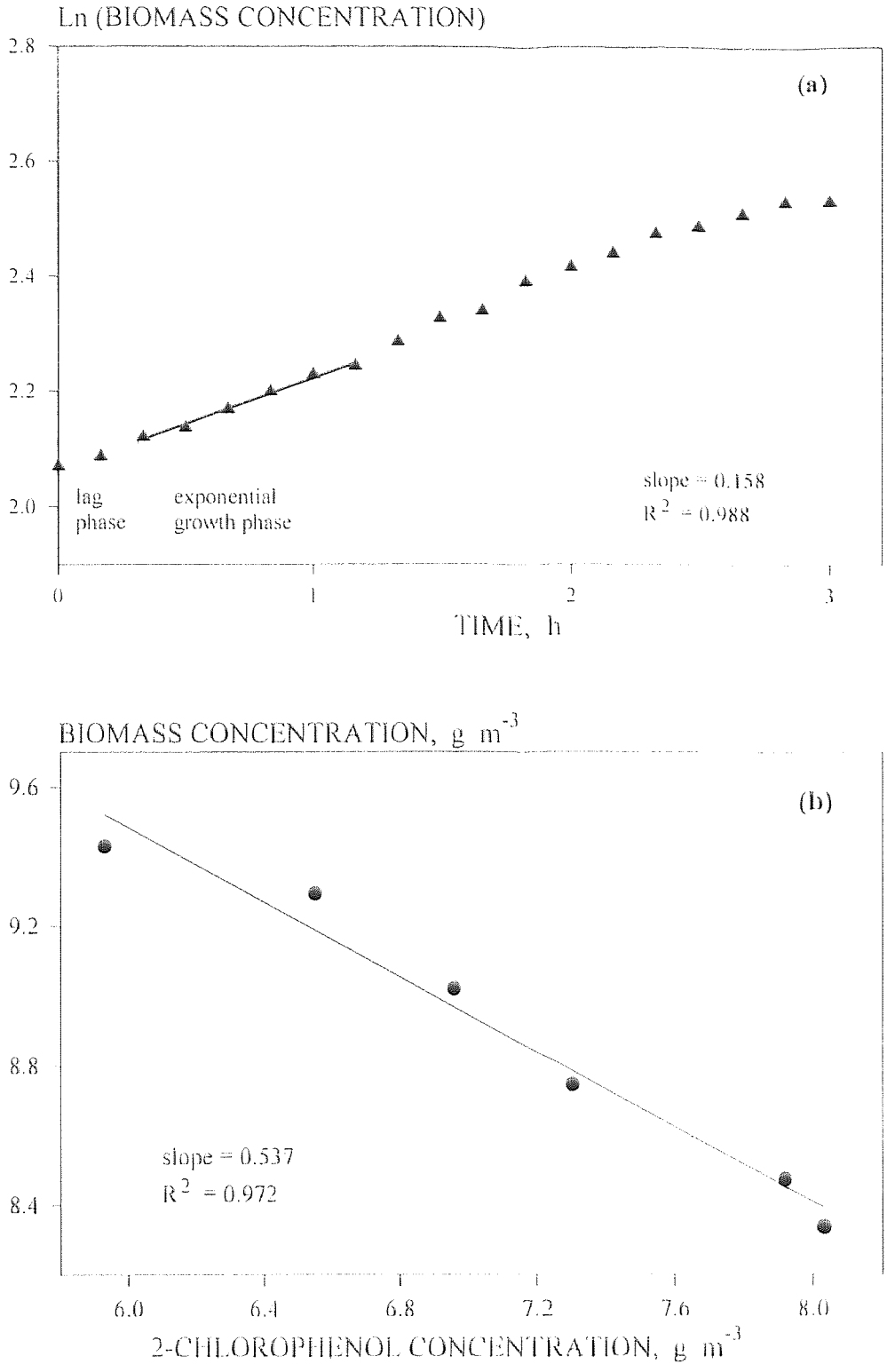

Figure E-11 Determination of the specific growth rate (a) and yield coefficient (b) of *P. pickettii* on 2-chlorophenol (Expt. K-19).

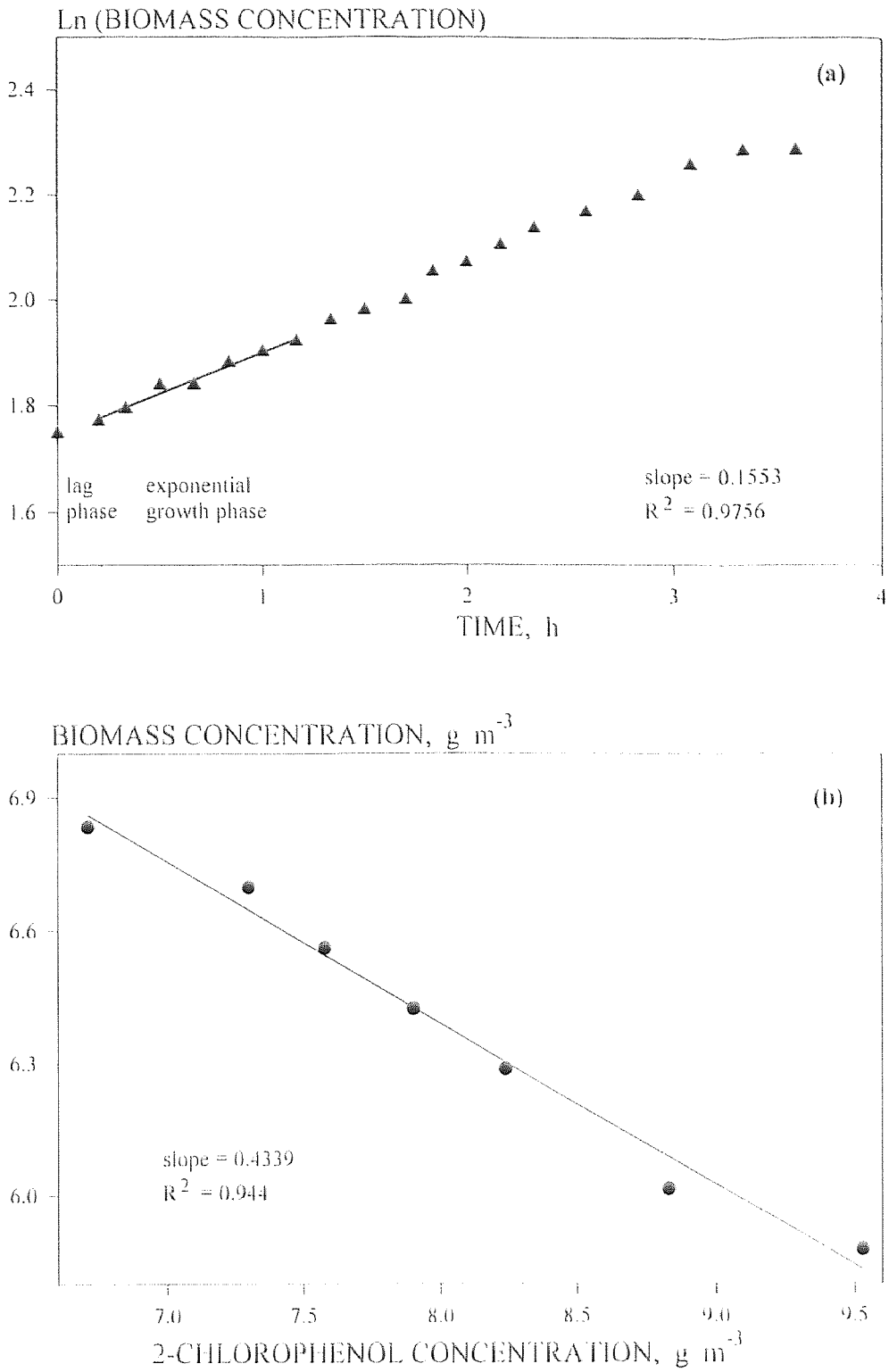

Figure E-12 Determination of the specific growth rate (a) and yield coefficient (b) of *P. pickettii* on 2-chlorophenol (Expt. K-20).

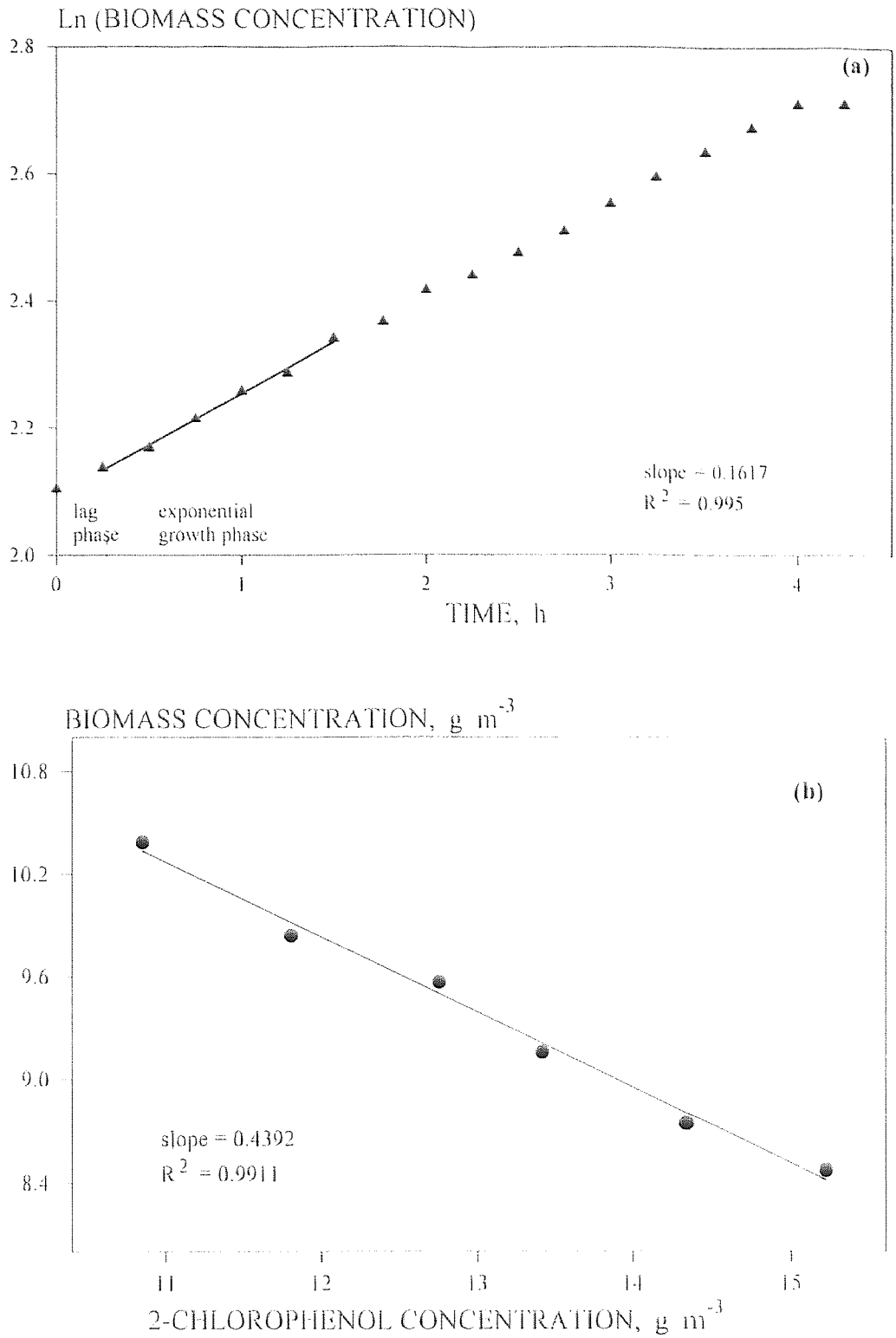

Figure E-13 Determination of the specific growth rate (a) and yield coefficient (b) of *P. pickettii* on 2-chlorophenol (Expt. K-21).

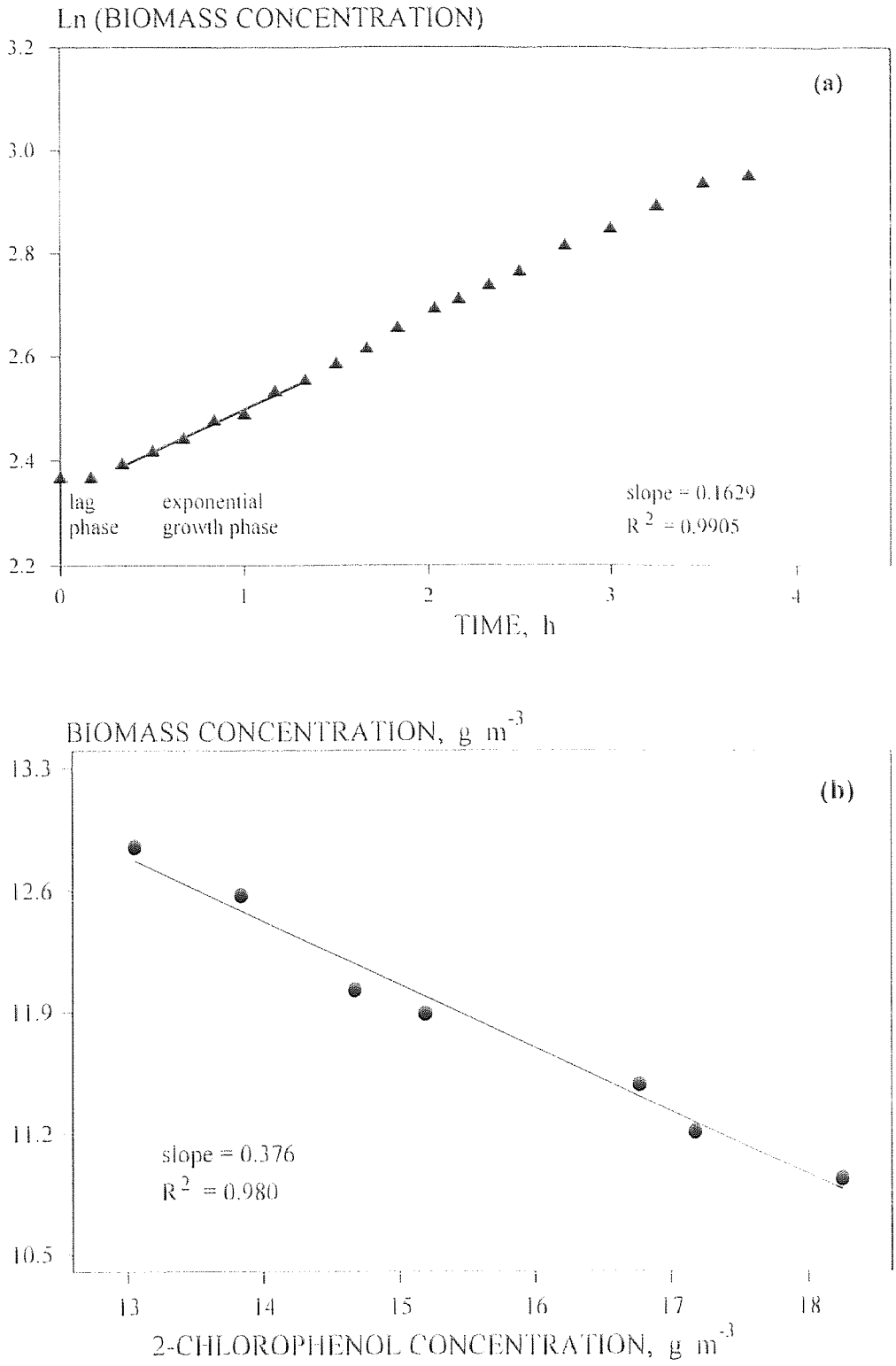

Figure E-14 Determination of the specific growth rate (a) and yield coefficient (b) of *P. pickettii* on 2-chlorophenol (Expt. K-22).

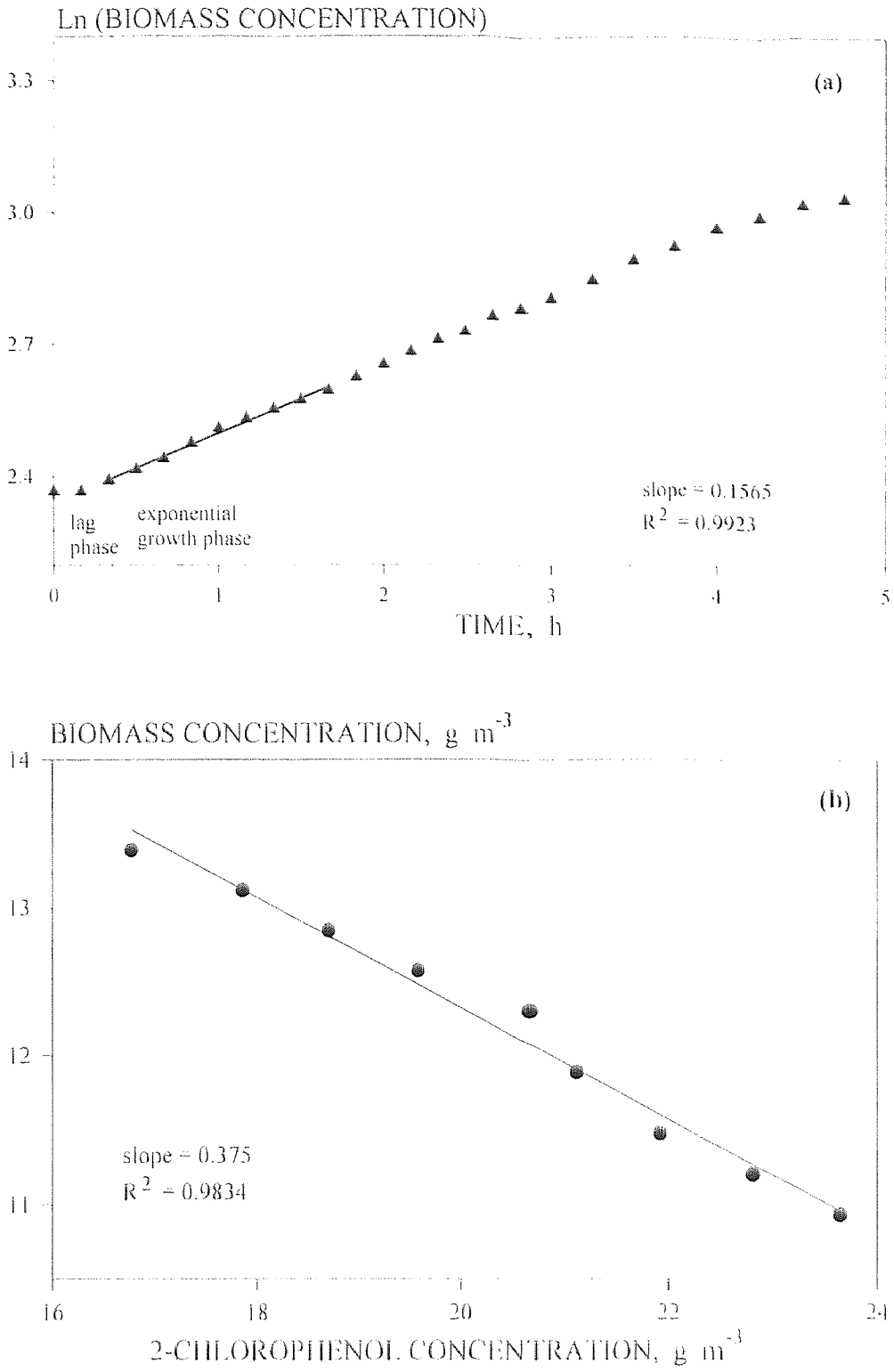

Figure E-15 Determination of the specific growth rate (a) and yield coefficient (b) of *P. pickettii* on 2-chlorophenol (Expt. K-23).

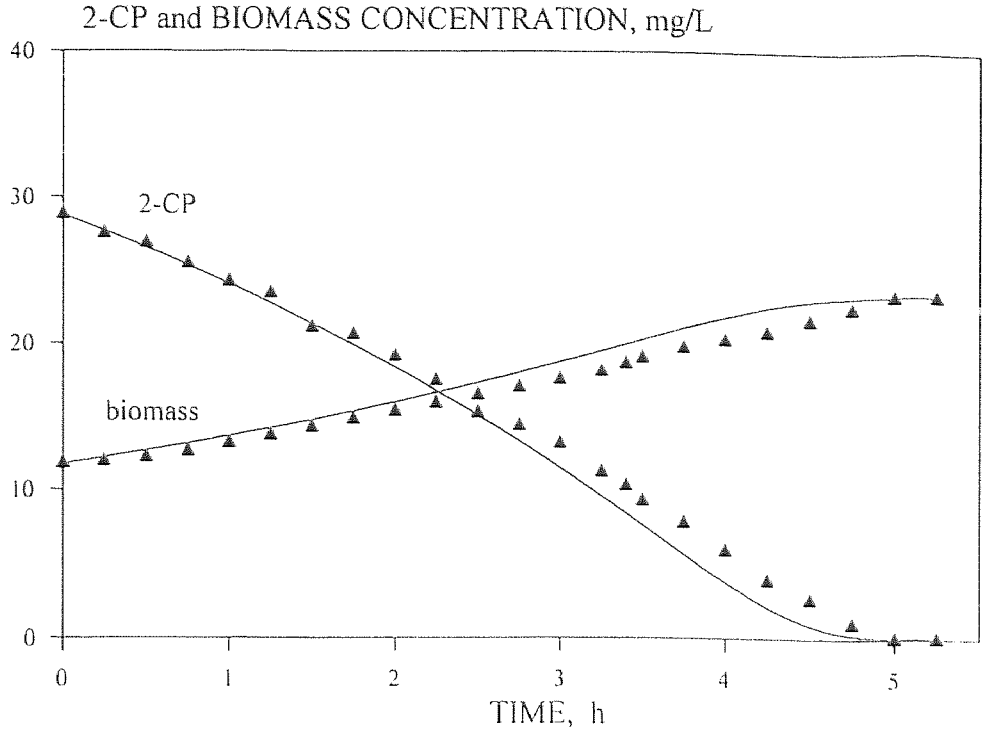

Figure E-16 Comparison between experimentally obtained and model predicted concentration profiles for 2-chlorophenol and biomass (# mo-k-8).

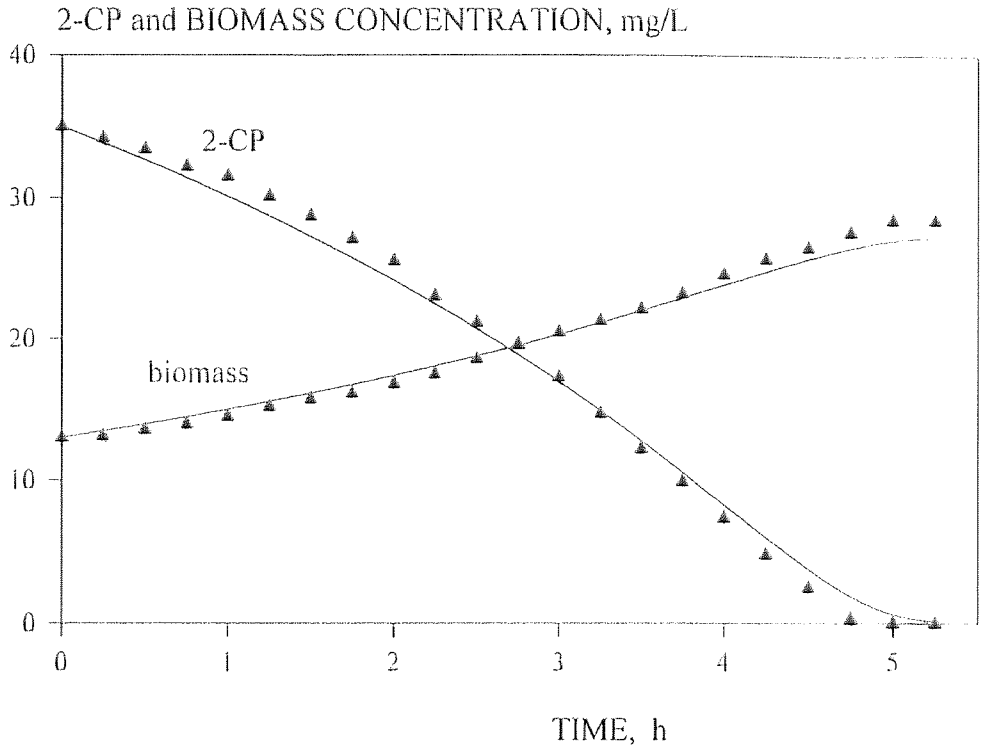

Figure E-17 Comparison between experimentally obtained and model predicted concentration profiles for 2-chlorophenol and biomass (# mo-k-9).

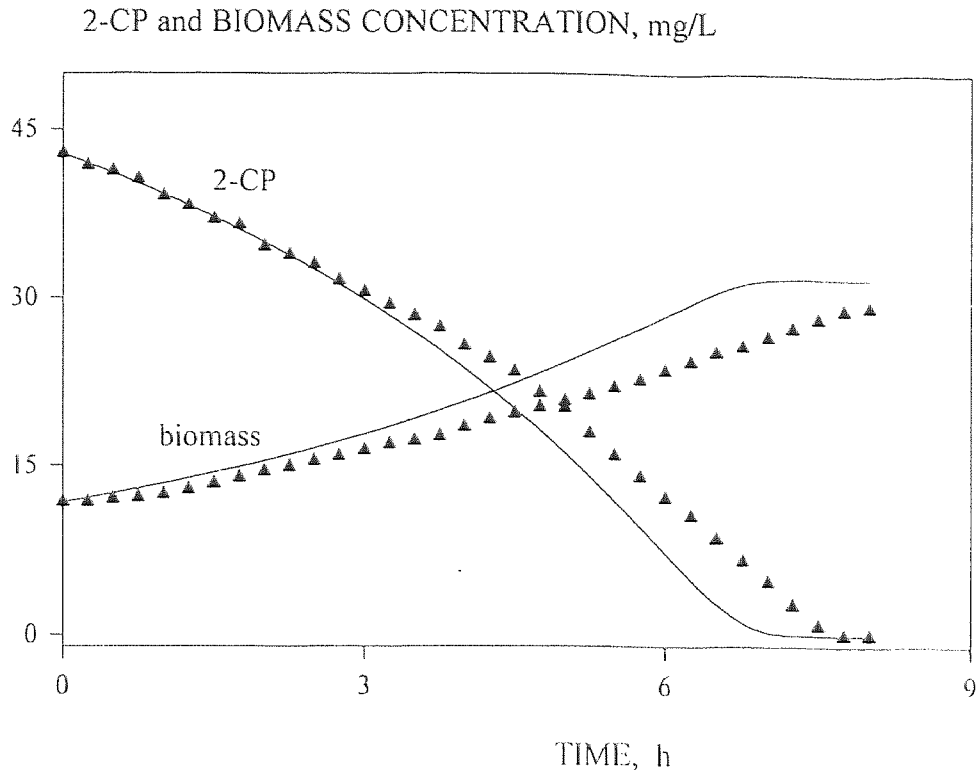

Figure E-18 Comparison between experimentally obtained and model predicted concentration profiles for 2-chlorophenol and biomass (# mo-k-10).

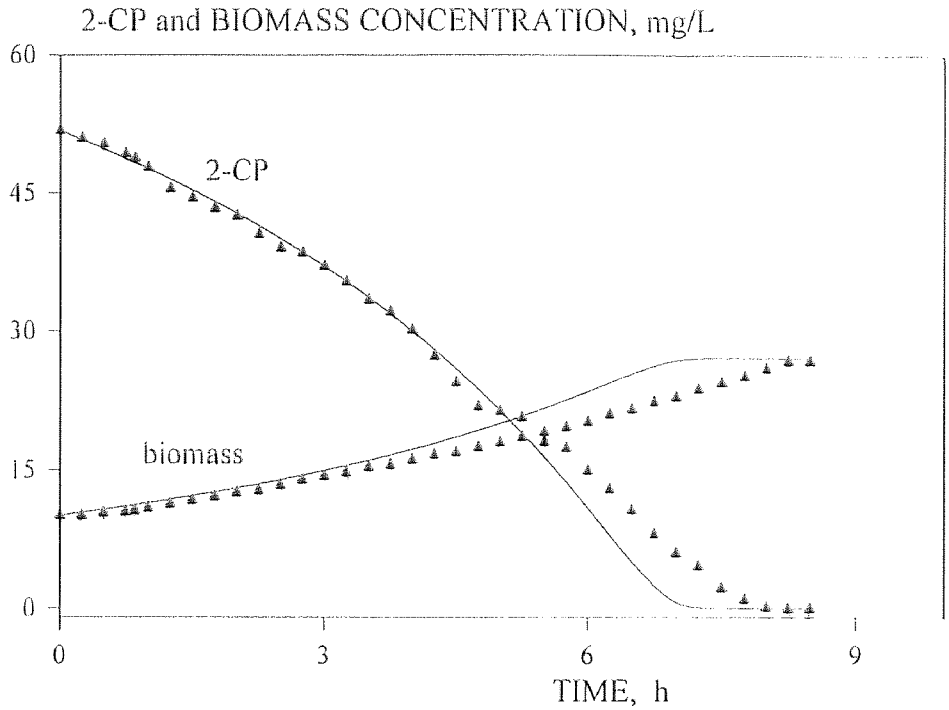

Figure E-19 Comparison between experimentally obtained and model predicted concentration profiles for 2-chlorophenol and biomass (# mo-k-11).

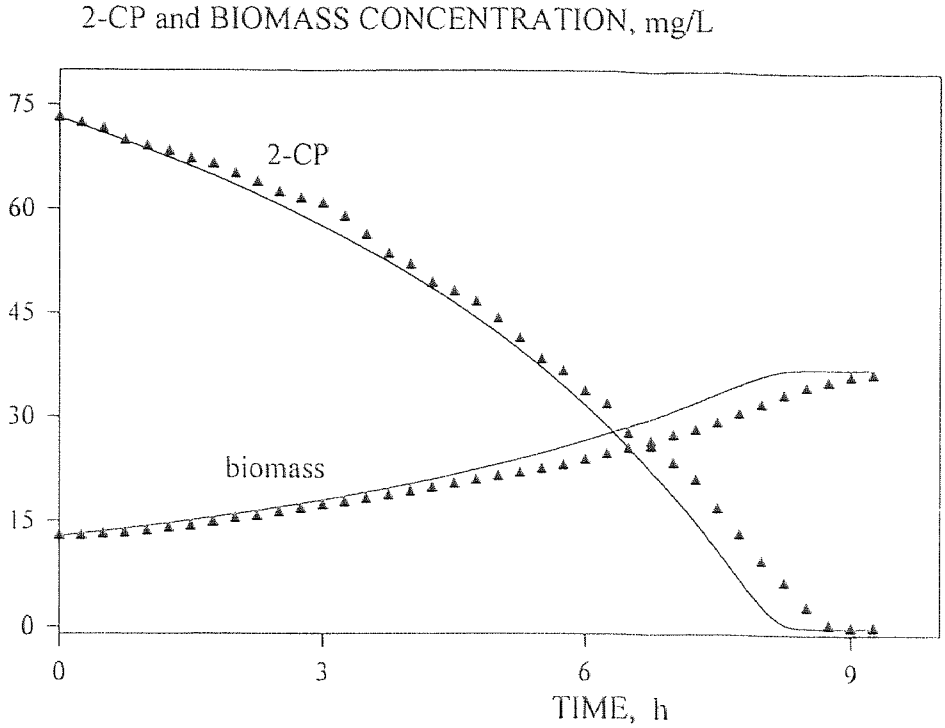

Figure E-20 Comparison between experimentally obtained and model predicted concentration profiles for 2-chlorophenol and biomass (# mo-k-12).

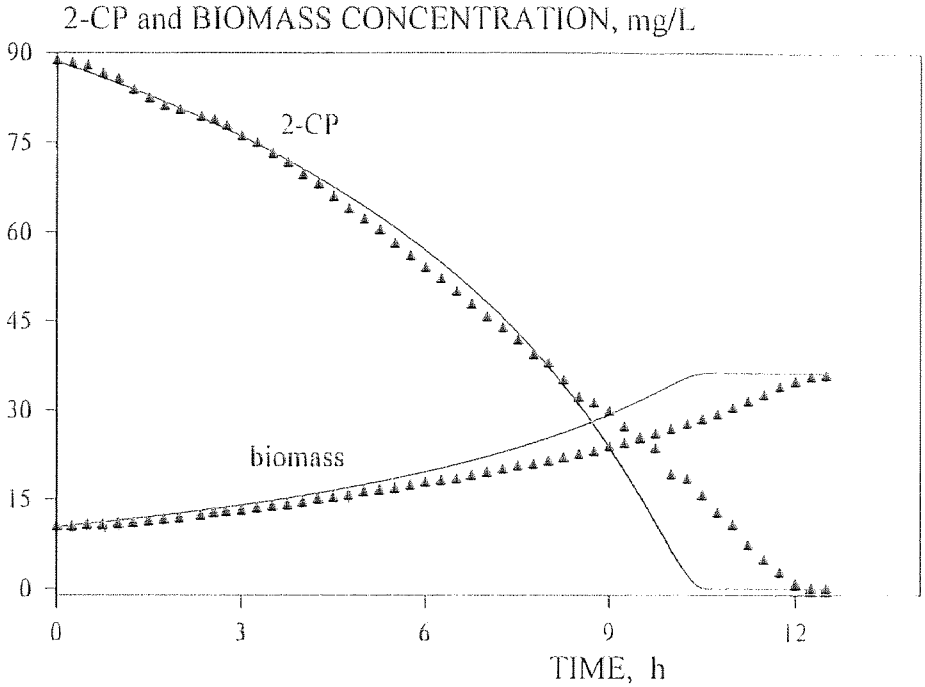

Figure E-21 Comparison between experimentally obtained and model predicted concentration profiles for 2-chlorophenol and biomass (# mo-k-13).

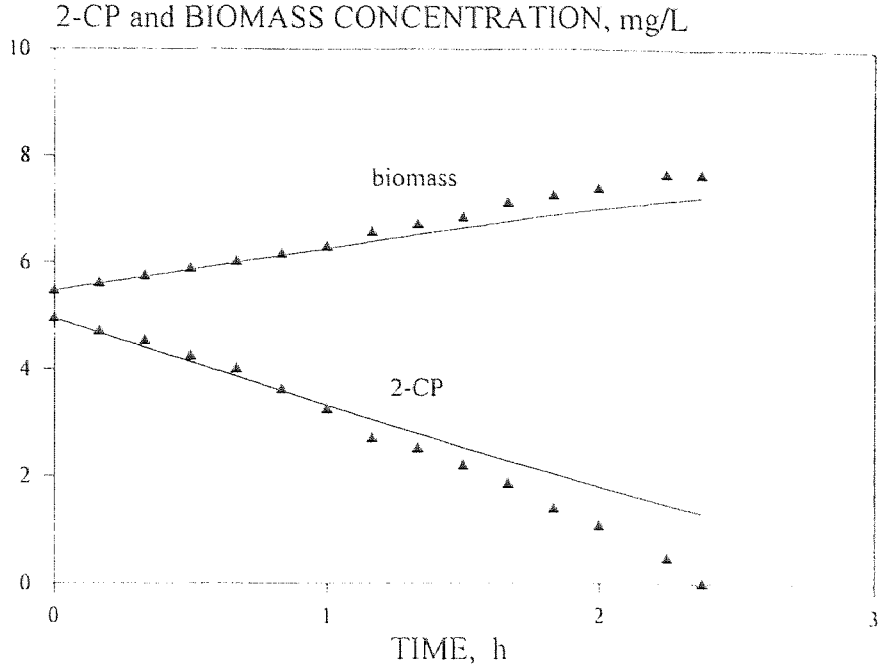

Figure E-22 Comparison between experimentally obtained and model predicted concentration profiles for 2-chlorophenol and biomass (# mo-k-15).

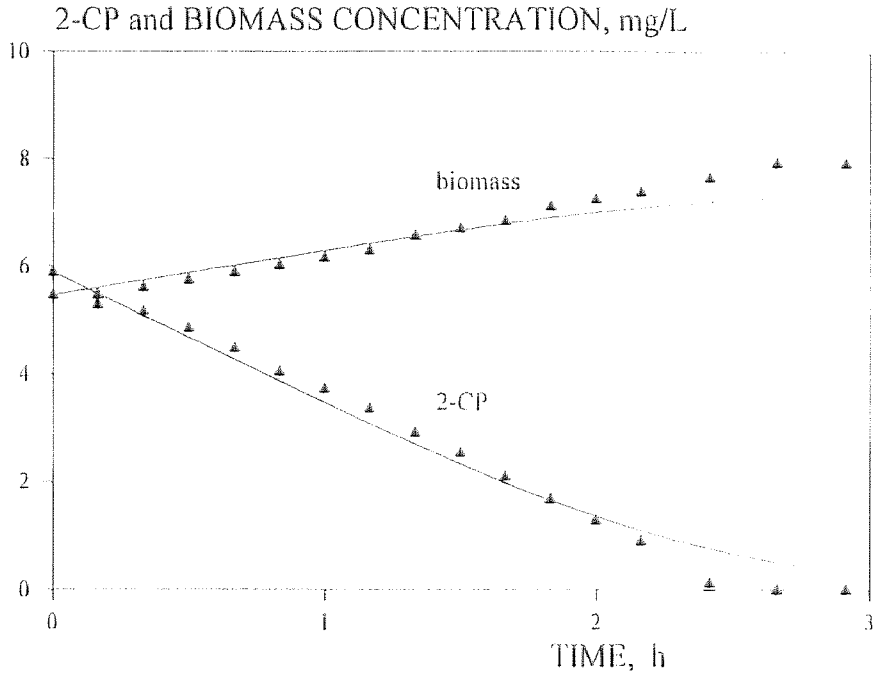

Figure E-23 Comparison between experimentally obtained and model predicted concentration profiles for 2-chlorophenol and biomass (# mo-k-16).

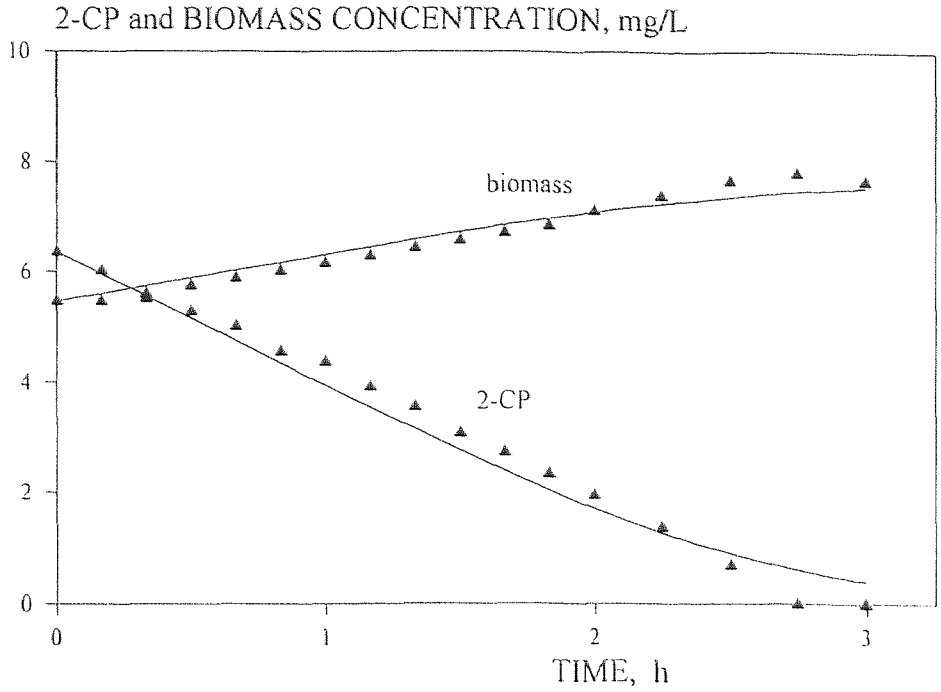

Figure E-24 Comparison between experimentally obtained and model predicted concentration profiles for 2-chlorophenol and biomass (# mo-k-17).

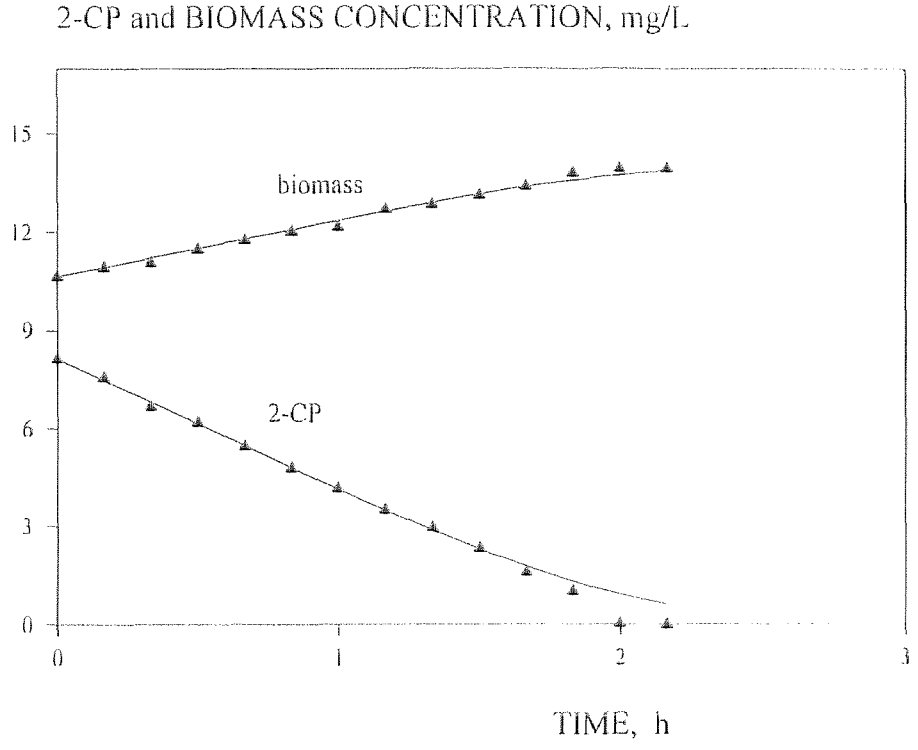

Figure E-25 Comparison between experimentally obtained and model predicted concentration profiles for 2-chlorophenol and biomass (# mo-k-18).

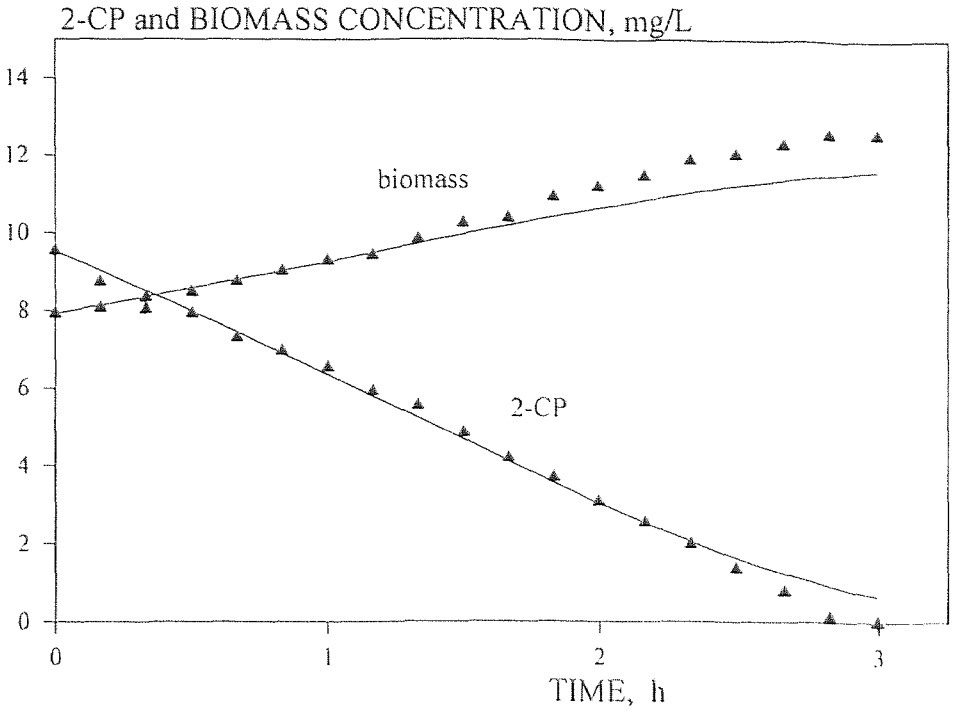

Figure E-26 Comparison between experimentally obtained and model predicted concentration profiles for 2-chlorophenol and biomass (# mo-k-19).

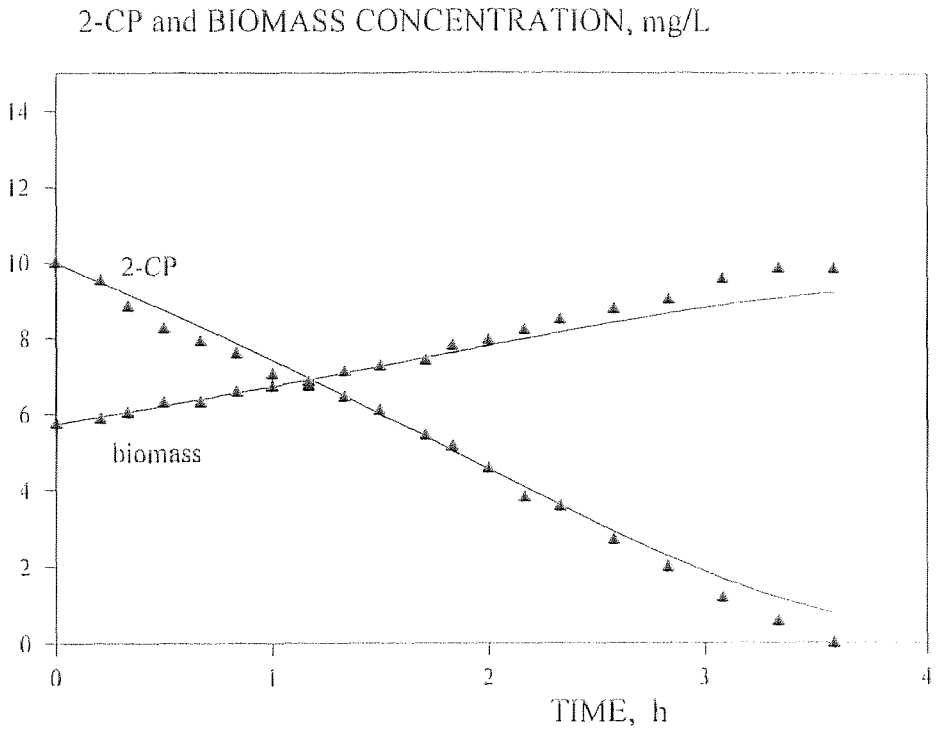

Figure E-27 Comparison between experimentally obtained and model predicted concentration profiles for 2-chlorophenol and biomass (# mo-k-20).

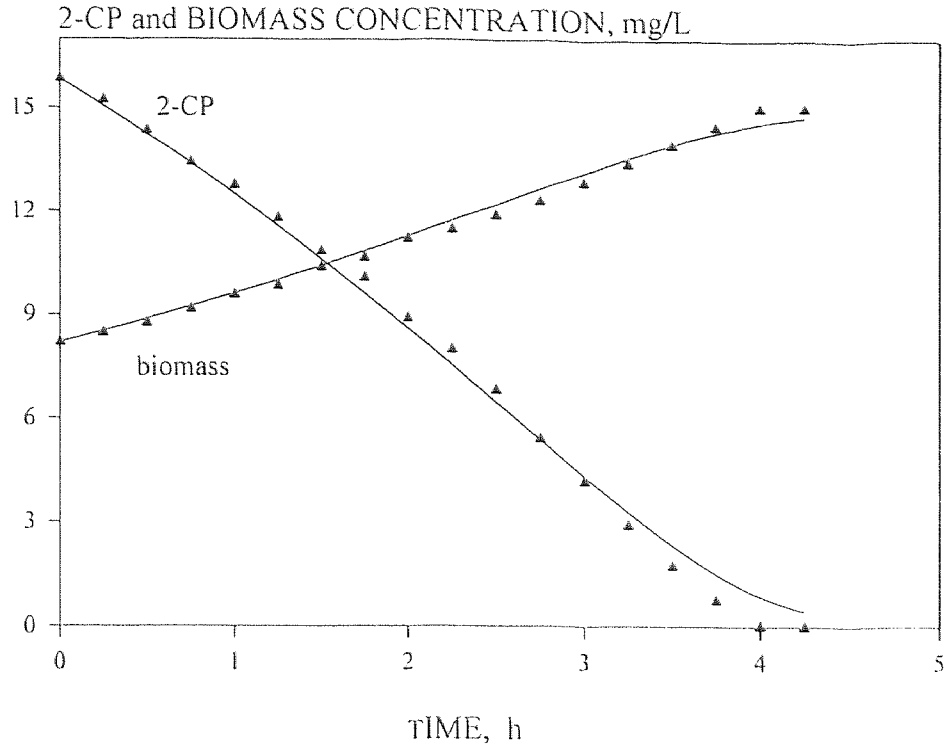

Figure E-28 Comparison between experimentally obtained and model predicted concentration profiles for 2-chlorophenol and biomass (# mo-k-21).

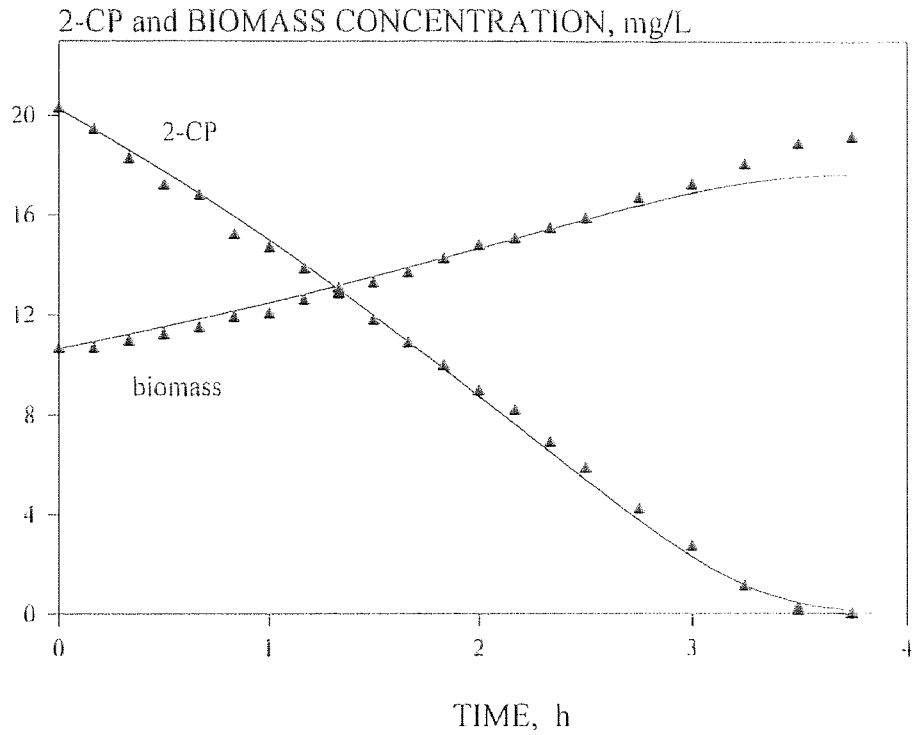

Figure E-29 Comparison between experimentally obtained and model predicted concentration profiles for 2-chlorophenol and biomass (# mo-k-22).

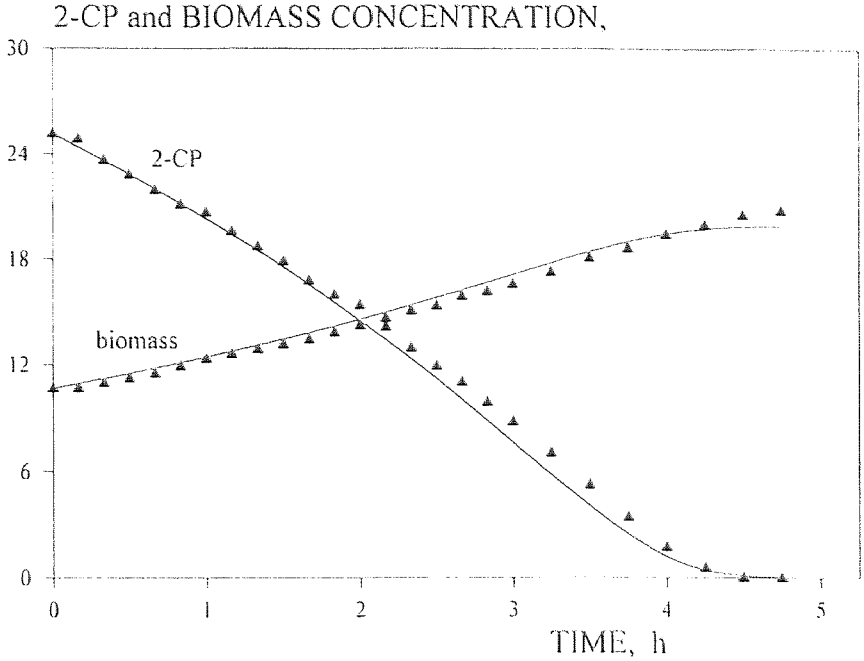

Figure E-30 Comparison between experimentally obtained and model predicted concentration profiles for 2-chlorophenol and biomass (# mo-k-23).

APPENDIX F

TABLES AND FIGURES RELATED TO ADSORPTION AND AXIAL DISPERSION EXPERIMENTS

Table F-1 Experimental data of batch adsorption based on 14.7 ppm 2-CP conc.

Time (h)	2-CP conc. in solution, (ppm)	solid phase conc. (q), mg 2-CP/kg of soil	(control) 2-CP conc. (ppm)
0	14.7	0	---
0.25	12.5	7.24	14.8
0.50	12.5	8.71	---
0.75	12.3	7.73	---
1.0	12.0	8.00	---
1.5	11.8	7.82	14.9
2.0	11.6	9.01	---
3.0	11.1	9.90	---
5.0	10.6	12.6	---
8.0	10.3	13.8	---
18.7	9.61	15.0	14.6
29.7	9.15	15.8	---
40.7	9.06	16.3	14.5

Average initial aqueous phase 2-CP concentration = 14.7 ppm
q_e = equilibrium solid phase concentration = 16.29 mg 2-CP per kg of soil
q_{inst} = 7.24 mg 2-CP per kg of soil
Equilibrium time = 40.7 hr. Temperature = 22 °C.

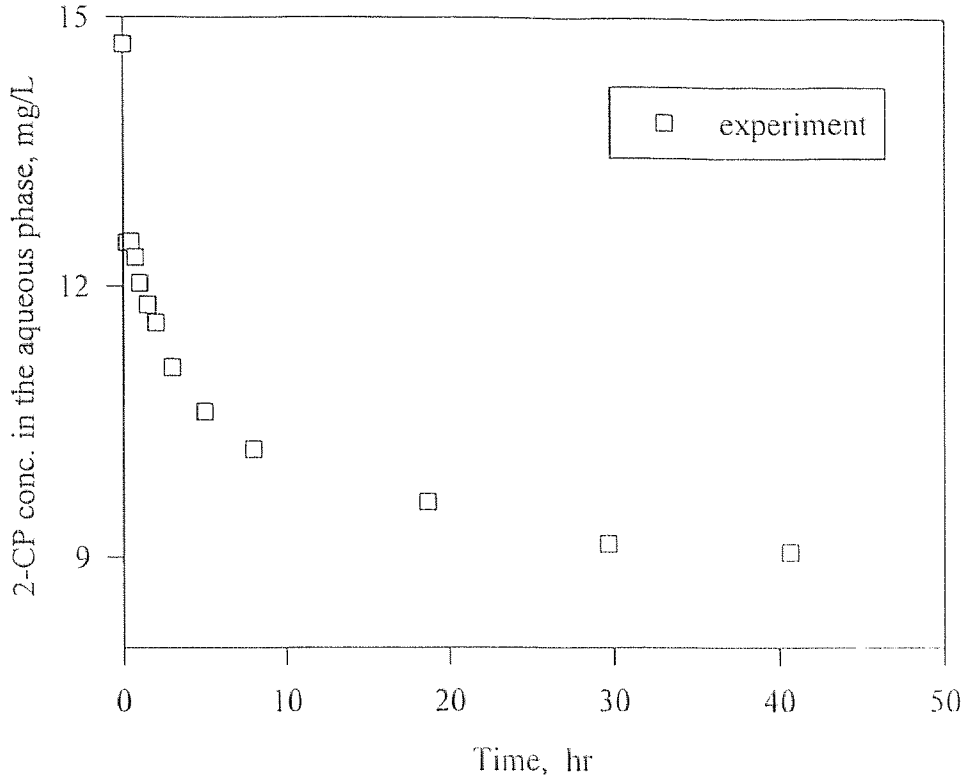

Figure F-1 2-CP concentration in the aqueous phase with time in presence of Pequest soil (Temp.: 22 °C; Liquid/Solid Mass Ratio=3.0, Ci=14.7 ppm).

Table F-2 Experimental data of batch adsorption based on 21.8 ppm 2-CP conc.

Time (h)	2-CP conc. in solution, (ppm)	solid phase conc. (q), mg 2-CP/kg of soil	(control) 2-CP conc. (ppm)
0.0	21.8	0.00	
0.25	18.2	10.8	21.8
0.5	18.1	11.1	21.8
1.0	17.9	11.8	21.8
2.0	17.5	12.9	21.8
3.5	16.8	15.0	21.7
5.75	15.7	18.3	---
8.58	14.6	21.5	21.8
22.5	14.3	22.6	21.9
31	14.3	22.6	21.8
44.5	14.3	22.4	21.9

Average initial aqueous phase 2-CP concentration = 21.8 ppm
q_e = equilibrium solid phase concentration = 22.43 mg 2-CP per kg of soil
q_{inst} = 10.79 mg 2-CP per kg of soil
Equilibrium time = 44.5 hr.; Temperature = 22 °C.

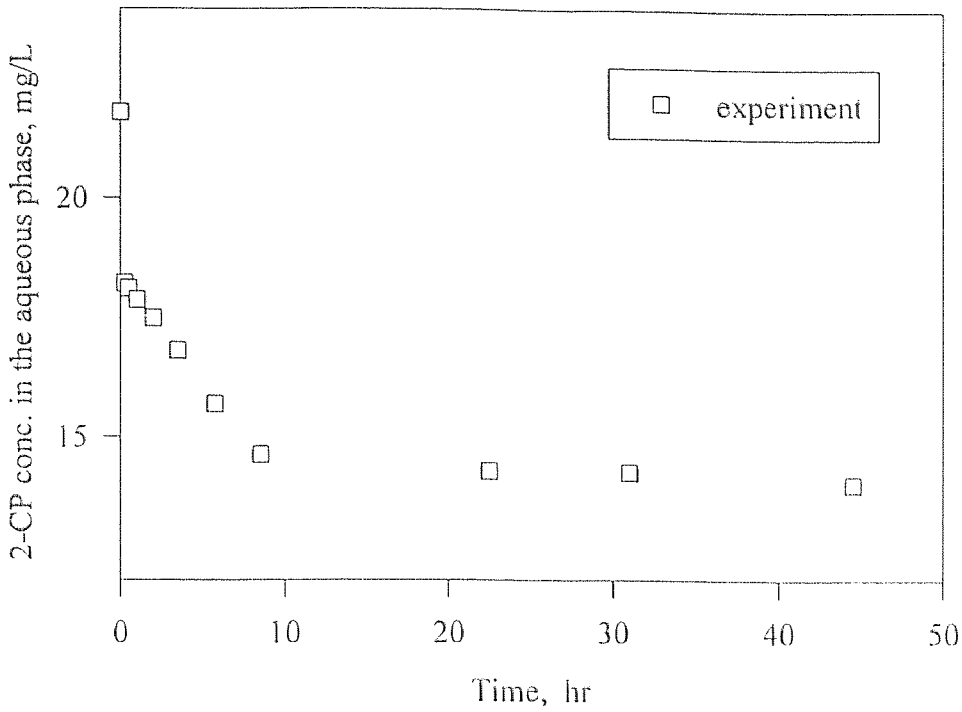

Figure F-2 2-CP concentration in the aqueous phase with time in presence of Pequest soil (Temperature = 22 °C; Liquid/Solid Mass Ratio=3.0, Ci=21.8 ppm).

Table F-3 Experimental data of 2-CP adsorption isotherm onto Pequest soil (equilibrium measurements after 55 hrs).

Sample	Concentrations of 2-CP in the liquid phase before mixing with soil	Concentrations of 2-CP in both (liquid and soil) phases after equilibrium	
	ppm	In the liquid phase, ppm	In the soil phase, mg 2-CP/ kg of soil
1	9.78	6.07	11.1
2	12.5	7.52	15.0
3	15.3	9.15	18.4
4	20.0	12.7	21.9
5	30.7	20.1	31.9
6	40.3	27.6	38.1
7	47.4	33.8	40.8
8	59.1	44.2	44.8
9	60.2	45.0	45.7

Table F-4 Experimental data of 2-CP adsorption isotherm onto Pequest soil* (equilibrium measurements after 55 hrs).

Sample No.	Concentrations of 2-CP in the liquid phase before addition of soil	Concentrations of 2-CP in both (liquid and soil) phases after equilibrium	
	ppm	In the liquid phase, ppm	In the soil phase, mg 2-CP/kg of soil
1R	9.78	6.20	10.7
2R	12.5	7.30	15.7
3R	15.3	9.57	17.5
4R	20.0	12.6	22.2
5R	30.7	20.1	31.9
6R	40.3	27.7	38.1
7R	47.4	33.9	40.6
9R	60.2	44.5	47.1

*This set of experiment is the repetition of those given in Table F-2

Table F-5 Axial dispersion experiment using chloride ion tracer (run# A-4).

Time (min)	Chloride ion concentration at the exit of the soil column (ppm)
0.0	0.000
15	0.000
30	0.000
40	0.000
50	0.000
60	0.000
70	0.000
80	0.000
90	0.015
100	0.010
110	0.043
120	0.090
130	0.121
140	0.167
150	0.230
160	0.312
170	0.584
180	0.811
190	1.061
200	1.185
210	1.361
220	1.438
230	1.412
240	1.303

Table F-5 (continued)

Time (min)	Chloride ion concentration at the exit of the soil column (ppm)
250	1.193
260	1.027
270	0.853
280	0.648
290	0.501
300	0.345
310	0.258
320	0.187
330	0.110
340	0.076
350	0.048
360	0.032
370	0.015
380	0.013
390	0.000
400	0.000
410	0.000
420	0.0000
430	0.000
440	0.000

- Flow rate = 1.1 mL/min
- 0.2 mL 2000 ppm NaCl solution was injected in port 1 of the column.
- Samples were taken from the column exit.
- Temperature = 23-24.5 °C

Table F-6 Axial dispersion experiment using chloride ion tracer (run# A-6).

Time (min)	Chloride ion concentration at the exit of the soil column (ppm)
0.00	0.000
30	0.000
40	0.000
50	0.000
60	0.000
70	0.000
80	0.000
90	0.000
100	0.006
110	0.013
120	0.023
130	0.113
140	0.190
150	0.287
160	0.400
170	0.600
180	0.816
190	1.024
200	1.185
210	1.260
220	1.315
230	1.340
240	1.230

Table F-6 (continued)

Time (min)	Chloride ion concentration at the exit of the soil column (ppm)
250	1.120
260	0.960
270	0.782
280	0.596
290	0.482
300	0.354
310	0.268
320	0.190
330	0.140
340	0.099
350	0.072
360	0.064
370	0.043
380	0.025
390	0.019
400	0.015
410	0.000
420	0.000
430	0.000
440	0.000
450	0.000

- Flow rate = 1.1 mL/min
- 0.2 mL 2000 ppm NaCl solution was injected in port 1 of the column.
- Samples were taken from the column exit.
- Temperature = 24-26 °C

APPENDIX G

TABLES AND FIGURES OF RESULTS FROM COLUMN EXPERIMENTS

Table G.1 Experimental results based on soil column biodegradation (run#1).

Time, hr	D-less time, θ	2-CP conc in Feed inlet (ppm)	D-less Feed in	2-CP conc in Feed outlet (ppm)	D-less Feed out
1.5	388.8	23.10	9.63	0.00	0.00
2.0	518.4	22.70	9.46	0.00	0.00
3.0	777.6	---	---	0.00	0.00
4.0	1036.8	23.20	9.67	0.93	0.39
5.0	1296.0	---	---	3.60	1.50
11.0	2851.2	24.22	10.09	8.35	3.48
12.0	3110.4	---	---	8.48	3.53
13.0	3369.6	---	---	9.09	3.79
14.0	3628.8	24.20	10.08	9.34	3.89
17.5	4536.0	24.30	10.13	10.54	4.39
19.2	4966.3	---	---	11.08	4.62
20.0	5184.0	---	---	11.59	4.83
21.2	5484.6	---	---	12.06	5.03
22.0	5702.4	---	---	12.17	5.07
23.5	6091.2	---	---	12.05	5.02
24.8	6415.2	---	---	12.01	5.00
26.5	6868.8	24.30	10.13	10.94	4.56
28.0	7257.6	24.08	10.03	10.35	4.31
29.3	7581.6	---	---	10.20	4.25
31.8	8250.3	23.85	9.94	11.10	4.63
32.5	8424.0	---	---	10.66	4.44
33.0	8553.6	---	---	11.41	4.75

Table G-1 (continued)

Time (hr)	D-less time, θ	2-CP conc in Feed inlet (ppm)	D-less Feed in conc.	2-CP conc in Feed outlet (ppm)	D-less Feed out conc.
33.5	8683.2	---	---	11.20	4.67
42.5	11016.0	24.30	10.13	11.62	4.84
43.0	11145.6	---	---	11.93	4.97
44.0	11404.8	---	---	12.07	5.03
45.0	11664.0	---	---	12.21	5.09
46.2	11964.7	---	---	12.72	5.30
47.0	12182.4	---	---	12.83	5.35
48.0	12441.6	---	---	12.27	5.11
50.5	13089.6	---	---	12.66	5.28
50.8	13162.2	---	---	13.00	5.42
51.0	13219.2	---	---	12.25	5.10
65.5	16977.6	23.20	9.67	12.19	5.08
90.0	23328.0	23.63	9.85	11.73	4.89
99.0	25660.8	23.24	9.68	12.70	5.29
100.5	26049.6	---	---	11.90	4.96
113.0	29289.6	23.73	9.89	12.10	5.04
120.0	31104.0	23.58	9.83	12.27	5.11
123.0	31881.6	23.60	9.83	13.02	5.43

D-less time = Dimensionless time, $\theta = (D_{se}\ t)/R^2$); where $D_{se}=7.2\times10^{-6}$ cm^2/s; R=0.01 cm.
D-less conc. = (2-CP concentration in ppm/Ks) and Ks=2.4 ppm in this case.
Average initial concentration of 2-CP = 23.7 ppm.
Approximate final steady concentration of 2-CP = 12.7 ppm.
% depletion with respect to 12.7 ppm = 46.4.

Table G.2 Experimental results based on soil column biodegradation (run#2).

Time (hr)	D-less time, θ	2-CP conc in Feed inlet (ppm)	D-less Feed in conc.	2-CP conc in Feed outlet (ppm)	D-less Feed out conc.
1.0	259.2	23.35	9.73	0.00	0.00
2.2	562.5			0.00	0.00
3.0	777.6			0.07	0.03
5.0	1296.0	23.20	9.67	3.40	1.42
7.0	1814.4			4.30	1.79
9.0	2332.8			5.60	2.33
11.0	2851.2			6.80	2.83
12.0	3110.4			8.20	3.42
14.0	3628.8	23.30	9.71	9.21	3.84
15.0	3888.0			9.51	3.96
16.0	4147.2			10.11	4.21
17.0	4406.4			11.05	4.60
18.5	4795.2			11.41	4.75
23.2	6005.6	23.24	9.68	12.82	5.34
24.0	6220.8			12.86	5.36
26.0	6739.2	23.08	9.62	12.68	5.28
28.0	7257.6			12.01	5.00
30.0	7776.0			11.76	4.90
32.0	8294.4			12.10	5.04
35.0	9072.0	23.50	9.79	12.66	5.28
36.3	9396.0			13.00	5.42
47.0	12182.4			12.90	5.38

Table G-2 (continued)

Time (hr)	D-less time, θ	2-CP conc in Feed inlet (ppm)	D-less Feed in conc.	2-CP conc in Feed outlet (ppm)	D-less Feed out conc.
48.0	12441.6	23.25	9.69	13.12	5.47
50.8	13154.4			12.62	5.26
54.0	13996.8			13.01	5.42
56.0	14515.2	22.80	9.50	13.50	5.63
71.0	18403.2	22.50	9.38	13.20	5.50
72.0	18662.4			12.89	5.37
80.0	20736.0	22.21	9.25	13.24	5.52
95.0	24624.0	23.11	9.63	12.98	5.41
106.0	27475.2	22.70	9.46	13.50	5.63
120.0	31104.0	22.45	9.35	12.66	5.28

D-less time = Dimensionless time, $\theta = (D_{se}\ t)/R^2$); where $D_{se}=7.2\times10^{-6}$ cm^2/s; R=0.01 cm
D-less conc = (2-CP concentration in ppm/Ks) and Ks=2.4 ppm in this case.
Average initial concentration of 2-CP = 22.97 ppm
Approximate final steady concentration of 2-CP = 12.8 ppm
% depletion with respect to 12.8 ppm = 44.3

Table G.3 Experimental results based 2-CP transport in soil column.

Time (hr)	D-less time, θ	2-CP conc in Feed inlet (ppm)	D-less Feed in conc.	2-CP conc in Feed outlet (ppm)	D-less Feed out conc.
4.0	1036.8	23.21	9.67	2.30	0.96
5.0	1296.0			6.10	2.54
6.0	1555.2			8.40	3.50
7.0	1814.4			11.50	4.79
8.0	2073.6			12.52	5.22
9.0	2332.8			14.80	6.17
10.0	2592.0			15.62	6.51
12.2	3151.8			17.96	7.48
14.0	3628.8			19.20	8.00
19.0	4924.8			20.60	8.58
18.2	4707.1			21.20	8.83
20.0	5184.0			20.92	8.72
22.3	5767.2			22.28	9.28
23.8	6176.7	23.58	9.83	22.00	9.17
27.1	7019.1			22.05	9.19
28.0	7257.6			21.51	8.96
31.5	8164.8			21.60	9.00
33.0	8553.6			22.00	9.17
35.0	9072.0			21.67	9.03
37.5	9720.0			21.92	9.14
41.5	10756.8			22.10	9.21
42.8	11080.8			21.79	9.08
43.7	11316.6	23.32	9.72	21.85	9.10

Table G-3 (continued)

Time (hr)	D-less time, θ	2-CP conc in Feed inlet (ppm)	D-less Feed in conc.	2-CP conc in Feed outlet (ppm)	D-less Feed out conc.
44.8	11599.2			21.61	9.00
45.3	11728.8			21.42	8.93
49.5	12830.4			21.50	8.96
50.5	13089.6			22.70	9.46
62.0	16091.1	23.52	9.80	22.85	9.52
63.0	16329.6			22.08	9.20
64.4	16692.5			21.61	9.00
67.0	17366.4			22.10	9.21
69.0	17884.8			21.54	8.98
72.0	18662.4	23.41	9.75	22.00	9.17
73.0	18921.6			22.06	9.19
85.8	22226.4			22.18	9.24
87.3	22615.2			22.22	9.26
90.0	23328.0			22.19	9.25
93.3	24170.4			22.00	9.17
96.5	25012.8			22.97	9.57
97.3	25207.2			23.20	9.67
108.3	28058.4			22.36	9.32
109.5	28382.4	23.63	9.85	22.19	9.25
114.5	29678.4			23.45	9.77

D-less time = Dimensionless time, $\theta = (D_{se} \cdot t)/R^2$); where $D_{se}=7.2 \times 10^{-6}$ cm^2/s; R=0.10 cm
D-less conc. = (2-CP concentration in ppm/Ks) and Ks=2.4 ppm in this case.
Average initial concentration of 2-CP = 23.44 ppm

REFERENCES

Abriola, L.M. and G.F. Pinder. 1985a. "A Multiphase Approach to the Modeling of Porous Media Contamination by Organic Compounds. 1. Equation Development." *Water Resources Research,* 21(1): 11-18.

Abriola, L.M. and G.F. Pinder. 1985b. "A Multiphase Approach to the Modeling of Porous Media Contamination by Organic Compounds. 2. Numerical Simulation." *Water Resources Research,* 21(1): 19-26.

Abriola, L.M. 1989. "Modelling Multiphase Migration of Organic Chemicals in Groundwater Systems-A Review and Assessment." *Enviro. Health Perspec.*,83: 117-143.

Ahn, Ik-Sung, L. W. Lion, and M.L. Shuler. 1996. "Microscale-Based Modeling of Polynuclear Aromatic Hydrocarbon Transport and Biodegradation in Soil." *Biotech. Bioeng.*, 51:1-14.

Andrews, J.F. 1968. "A Mathematical Model for the Continuous Culture of Microorganisms Utilizing Inhibitory Substrates." *Biotech. Bioeng.*, 10: 707-723

Armenante, P.M., D. Kafkewitz, C.-J. Jou, and G. Lewandowski. 1993. "Effect of pH on the Anaerobic Dechlorination of Chlorophenols in a Defined Medium." *Appl. Microbiol. Biotech.*, 39: 772-777.

Bahr, J. M. 1989. "Analysis of Nonequilibrium Desorption of Volatile Organics During Field Test of Aquifer Decontamination." *J. of Contaminant Hydrology.*, 4: 205-222.

Bailey, J.E. and D.F. Ollis. 1986. *Biochemical Engineering Fundamentals*. 2nd Edition, McGraw-Hill Book Company, New York, NY.

Baker, M.D., C.I. Mayfield, and W.E. Inniss. 1980. "Biodegradation of Chlorophenols in Soil, Sediment, and Water at Low Temperatures." *Water Research,* 14: 1765-1771.

Bakke, R. 1986. *Biofilm Detachment*. Ph.D. Dissertation, Montana State University, Bozeman, MT.

Ball, W.P. and P.V. Roberts. 1990. "Slow Diffusion of Sorbing Hydrophobic Organic Compounds in Sandy Aquifer Material." *199th ACS National Meeting at Boston,* 30(1): 313-317.

Bartels, I., H. -J. Knackmuss, and W. Reineke. 1984. "Suicide Inactivation of Catechol 2,3-Dioxygenase from *Pseudomonas putida* mt-2 by 3-Halocatechols." *Appl. Envion. Microbial.*, 47: 500-505.

Bayard, R. 1997. *Étude de l'adsorption/désorption de Pollutants Organiques dans les Sols. Approche Méthodologique et Application au Pemtachlorophénol et aux Hydrocarbures Aromaticques Polycycliques*, Ph.D. Dissertation, INSA de Lyon, France.

Bhaumik, S., S. Majumdar, and K.K. Sirkar. 1996. " Hollow-Fiber Membrane-Based Rapid Pressure Swing Adsorption." *AIChE J.*, 42(2): 409.

Boyd, S.A. 1982. "Adsorption of Substituted Phenols by Soil." *Soil Sci.*, 134: 337-343.

Boyd, S.A., D.R. Shelton, D. Berry, and J.M. Tiedje. 1983. "Anaerobic Biodegradation of Phenolic Compounds in Digested Sludge." *Appl. Envion. Microbiol.*, 46: 50-54.

Boyd, S.A. and D.R. Shelton. 1984. "Anaerobic Biodegradation of Chlorophenols in Fresh Acclimated Sludge." *Appl. Envion. Microbiol.*, 47: 272-277.

Borden, R. C., M. D. Lee, J. T. Wilson, C. H. Ward, and P. B. Bedient. 1984. "Modeling the Migration and Biodegradation of Hydrocarbons Derived from a Wood-Creosoting Process Waste." In: *Proceedings of the NWWA/API Conference on Petroleum Hydrocarbons and Organic Chemicals in Ground Water - Prevention, Detection and Restoration*. National Water Well Association. 130-143.

Borden, R. C. and P. B. Bedient. 1986. "Transport of Dissolved Hydrocarbons Influenced by Oxygen-Limited Biodegradation 1. Theoretical Development." *Water Resources Research*, 22: 1973-1982.

Borden, R. C., P. B. Bedient, M.D.Lee, C.H.Ward, and J.T. Wilson. 1986. "Transport of Dissolved Hydrocarbons Influenced by Oxygen-Limited Biodegradation 2. Field Application." *Water Resources Research*, 22: 1983-1990.

Bosma, T.N.P. 1994. *Simulation of Subsurface Biotransformation*, Ph.D. Dissertation, The Agricultural University of Wageningen, Netherlands.

Bouchard, D.C., A.L. Wood, M.L. Campbell, P. Nkedi-Kizza, and P.S.C. Rao. 1988. "Soprion Equilibrium During Solute Transport." *J. of Contaminant Hydrology*, 2: 209-223.

Bouwer, E.J. 1992. "Microbial Remediation: Strategies, Potentials, and Limitations." *In: Proceedings of the European Conference on Integrated Research for Soil and Sediment Protection and Remediation*. Maastricht, The Netherlands. 1-11.

Bouwer, E.J. 1992a. "Bioremediation of Organic Contaminants in the Subsurface," pp. 287-318. In: R. Mitchell (ed.), *Environmental Microbiology*. Wiley and Sons Inc., New York, NY.

Bouwer E.J. and P.L. McCarty. 1984. "Modeling of Trace Organics Biotransformation in the Subsurface." *Ground Water*, 22: 433-440.

Bouwer, E. J. and P.L. McCarty. 1985. "Utilization Rates of Trace Halogenated Organic Compounds in Acetate-supported Biofilms." *Biotech. Bioeng.*, 27: 1564-1571.

Bouwer, E. J. and G.D. Cobb, 1987. "Modeling of Biological Processes in the Subsurface." *Water Sci. and Technol.*, 19: 769-779.

Bouwer, E.J. 1989. "Transformation of Xenobiotics in Biofilms." pp251-267. In: W.G. Characklis and P.A. Wilderer (eds.), *Structure and Function of Biofilms*. Wiley and Sons Inc., New York, NY.

Bouwer, E. J., C.T. Chen, and Y.H. Li. 1992. "Transformation of Petroleum Mixture in Biofilms." *Water Sci. and Technol.*, 26: 637-646.

Brian III, B.F., I. Zwiebel, and R.S. Artigue. 1987. "Numerical Simulation of Fixed-bed Adsorption Dynamics by the Method of Lines." *AIChE Symp. Ser.*, 83: 80-86.

Brusseau, M. L. and P.S.C. Rao. 1989. "Sorption Nonideality during Organic Contaminant Transport in Porous Media." *Critical Reviews in Environmental Control.*, 19: 33-99.

Brusseau, M. L., R.E. Jessup, and P.S.C. Rao. 1991. "Nonequilibrium Sorption of Organic Chemicals: Elucidation of Rate-Limiting Processes." *Environ. Sci. Tech.*, 25(1): 134-142.

Brusseau, M. L. 1992. "Transport of Rate-Limiting Sorbing Solute in Heterogeneous Porous media: Application of a One-Dimensional Multifactor Nonideality Model to Field Data." *Water Resources Research*, 28: 2485-2497.

Caldwell, D.E. and J.R. Lawrence. 1986. "Growth Kinetics of *Pseudomonas fluorescens* Microcolonies within the Hydrodynamic Boundary Layers of Surface Microenvironment." *Microbiol.Ecol.*, 12: 299-312.

Calvet, R. 1989. "Adsorption of Ogranic Chemicals in Soils." *Environ. Health Persp.*, 83: 145-177.

Cerniglia, C.E. 1993. "Biodegradation of Polycyclic Aromatic Hydrocarbons." *Current Opinions in Biotech.*, 4: 331-338.

Chen, Y.-M., L.M. Abriola, P.J.J. Alvarez, P.J.Anid, and T.M. Vogel. 1992. "Modeling Transport and Biodegradation of Benzene and Toluene in sandy Aquifer Material: Comparison with Experimental Measurements." *Water Resources Research*, 28(7): 1833-1847.

Chaudhry, G.R. and S. Chapalamadugu. 1991. "Biodegradation of Halogenated Organic Compounds." *Microbiol. Rev.*, 55(1): 59-79.

Chung, G.-Y, B.J. McCoy, and Kate M. Scow. 1993. "Criteria to Assess When Biodegradation is Kinetically Limited by Intraparticle Diffusion and Sorption." *Biotech. Bioeng.*, 41: 625-632.

Costerton, J.W., R.T. Irvin, and K.-J. Cheng. 1981. "The Bacterial Glycocalyx in Nature and Disease." *Ann. Rev. Microbiol.*, 35: 299-324.

Craver, M.B. 1976. "The Choice of Algorithms in Automated Method of Lines Solution of Partial Differential Equations." In: L. Lapidus and W.E. Schiesser (eds.), *Numerical Methods for Differential Systems*. Academic Press, New York, NY.

Crittenden, J. C., N. J. Hutzler, D. G. Geyer, J. L. Oravitz, and G. Friedman. 1986. "Transport of Organic Compounds with Saturated Groundwater Flow: Model Development and Parameter Sensitivity." *Water Resources Research*, 22: 271-284.

Cunningham, A.B., W.G. Characklis, F. Abedeen, and D. Crawford, 1991. "Influence of Biofilm Accumulation on Porous Media Hydrodynamics." *Env. Sci. Technol.*, 25: 1305-1311.

Davis, M.E. 1984. "Numerical Methods and Modeling for Chemical Engineers." John Wiley and Sons, New York, NY.

Dhawan, S., L.T. Fan, L.E. Erickson, and P. Tuitemwong. 1991. "Modeling, Analysis and Simulation of Bioremediation of Soil Aggregates." *Environmental Progress*, 10: 251-260.

Dietrich, G. and J. Winter. 1990. "Anaerobic Degradation of Chlorophenol by an Enrichment Culture." *Appl. Microbiol. Biotechnol.*, 34: 253-258.

Dhawan, S., L.E. Erickson, and L.T. Fan. 1993. "Model Development and Simulation of Bioremediation in Soils Beds with Aggregates." *Ground Water*, 31: 271-284.

Doran, P.M. 1985. *The Effect of Immobilization on the Metabolism of Yeast*. Ph.D. Dissertation, California Institute of Technology, Pasadena, CA.

Dorn, E., M. Hellwig, W. Reineke, and H. -J. Knackmuss. 1974. "Isolation and Characterization of a 3-chlorobenzoate degrading *Pseudomonad*." *Arch. Microbiol.*, 99: 61-70.

Dikshitulu, S. 1993. *Competition Between Two Microbial populations in a Sequencing Fed-Batch Reactor and its Implication for Waste Treatment Applications*. Ph.D. Dissertation, Dept. of Chemical Engineering, New Jersey Institute of Technology, Newark, NJ.

EPA Document. 1997. "Cleaning Up the Nations's Waste Sites: Markets and Technology Trends." EPA-542-R-96-005A.

Fava, F., P.M. Armenante, and D. Kafkewitz. 1995. "Aerobic Degradation and Dechlorination of 2-chlorophenol, 3-chlorophenol, and 4-chlorophenol by a *Pseudomonas pickettii* strain." *Letters in Appl. Microbiol.*, 21: 307-312.

Freeman, R.A. and J.M. Schroy. 1986. "Modeling the Transport of 2, 3, 4, 8-TCDD and Other Volatility Chemicals in Soils." *Environmental Progress*, 5: 28-33.

Goltz, M.N. and P.V. Roberts. 1986. "Three-dimensional Solutions for Solute Transport in an Infinite Medium with Mobile and Immobile Zones." *Water Resources Research*, 22: 1139-1148.

Goltz, M.N. and P.V. Roberts. 1988. "Simulations of Physical Nonequilibroum Solute Transport Models: Applications to a Large-Scale Field Experiment." *J. of Contaminant Hydrology*, 3: 37-63.

Gordon, A.S. 1983. "Effects of Inorganic Particles on Metabolism by a Periphytic Marine Bacterium." *Appl. Environ. Microbiol.*, 45: 411-417.

Häggblom, M.M. 1992. "Microbial Breakdown of Halogenated Aromatic Pesticides and Related Compounds." *FEMS Microbiol. Rev.*, 103: 29-72.

Häggblom, M.M, J.H.A. Apajalahti, and M.S. Salkinoja-Salonen. 1988. "Degradation of Chlorinated Phenolic Compounds Occurring in Pulp Mill Effluents." *Water Sci. and Technol.*, 20:205-208.

Harmon, T.C., W.P. Ball, and P.V. Roberts, 1989. "Nonequilibrium Transport of Ogranic Contaminants in Groundwater." In: Reactions and Movement of Organic Chemicals in Soils, Edited by B.L. Sawhney and K. Brown, Soil Science Society of America and American Society of Agronomy, Madison, WI. SSSA Special Publication Number 22, 405-437.

Hausenbuiller, R. I. 1978. *Soil Sci.* Brown Company Publishers, Dubuque, Iowa.

Hrudey, S.E., E. Knetting, S. Daignault, and P.M. Fedorak. 1987. "Anaerobic Biodegradation of Monochlorophenols." *Envion. Technol. Letters, 8:65-76.*

Hrudey, S.E. and S.J. Pollard. 1993. "The Challenges of Contaminated Sites: Remediation Approaches in North America." *Environ. Rev.*, 1: 55-72.

Hutzler, N.J., J.C. Crittenden, J. S. Gierke, and A.S. Johnson. 1986. "Transport of Organic Compounds with Saturated Groundwater Flow: Experimental Results." *Water Resources Research*, 22: 285-295.

Janke, D., W. Ihn, and D. Tresselt. 1989. "Critical Steps in Degradation of Chloroaromatics by *Rhodococci*. IV. Detailed Kinetics of Substrate Removal and Product Formation by Resting Pre-Adapted Cells." *J. of Basic Microbiol.*, 29: 305-314.

Jeffrey, W.H. and J.H.Paul. 1986. "Activity of an Attached and Free-living *Vibrio* sp. as measured by Thymidine Incorporation, p-Iodonitrotetrazolium Reduction and ATP/ADP Ratios." *Appl. Environ. Microbiol.*, 51: 150-156.

Jolly, R.L., G. Jones, W.W. Pitt, and J.E. Thomson. 1976. "Determination of Chlorination Effects on Organic Constituents in Natural Process Waters using High Pressure Liquid Chromatography." pp 233-245. In: L. Keith (ed.), *Identification and Analysis of Organic Pollutants in Waters.* Ann Arbor Science, Ann Arbor, MI.

Kafkewitz, D., F. Fava, and P.M., Armenante. 1996. "Effect of Vitamins on the Aerobic Degradation of 2-Chlorophenol, 4-Chlorophenol, and 4-Chlorobiphenyl." *Appl. Microbiol. Biotech.*, 46: 414.

Kaschabek, S.R. and W. Reineke. 1993. "Degradation of Chloroaromatics: Purification and Characterization of Maleylacetate Reductase from *Pseudomonas sp.* strain B13." *J. of Bacteriol.*, 175: 6093-6081.

Kieft, T.L. and D.E. Caldwell. 1984. "Chemostat and In-Situ Colonization Kinetics of *Thermotrix thiopara* on Calcite and Pyrite Surfaces." *Geomicrobiol. J.*, 3:217-229.

Kissel, J.C., P.L. McCarty, and R.L. Street. 1984. "Numerical Simulation of Mixed-Culture Biofilm." *J. of Environ. Engineering*, 110: 393-411.

Knackmuss, H.-J. and M. Hellwig. 1978. "Utilization and cooxidation of Chlorinated Phenols by *Pseudomonas sp.* B13." *Arch. Microbiol.*, 117: 1-7.

Kobayashi, K. 1978. "Metabolism of Pentachlorophenol in Fishes." pp 89-105. In: K.R. Rao (ed.), *Environmental Science Research, vol 12: Pentachlorophenol. Chemistry, Pharmacology and Environmental Toxicology.* Plenum Press, New York, NY.

Kringsted, K.P. and K. Lindstrom. 1984. "Spent Liquors from Pulp Bleaching." *Environ. Sci. Technol.*, 18: 236A-248A.

Lapidus, L. and J. H. Seinfeld. 1971. *Numerical Solution of Ordinary Differential Equations*. Academic Press, New York, NY.

Levenspiel, O., 1972. *Chemical Reaction Engineering*. John Wiley and Sons, New York, NY.

McCarty, P. L., M. Reinhard, and B. E. Rittmann. 1981. "Trace Organics in Ground Water." *Environ. Sci. Technol.*, 15: 40-51.

McCarty, P. L., B. E. Rittmann, and E. J. Bouwer. 1984. "Microbiological Processes Affecting Chemical Transformations in Groundwater." In *Groundwater Pollution Microbiology*, eds. G. Bitton and C. P. Gerba. Wiley Interscience, New York, NY.

MacQuarrie, K.T.B., E.A. Sudicky, and E.O. Frind, 1990. "Simulation of Biodegradable Organic contaminants in Groundwater. 1: Numerical Formulation in Principal Directions." *Water Resources Research*, 26: 207-222.

Mikesell, M.D. and S.A. Boyd. 1986. "Complete Reductive Dechlorination and Mineralization of Pentachlorophenol by Anaerobic Microorganisms." *Appl. Environ. Microbio.*, 52: 861-865.

Miller, C.T. and W.J. Weber Jr. 1986. "Sorpotion of Hydrophobic Organic Pollutants in Saturated Soil Systems." *J. of Contaminant Hydrology*, 1: 243-261.

Mitchell, A.R. and D.F. Griffiths. 1980. *The Finite Difference Method in Partial Differential Equations*. Wiley Interscience, New York, NY.

Molz, F.J., M.A. Widdowson, and L.D. Benefield. 1986. "Simulation of Microbial Growth Dynamics Coupled to Nutrient and Oxygen Transport in Porous Media." *Water Resources Research*, 22: 1207-1216.

Monod, J. 1942. "*Recherches sur la croissance des cultures bactériennes.*" Hermann et Cie., Paris.

Ogram, A. V., R. E. Jessup, L. T. Ou, and P. S. Rao. 1985. "Effects of Sorption on Biological Degradation Rates of 2,4-Dichlorophenoxy Aeetic Acid in Soils." *Appl. Environ. Microbiol.*, 49: 582-587.

Parker, J.C. and M. Th. van Genuchten. 1984. "Flux-Averaged and Volume-Averaged Concentrations in Continuum Approaches to Solute Transport." *Water Resources Research*, 20, 866-872.

Pickens, J. F., R. E. Jackson, K. J. Inch, and W. F. Merritt. 1981. "Measurement of Distribution Coefficients Using a Radial Injection Dual-Tracer Test." *Water Resources Research*, 17: 529-544.

Pinder G.F. and L.M. Abriola. 1986. "On the Simulation on Non-aqueous Phase Orgamic Compounds in the Subsurface." *Water Resources Research*, 22(9): 109S-119S.

Pritchard, P.H., E.J. O'Neill, C.M. Spain, and D.G. Ahearn. 1987. "Physical and Biological Parameters that Determine the Fate of p-Chlorophenol in Laboratory Test Systems." *Appl. Environ. Microbio.*, 53: 1833-1838.

Press, W.H., B.P. Flannery, S.A. Teukolsky, and W.T. Vetterling. 1990. "Numerical Recipes." Cambridge University Press, NY.

Raghavan, N.S. and D.M. Ruthven. 1983. "Numerical Simulation of Fixed-bed Adsorption Column by the Method of Orthogonal Collocation." *AIChE J.*, 29: 922-925.

Rao, P.S.C., R.E. Jessup, D.E. Rolston, J. M. Davidson, and D. P. Kilcrease. 1980a. "Experimental and Mathematical Description of Nonadsorbed Solute Transfer by Diffusion in Spherical Aggregates." *Soil Sci. Soc. Am. J.*, 44: 648-688.

Rao, P.S.C., D.E. Rolston, R.E. Jessup, and J. M. Davidson. 1980b. "Solute Transport in Aggregated Porous Media: Theoretical and Experimental Evaluation." *Soil Sci. Soc. Am. J.*, 44: 1139-1146.

Rao, P.S.C., R.E. Jessup, and T. M. Addiscott. 1982. "Experimental and Theoretical Aspects of Solute Diffusion in Spherical and Nonspherical Aggregates." *Soil Sci.*, 113, 342-349.

Reineke, W. and H.-J. Knackmuss. 1988. "Microbial Degradation of Haloaromatics." *Ann. Rev. Microbiol.*, 42: 263-287.

Rifai, H.S. and P.B. Bedient. 1990. "Comparison of Biodegradation Kinetics with an Instantaneous Reaction Model for Groundwater." *Water Resources Research*, 26: 637-645.
637-645.

Rittmann, B.E. and P.L. McCarty, 1980a. "Model of Steady-state Biofilm Kinetics." *Biotech. Bioeng.*, 22: 2343-2357.

Rittmann, B.E. and P.L. McCarty, 1980b. "Evaluation of Steady-state Biofilm Kinetics." *Biotech. Bioeng.*, 22: 2359-2373.

Rittmann, B.E., 1993. "The Significance of Biofilms in Porous Media." *Water Resources Research*, 29: 2195-2202.

Robinson, K. G., W. S. Farmer, and J. T. Novak. 1990." Availability of Sorbed Toluene in Soils for Biodegradation by Acclimated Bacteria." *Water Resources*, 24: 345-350.

Roberts, P.V., M.N. Goltz, R.S. Summers, J.C. Crittenden, and P. Nkedi-Kizza. 1987. "The Influence of Mass Transfer on Solute Transport in column Experiments with an Aggregated Soil." *J. of Contaminant Hydrology*, 1: 375-393.

Sabatini, D.A. and T. A. Austin. 1990. "Sorption and Transport of Pesticides in Ground Water: Critical Review." *J. of Irrigation and Drainage Engineering*, 116(1): 3-15.

Schmidt, E. and H.-J. Knackmuss. 1980. "Chemical Structure and Biodegradability of Halogenated Aromatic Compounds. Conversion of Chlorinated Muconic Acids into Maleoylacetic Acid." *Biochem. J.*, 192: 339-347.

Shareefdeen, Z.M. 1994. *Engineering Analysis of a Packed-bed Biofilter for Removal of Volatile Organic Compound (VOC) Emissions*, Ph.D. Dissertation, Dept. of Chemical Engineering, New Jersey Institute of Technology, Newark, NJ.

Semprini, L. and P. L. McCarty. 1991. "Comparison Between Model Simulations and Field Results for In-situ Biorestoration of Chlorinated Aliphatics: Part 1. Biostimulation of Methanotrophic Bacteria." *Ground Water*, 29: 365-374.

Shreve, G.S. and T. M. Vogel. 1993. "Comparison of Substrate Utilization and Growth Kinetics Between Immobilized and Suspended *Pseudomonas* Cells." *Biotech. Bioeng.*, 43: 370-379.

Shuler, M. L. and F. Kargi. 1992. *Bioprocess Engineering: Basic Concepts*. Prentice-Hall, Englewoods Cliffs, NJ.

Sims, J. L., R.C. Sims, and J.E. Mathews. 1990. "Approach to Bioremediation of Contaminated Soil" *Hazardous Waste and Hazardous Materials*, 7: 117-149, EPA/600/J-90/203.

Smith, M.A. 1991. "Identification, Investigation and assessment of contaminated land." *J. Inst. Water Environment Manage.*, 5: 617-623.

Smith, J.A. and J.T. Novak. 1987. "Biodegradation of Chlorinated Phenols in Subsurface Soil." *Water Air Soil Pollution*, 33: 29-42.

Spain, J.C. and D.T. Gibson. 1988. "Oxidation of Substituted Phenols by *Pseudomonas putida* F1 and *Pseudomonas sp.* strain JS6." *Appl. Environ. Microbiol.*, 54: 1399-1404.

Srinivasan, P., and J. W. Mercer. 1988. "Simulation of Biodegradation and Sorption Processes in Groundwater." *Ground Water*, 26:475-487.

Suflita, J.M., A. Horowitz, A. Shelton, and D.R. Tiedje. 1982. "Dehalogenation: a novel pathway for the anaerobic biodegradation of haloaromatic compounds." *Science*, 218: 1115-1117.

Sykes, J. F., S. Soyupak, and G. J. Farquhar. 1982. "Modeling of Leachate Organic Migration and Attenuation in Groundwater Below Sanitary Landfills." *Water Resources Research*, 18: 135-145.

Taylor, S. W. and P.R. Jaffé. 1990a. "Biofilm Growth and the Related Changes in the Physical Properties of a Porous Medium: 1. Experimental Investigations." *Water Resources Research*, 26: 2153-2159.

Taylor, S. W., P.C.D. Milly, and P.R. Jaffé. 1990. "Biofilm Growth and the Related Changes in the Physical Properties of a Porous Medium: 2. Permeability." *Water Resources Research*, 26: 2161-2169.

Taylor, S. W. and P.R. Jaffé 1990b. "Biofilm Growth and the Related Changes in the Physical Properties of a Porous Medium: 3. Dispersivity." *Water Resources Research*, 26: 2171-2180.

Valo, R., V. Kitunen, M. Salkinoja-Salonen, and S. Raisanen. 1984. "Chlorinated Phenols as Contaminants of Soil and Water in the Vicinity of Two Finish Sawmills." *Chemosphere*, 13(8): 835-844.

Vandevivere, P. and P. Baveye, 1992. "Effect of Bacterial Extracellular Polymers on the Saturated Hydraulic Conductivity of Sand Columns." *Appl. Environ. Microbiol.*, 58: 1690-1698.

van Genuchten, M. Th. and P.J. Wierenga, 1976. "Mass Transfer Studies in Sorbing Porous Media: Analytical Solutions." *Soil sci. Soc. Am. J.*, 40(3): 473-480.

van Loosdrecht, M.C.M., J, Lyklema, W. Norde, and A.J.B. Zehnder. 1982. "Influence of Interfaces on Microbial Activity." *Microbiol. Rev.*, 54: 75-87.

Walas, S. M. 1991. *Modeling with Differential Equations in Chemical Engineering*. Butterworth-Heinemann, Inc., Stoneham, MA.

Wang, K. W. 1995. *Biodegradation of Mixed Wastes: Basic Kinetics and Reaction Engineering for Cyclic Reactor Operation,* Ph.D. Dissertation, Dept. of Chemical Engineering, New Jersey Institute of Technology, Newark, NJ.

Wanner, Q. and P. Reichert, 1996. "Mathematical Modelling of Mixed-Culture Biofilms." *Biotech. Bioeng.*, 49: 172-184.

Weber, W.J. Jr. and E.H. Smith, 1987. "Simulation and Design Models for Adsorption Processes." *Environ. Sci. Tech.*, 21: 1040-1050.

Widdowson, M.A., F.A. Molz, and L.D. Benefield, 1988. "A numerical Transport Model for Oxygen and Nitrate-based Respiration Linked to Substrate and Nutrient availability in Porous Media." *Water Resources Research,* 24: 1553-1565.

Wilke, C. R. and P. Chang. 1955. "Correlation of Diffusion Coefficients in Dilute Solutions." *AIChE J.*, 1(2): 261.

Wilson, E.J. and C.J. Geankoplis. 1966. "Liquid Mass Transfer at Very Low Reynolds Numbers in Packed Beds." *AIChE J.*, 5: 9-14.

Zhang, T.C. and P.L. Bishop. 1994. "Density, Porosity, and Pore Structure of Biofilms." *Water Research,* 28: 2267-2277.